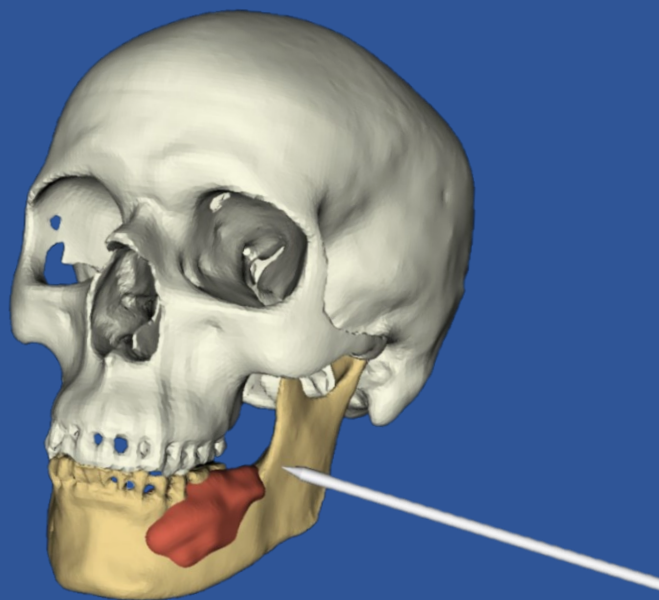# Electromagnetic navigation in mandible reconstruction surgery

Introduction and assessment of a noninvasive method for patient registration

Master's thesis

Anna Fleur de Geer

Electromagnetic navigation in mandible reconstruction surgery

Introduction and assessment of a noninvasive method for patient registration

Anna Fleur de Geer

Student number: 4397452

14-02-2022

Thesis in partial fulfilment of the requirements for the joint degree of Master of Science in

Technical Medicine

Leiden University; Delft University of Technology; Erasmus University Rotterdam

Master thesis project (TM30004; 35 ECTS)

Dept. of Head and Neck Oncology and Surgery, Netherlands Cancer Institute – Antoni van Leeuwenhoek hospital

Dept. of BioMechanical Engineering, TU Delft

September 2020 – February 2022

Supervisors

Dr. M.B. Karakullukcu, MD	(Medical supervisor)
Dr. ir. A.J Loeve	(Technical supervisor)
Dr. M.J.A. van Alphen	(Daily supervisor)
Dr. ir. R.P.J. van Veen	(Daily supervisor)

Thesis committee members

Prof. dr. F.W. Jansen, MD	(Chairman)
Dr. M.B. Karakullukcu, MD	(Medical supervisor)
Dr. ir. A.J. Loeve	(Technical supervisor)
Dr. M.J.A. van Alphen	(Daily supervisor)
Dr. L. van Erven, MD	(Additional member)

An electronic version of this thesis is available at https://repository.tudelft.nl

Preface and acknowledgements

During the second year of the master Technical Medicine, I did an internship in the NKI-AvL at the Department of Head and Neck Oncology and Surgery. During this internship, I became familiar with the possibilities of using 3D technology to improve surgical planning and intraoperative guidance. I got the opportunity to assist surgeons during mandible reconstruction surgery and I was intrigued by the amount of technology that was used during this surgery; 3D printed patient-specific cutting guides were used as part of the standard surgical workflow and surgical navigation was performed as part of a clinical study. When I was looking for a graduation project, the choice was easily made when I heard that I could do research in the NKI-AvL on surgical navigation in mandible reconstruction surgery.

As excited as I was to start with my graduation project in September 2020, in August my father got suddenly diagnosed with cancer and was referred to the NKI-AvL for treatment. This changed my graduation planning and also my perception of the hospital. The NKI-AvL was no longer only a hospital where innovative research was performed, but also a hospital where my father was being treated. I want to thank my supervisors for giving me all the time I needed during my father's treatment and after his death. Although I still have mixed feelings when I enter the hospital, I am glad that I continued with my research. As a researcher you can make a huge difference for cancer patients both in terms of survival and the quality of life. Therefore, I aspire to keep working on research focusing on improving the diagnostic process and treatment of cancer patients after my graduation.

To give my future scientific career a head start and to extend my stay in the NKI-AvL, I decided to do an elective project (15 ECTS) parallel to performing my graduation research. Besides writing my thesis, I have followed a course for scientific writing, submitted two articles to med(tech) journals, and submitted two grant proposals for funding to be able to continue with my research as a doctoral candidate. Although I did not get the funding, I have learned a lot and I am sure that this knowledge will be valuable when I pursue a career in research after my graduation.

The research conducted in this thesis would not have been possible without the excellent guidance of my supervisors. Arjo, thank you for teaching me to think a bit more outside the box and for your very critical but also valuable feedback. Although you did not know the project beforehand, you have always been very enthusiastic to supervise me. Baris, thank you for welcoming me in the clinic. You made me step out of my comfort zone when I had to perform several medical treatments from which I did not know I could do them on my own. With your constructive feedback, I have improved my medical skills as a Technical Physician. Also, I will never forget your wise words when I was working on the manuscripts and grant proposals *"Perfect is the enemy of good"*. Maarten, and Robert, thank you for welcoming me in the 3D lab and for our many brainstorm sessions. When I had a question, I could always walk by for a quick chat which was very helpful. I would also like to thank Harald, Wout, Jasper, Laura, and Marijn for letting me participate during their research meetings about surgical navigation, for their help with the navigation system, and for the brainstorm sessions regarding my experiments. In addition, I would like to thank Susan for her help during the first months of my research. Susan, you made me familiar with the navigation procedure for mandible surgery and you encouraged me to continue with your research when you left the NKI-AvL after obtaining your PhD title.

Finally, I would like to thank the other students of the 3D lab for our daily coffee and lunch sessions where we laughed a lot, my friends and family for their support, and Joris who always cooked for me when I was working late and who made me laugh by telling silly jokes when I was stressed.

Fleur de Geer,
Amsterdam, January 2022

Summary

In patients with oral cavity cancer invading the mandible, a segmental bone resection is performed and the original contour of the mandible is reconstructed with a free fibula flap. Virtual surgical planning is performed prior to surgery to determine the locations and orientations of the osteotomy planes on the mandible and fibula. Currently, patient-specific cutting guides are designed and three-dimensional printed to translate the virtual surgical plan to the patient in the operating room. However, these cutting guides are not ideal; they lack adaptability when the intraoperative situation is different than expected, e.g. due to tumor progression. Alternatively, surgical navigation could be used to translate the virtual surgical plan to the patient. To enable surgical navigation, accurate alignment of the preoperative imaging data, including the virtual surgical plan, and the patient is required, i.e. image-to-patient registration. In this thesis, a simple, accurate, and noninvasive registration method for electromagnetic navigation of the mandible is introduced and assessed.

Chapter 1 gives an introduction to the clinical background of mandible reconstruction surgery and the technical background of surgical navigation. The clinical problem, a potential solution and the thesis objectives are also discussed.

The systematic review in **Chapter 2** gives an overview of currently used registration methods in navigated mandibular surgery: point registration, surface registration, hybrid registration, and computer vision based registration. The main conclusion of the review was that there is always a tradeoff between the usability, registration time, accuracy, and invasiveness of a registration method.

Chapter 3 introduces a simple and noninvasive registration method for mandible navigation: hybrid registration. This method consists of two steps: 1) point registration; performed for initialization using three anatomic landmarks on the mandible, and 2) surface registration; performed for optimization using the surgically exposed mandibular bone surface after removal of soft tissue.

In previous research in the NKI-AvL, an applicator was used to fixate an electromagnetic sensor to the mandible to track its movements during navigated surgery. The design of this applicator, however, enabled movement of the sensor in the applicator, which resulted in inaccurate navigation. Therefore, in **Chapter 4,** a renewed design for the sensor applicator is proposed.

In **Chapter 5**, the optimal approach for hybrid registration of the mandible is determined in phantom experiments. Different registration configurations, i.e. different surface point areas and number and configuration of surface points, were evaluated as well as registration with different patient anatomies. In all experiments, the target registration error (TRE) was below 2.0 mm, which meets the practical clinical requirements for mandible reconstruction surgery. The results suggest that only a small surface area of the mandible, marked by limited surface points, is required to obtain accurate registration.

Chapter 6 describes the preliminary results of hybrid registration of the mandible in four patients during surgery. Registration could be performed within on average 4.5 minutes. Mean TRE values of 3.4 mm for anatomic landmarks and 2.3 mm for cutting guide landmarks were obtained, indicating that the registration procedure should be further optimized to achieve clinically acceptable registration accuracy.

Chapter 7 provides an overall conclusion and future perspectives. Although the preliminary results of the patient study for mandible navigation are promising, the registration method should be further optimized and evaluated in more patients before implementation into clinical practice is possible. Ultimately, we want to use electromagnetic navigation to position a universal cutting guide during mandible reconstruction surgery. Multiple challenges still lie ahead before this can become reality in the NKI-AvL.

List of abbreviations

Abbreviation	Definition
3D	three-dimensional
ALT	anterolateral thigh flap
AR	augmented reality
CAD	computer-assisted design
CAM	computer-assisted manufacturing
CAS	computer-assisted surgery
CBCT	cone beam computed tomography
CSD	central sterilization department
CT	computed tomography
DOF	degrees-of-freedom
DRF	dynamic reference frame
ED	Euclidean distance
EM	electromagnetic
EMTS	electromagnetic tracking system
FFF	free fibula flap
FG	field generator
FRE	fiducial registration error
HPV	human papillomavirus
ICP	iterative closest point
IMF	intermaxillary fixation
MRI	magnetic resonance imaging
NKI-AvL	Netherlands Cancer Institute – Antoni van Leeuwenhoek
OCC	oral cavity cancer
OPG	orthopantomogram
OR	operating room
PET	positron emission tomography
RMSE	root mean squared error
SCC	squamous cell carcinoma
SCU	sensor control unit
SD	standard deviation
SIU	sensor interface unit
TMJ	temporomandibular joint
TP	technical physician
TRE	target registration error
UMC	university medical center
US	ultrasound
VSP	virtual surgical planning

Table of contents

Chapter 1

General introduction

1.1 Clinical background

1.1.1 Anatomy of the mandible

The mandible is the largest facial bone and represents the contour of the lower third of the face. The main function of the mandible is mastication, but it also plays a role in swallowing, speaking, and breathing [1, 2]. The mandible consists of a body and two rami (Figure 1.1) [2]. The mandibular body is curved like a horseshoe and creates the lower jaw line. The mandibular body serves as the basis for the lower teeth and its outer surface is characterized by two mental foramen where the mental nerve passes from inside the mandible to innervate the chin and lower teeth [3]. The mandibular body ends at the angles of the mandible where the rami join. At the cranial part of each ramus, the condylar process articulates with the temporal bone to form the temporomandibular joint (TMJ). The TMJ facilitates movement of the mandible together with four primary mastication muscles that insert at the ramus: m. masseter, m. temporalis, m. lateral pterygoid, and m. medial pterygoid [2, 4].
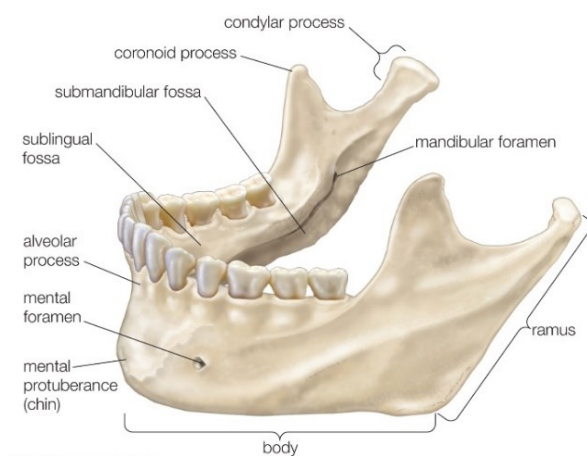
Figure 1.1 *Bony anatomy of the mandible [5].*

1.1.2 Cancer involving the mandible

1.1.2.1 Epidemiology

Primary mandibular bone tumors are rare, but the mandible is often involved in cancers of the oral cavity [6]. Oral cavity cancer (OCC) is the most common type of head and neck cancer in the Netherlands and its incidence is rising; in 2020, 920 patients were diagnosed with OCC in the Netherlands [7]. Worldwide, the incidence of lip and oral cavity cancer was 377,713 in 2020 from which 70% of the patients were men [8]. OCC is most frequent in South Central Asia and Melanesia due to betel nut chewing. In Eastern and Western Europa, Australia, and New Zealand, incidence rates are also high which has been linked to tobacco smoking, alcohol consumption, and infection with the human papillomavirus (HPV) [8]. The risk of developing OCC increases with age, and alcohol consumption and tobacco smoking have a synergistic relationship [6, 9]. Squamous cell carcinoma (SCC) account for 90% of OCC. Other common tumor types invading the mandible are osteosarcoma, chondrosarcoma, rhabdomyosarcoma, and benign tumors such as ameloblastoma and giant cell tumors [9].

1.1.2.2 Diagnosis

In early stage of OCC irregular white, red or mixed patches appear on the mucosa. However, when patients present themselves at the hospital it is often because of pain, which indicates a more advanced disease stage. Other common symptoms include dysphagia, odynophagia, a hoarse voice, otalgia, weight loss, and lymphadenopathy [9]. In the NKI-AvL, physical examination with visual inspection and palpation is performed as a first step in the diagnostic process. If suspicious lesions are found, a biopsy is performed. If malignant cells are present in the lesion, additional imaging is performed; magnetic

resonance imaging (MRI) is preferred to evaluate the tumor itself and soft tissue involvement, an orthopantomogram (OPG) to evaluate the presence and quality of the lower teeth and to get a general impression of the status of the mandibular bone, computed tomography (CT) to assess possible bone invasion, ultrasound (US) imaging with cytologic punction to investigate suspected lymph nodes and the presence of lymphadenopathy, and positron emission tomography (PET) to assess possible locoregional or distant metastases and confirm bone invasion if the CT scan is inconclusive [10, 11].

1.1.2.3 Treatment

Surgery is the main curative treatment of OCC, often followed by adjuvant (chemo)radiotherapy [12]. The extent of surgery depends on the size and staging of the tumor and often includes a radical or selective neck dissection to excise lymph nodes [6, 9]. In tumors invading the mandible, staged as T4, a bone resection is indicated to obtain adequate surgical margins [10, 13]. In these patients, a segmental mandibulectomy is performed (Figure 1.2). To restore the mandible's continuity and function, a reconstruction of the defect is indicated. When the tumor is located against the bone, not invading the bone, a marginal mandibulectomy is performed (Figure 1.2). With a marginal mandibulectomy the inferior border of the mandible remains intact hereby preserving its contour and function and decreasing the patient's functional and aesthetic morbidity [10].
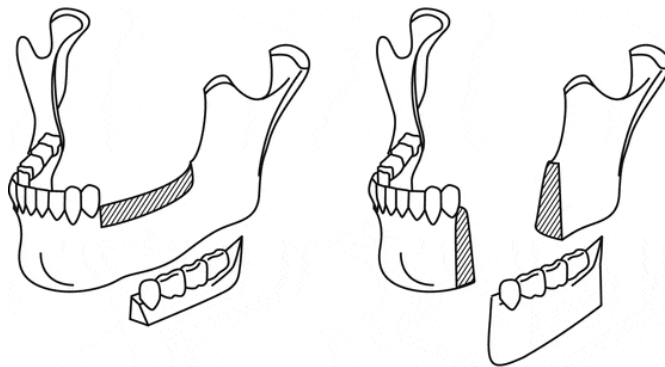
Figure 1.2 *Types of mandibulectomy: marginal mandibulectomy (left) and segmental mandibulectomy (right)* [14].

1.1.2.4 Surgical margins

Postoperatively, the resected specimen is examined by a histopathologist to investigate the surgical margins. Histologically, for soft tissue specimens, surgical margins are defined as 'adequate' or 'clear' when the tumor is surrounded by at least 5 mm healthy tissue, as 'close' when the tumor is surrounded by 1-5 mm healthy tissue, and as 'positive' when the tumor is surrounded by less than 1 mm healthy tissue [10]. For bone specimens, margins are considered 'positive' when tumor tissue is found in the resection plane. Positive resection margins are associated with poor prognosis both in terms of locoregional recurrence and overall survival [14, 15]. Hence, it is important to radically remove the tumor during surgery. The tumor, often including both a soft tissue component and a bone component, is resected with 10 mm of surrounding healthy tissue in all planes because soft tissue will shrink after resection and the extent of bone invasion is often difficult to determine beforehand [16, 17]. Ultimately, the goal of surgery is to radically remove the tumor while sparing vital structures as much as possible.

1.1.3 Mandible reconstruction

In patients requiring a segmental resection, a reconstruction is performed to restore the mandible's contour and function [18]. In patients with primary benign tumors, non-vascularized bone grafts can be used for the reconstruction of small bone defects (up to 5 cm) [18, 19]. In patients with malignant tumors, the mouth floor or tongue are often involved and soft tissue reconstruction is indicated as well.

Sometimes, the bone defect is bridged by a (titanium) reconstruction plate and the soft tissue defect is covered by a fasciocutaneous flap, e.g. an anterolateral thigh (ALT) flap. However, intra- and extraoral plate exposure and plate fracture are commonly seen complications in these patients [20, 21]. Alternatively, in some patients the bone defect doesn't need to be reconstructed and only a soft tissue reconstruction is carried out. However, vascularized bone grafts with a skin paddle usually lead to improved outcomes with decreased overall costs compared to non-vascularized grafts, soft tissue reconstructions, and combined plate and soft tissue reconstructions [18]. Absolute indications for the use of vascularized bone grafts are bone defects larger than 6 cm, the need for soft tissue reconstruction, and poorly vascularized covering tissue [18, 22]. The most widely used donor sites for vascularized bone grafts include the fibula, iliac crest, scapula, and radius. Each flap has its own advantages and disadvantages, but the fibula possesses a number of characteristics that have made it the working horse and golden standard for reconstruction of the mandible [18, 22].

1.1.3.1 Free fibula flap

The fibula is a long non weight-bearing bone in the lower leg, consisting of a head, neck, shaft, and distal end containing the lateral malleolus (Figure 1.3a). Its main function is to provide stability to the ankle joint and provide attachment for several muscles of the leg [23]. Because of its non weight-bearing function, the middle section of the fibula can be harvested with low risk of donor site comorbidity; the fibular head and distal end are kept intact (Figure 1.3b). The fibula is thin and long while maintaining great vascularity that allows for easy graft uptake [23]. The main advantages of using a free fibula flap (FFF) for mandible reconstruction (Figure 1.3b) include the long segment that can be harvested (up to 25 cm), its tolerance for multiple osteotomies due to the segmental and intraosseous blood supply, its adequate bone stock to support osseointegrated implants, its long vascular pedicle, its large and reliable skin paddle, and the possibility to operate on both the mandible and fibula at the same time [6, 18]. After harvesting, the fibula is fixated in the native mandible with a patient-specific reconstruction plate, a pre-bent reconstruction plate, or with mini plates [24].

1.1.3.2 Current workflow in the NKI-AvL

In the past, mandible reconstruction surgery was performed with a free hand approach. The success rates of the vascularized bone flaps, as well as functional and aesthetic outcomes were highly dependent on the surgeon's experience [25]. To obtain increased reconstruction accuracy, more predictable surgical outcomes, and shorter operating and ischemic times, virtual surgical planning (VSP) has been introduced in mandible reconstruction surgery [25-27]. Using VSP, surgeons can visualize the tumor, perform mandibular resection, determine the number and orientation of required fibula segments, and perform fibular osteotomies and free flap inset through the VSP system prior to surgery [25]. Using computer-assisted design and -manufacturing (CAD-CAM) techniques, patient-specific mandibular and fibular cutting guides can be designed and three-dimensional (3D) printed to accurately transfer the virtual surgical plan to the patient in the operating room (OR) (Figure 1.4) [27].

The NKI-AvL works together with the Radboud University Medical Center (Radboud UMC) and KLS Martin (Tuttlingen, Germany), a medically certified 3D printing company, to design and fabricate the cutting guides. First, the treatment plan is discussed in the multidisciplinary 3D reconstruction board meeting in the NKI-AvL. Then, VSP is performed by a Technical Physician (TP) and a surgeon from the Head and Neck Surgery department: a 3D model of the mandible is constructed from the preoperative imaging data and the locations and orientations of the osteotomy planes are determined. The 3D model together with the osteotomy planes is discussed with a TP in the Radboud UMC in a videoconference. Afterwards, the TP determines the number of fibula segments with length and angle specifications and designs the cutting guides. The virtual surgical plan and the cutting guides require approval from the surgeon in the NKI-AvL. When approved, the cutting guides are send to KLS Martin for 3D printing.

Subsequently, the cutting guides are transported to the NKI-AvL, checked by the surgeon, and disinfected and sterilized for surgical use by the sterilization department. A complete overview of the workflow is visualized in Figure 1.7.
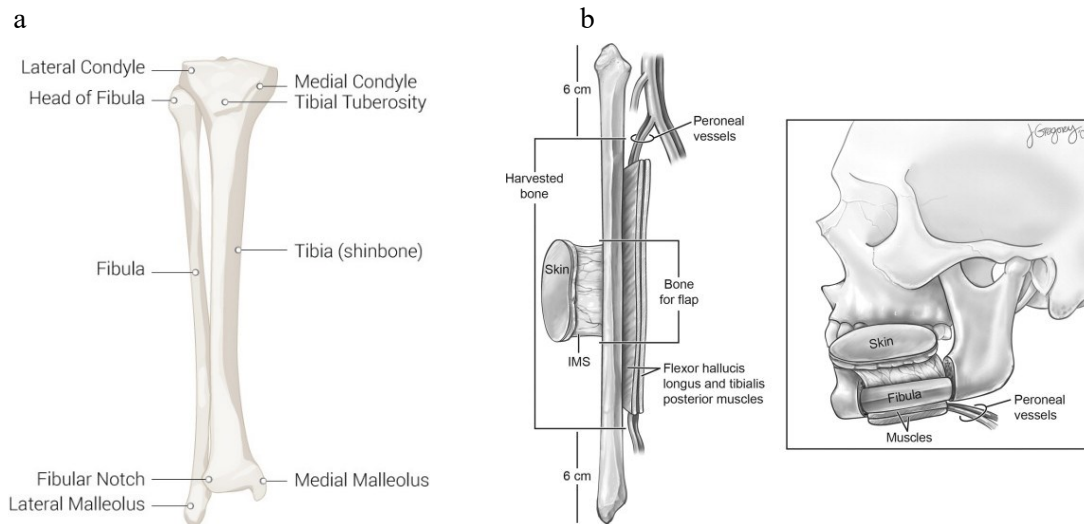
Figure 1.3 *a) Anatomy of the fibula, b) anatomy of the free fibula flap and an example of a restored mandible with the flap in situ [23, 28].*
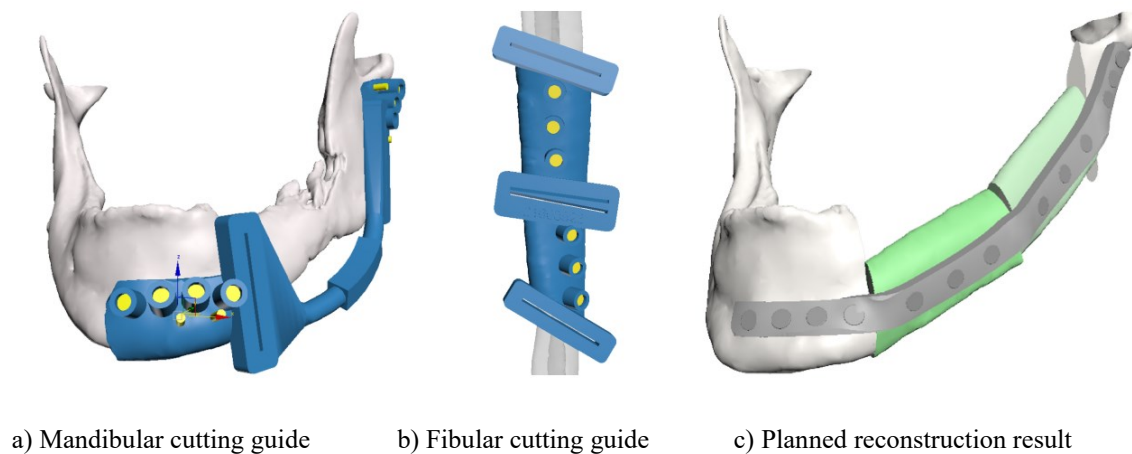
a) Mandibular cutting guide   b) Fibular cutting guide   c) Planned reconstruction result

Figure 1.4 *Example of patient-specific cutting guides used during surgery in the NKI-AvL. The guides are fixated to the bone with screws through the small holes indicated in yellow. The bone is cut by sliding a saw through the cutting slots.*

1.2 Clinical problem

Although the currently used cutting guides help obtain faster and more reliable surgery compared to the original free hand technique [29], the cutting guides are not ideal. The most important shortcoming is their lack of adaptability when the intraoperative situation is different than expected [30]. The time interval between preoperative planning and surgery should not exceed two weeks, but can take up to four weeks because of the time consuming logistics with the two external companies that are required for the design and fabrication process of the cutting guides. In the meantime, an aggressive tumor can grow rapidly making the virtual surgical plan outdated since the surgical margins will be inadequate. Moreover, in some cases the cutting guide does not fit because of remaining soft tissue between the mandible and the cutting guide (Figure 1.5) or because of a mandible fracture due to osteoradionecrosis. Since the current cutting guides do not allow for alterations of the surgical plan, the cutting guides cannot be used. For these patients, the cutting guides are cut into separate parts or free hand surgery is used. Moreover, the dependency on two external companies leads to high costs since multiple stakeholders such as engineers, surgeons, and sterilization personnel are involved. Also, the material of the cutting guides is not robust, which enables the saw to cut through the guides instead of following them; this can result in skewed osteotomy planes, which can result in poor reconstruction results [31]. Lastly, the cutting guides are pollutive for the environment since they are made from plastic, for single use only, and require transport from the 3D printing company to the hospital for every patient individually.

Figure 1.5 *An example of a patient treated in the NKI-AvL where the cutting guide did not fit on the mandible and had to be cut in two separate parts because of a large tumor invading the oral cavity, mandible, and facial skin: a) the tumor is causing swelling and redness in the skin, b) the tumor during surgery, before the cutting guide is attached, c) the tumor with the cutting guide attached in two separate parts, d) the tumor after bone resection, the cutting guide parts are still in place, adapted from [32].*

1.3 Proposed solution

To overcome the limitations of the currently used patient-specific cutting guides, another method is preferred to translate the virtual surgical plan to the patient in the OR. A potential method is to use surgical navigation. Surgical navigation allows real-time visualization of the position and orientation of surgical instruments in relation to the patient's anatomy. The proposed solution is to use universal, navigated, titanium cutting guides that can be adapted for every patient [33]. The preoperative planning is similar to the current workflow: 3D models are constructed from preoperative imaging data and the locations and orientations of the osteotomy planes on the mandible and fibula are determined by a TP and a surgeon from the Head and Neck Surgery department. Intraoperatively, the cutting guide is positioned on the bone according to the virtual surgical plan (Figure 1.6). The only prerequisite to be able to perform the surgery is the preoperative imaging data; this makes the whole workflow significantly shorter (Figure 1.7). If the planning of the Radiology and Surgery departments allow it, surgery can be performed directly after diagnosis which is a huge advantage compared to the current method.

The proposed cutting guides will:

1. enable the surgeon to adapt the surgical plan shortly before or even during surgery;
2. obviate the need for external partners, hereby reducing the costs and shorten the waiting time between planning and surgery;
3. provide accurate guidance of the saw due to robustness of the material;
4. be reusable and sustainable, hereby reducing the ecological footprint of this surgery.
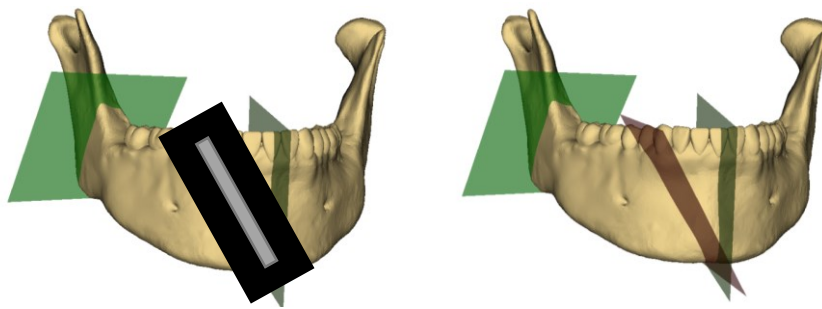
Figure 1.6 *Overview of the proposed solution: positioning of a universal, navigated, titanium cutting guide (left) according to the virtual surgical plan (right). The cutting guide is indicated in black with the cutting slot in grey. The planned osteotomy planes are indicated in green, the current osteotomy plane is indicated in red. The surgeon moves the cutting guide until the position of the planned osteotomy plane is reached, then the cutting guide is fixated and the bone is sawn.*
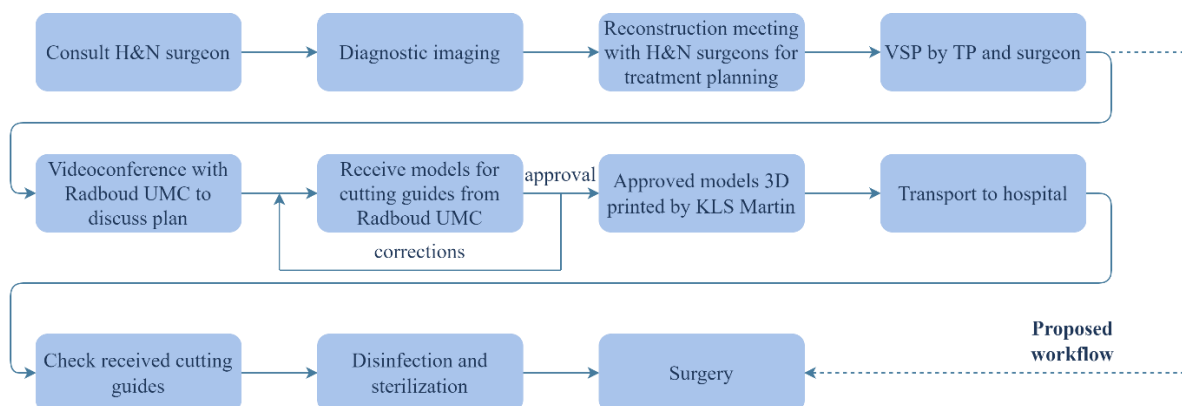
Figure 1.7 *Overview of the current and proposed workflow for mandible reconstruction surgery in the NKI-AvL. H&N = head and neck, VSP = virtual surgical planning, TP = technical physician.*

1.4 Technical background

1.4.1 Surgical navigation workflow

Surgical navigation can be divided into two phases: a preoperative phase and an intraoperative phase. The complete workflow is visualized in Figure 2.1. The preoperative phase starts with imaging (CT and/or MRI scanning). From the imaging data, the relevant anatomy is segmented and 3D models are constructed. A virtual surgical plan is created based on the 3D models. During surgery, the preoperative imaging data, 3D models, and the virtual surgical plan are visualized on a screen in the OR. First, the preoperative imaging data, including the virtual surgical plan, is aligned with the intraoperative anatomy of the patient, i.e. image-to-patient registration. Subsequently, the real-time position of tracked surgical instruments can be visualized on the screen relative to the patient's anatomy.

1.4.2 Tracking methods

Tracking is a key component in surgical navigation, allowing the continuous localization of surgical instruments relative to the patient's anatomy. Two main methods exist: optical tracking and electromagnetic (EM) tracking. In optical tracking, infrared reflecting markers are attached to the patient and surgical instruments. These markers are recognized by an infrared camera system and localized in space. The main drawback of optical tracking is the requirement of a continuous line-of-sight from the camera to the markers [34]. This limits the surgeon's movements and is, therefore, challenging in small working areas such as the oral cavity. Therefore, EM tracking has emerged as a solution to this problem. In EM tracking, a field generator (FG) is used to create an EM field that creates currents in EM sensors attached to the patient and surgical instruments. These currents are used by the EM system to calculate the distance from the sensors to the FG to define the position and orientation of the sensors in the reference frame of the EM system. Therefore, the FG should be located in proximity to where the sensors are positioned on the patient. The main drawback of EM tracking is that the tracking accuracy can be compromised by magnetic field distortion due to nearby ferromagnetic objects such as surgical instruments, instrument tables, and standard patient tables [35, 36].

1.4.3 Aurora electromagnetic tracking system

In the NKI-AvL, an EM tracking system is currently being used for surgical navigation during oncologic surgery; the NDI Aurora V2 (Northern Digital Inc., Waterloo, Canada) [37]. This system consists of four main components: a FG, EM sensors, a sensor interface unit (SIU), and a system control unit (SCU). Two FGs are available in the NKI-AvL: a tabletop FG and a planar FG (Figure 1.8). The tabletop FG is mostly used in abdominal cancer surgery since it can be easily attached inside a special carbon patient table before surgery. However, this patient table is suboptimal for use during mandible reconstruction surgery since the separate leg positioning add-on, desirable for surgery of the fibula, cannot be attached. Therefore, the planar FG is used for navigation during mandible reconstruction surgery. This FG is mounted on a positioning arm that can be placed in the proximity of the patient's head (Figure 1.9).

The planar FG creates a 50 x 50 x 50 cm EM field that induces currents in the EM sensors when these are placed inside the EM field. These currents are amplified and digitized by the SIU. The SCU detects the amplified signal and calculates the position and orientation of the sensors and passes this information to a host computer [37].

Two types of EM sensors are available, five degrees-of-freedom (5DOF) sensors and six degrees-of-freedom (6DOF) sensors [38]. The 5DOF sensors provide the x, y, and z position of the sensor and two of its orientations; pitch and yaw. The 6DOF sensors provide an additional third orientation of the sensor; roll (Figure 1.10). Therefore, unique positions of the patient and surgical instruments can be determined by using a single 6DOF sensor or two combined 5DOF sensors. In mandible reconstruction

surgery, 6DOF sensors are used. The tracking accuracy of a 6DOF sensor combined with the planar FG is 0.48 mm and 0.30° in laboratory setting [37].

Figure 1.8 The Aurora tabletop field generator (left) and planar field generator (right) [37].

Figure 1.9 The planar field generator mounted on a positioning arm, located near the head of the patient [37].

1.4.4 Image-to-patient registration

Registration is the process of transforming data coordinates from one coordinate system to another. During a simple rigid registration, the optimal translation and rotation of coordinate system A to coordinate system B is calculated resulting in a translation vector ($^{B}t_A$) and a rotation matrix ($^{B}R_A$) which can be combined as a transformation matrix $^{B}T_A = \begin{bmatrix} ^{B}R_A & ^{B}t_A \\ 0 & 1 \end{bmatrix}$. $^{B}T_A$ is the transformation from coordinate system A to coordinate system B that can be applied to transform points from coordinate system A (^{A}p) to points in coordinate system B (^{B}p) with Equation 1.1 [39]:

$$^{B}p = {}^{B}T_A * {}^{A}p \qquad\qquad 1.1$$

During surgical navigation, this technique is applied to align the preoperative imaging data, including the virtual surgical plan, with the patient in the OR, i.e. 'image-to-patient' registration.

Two main registration methods exist for navigated surgery: point registration and surface registration [40]. In point registration, at least three distinct points are required to register the preoperative imaging data with the patient [41]. Preoperatively, these points are annotated in the 3D model that is constructed from the preoperative imaging data. Intraoperatively, the surgeon pinpoints these points on the patient with a tracked probe and their coordinates are matched with the corresponding points in the 3D model by the navigation software. Both anatomic landmarks and artificial markers can be used as registration points. Surface registration is a marker-free method using a series of points on anatomical surfaces such as the facial skin. The surgeon collects these points with a tracked probe or with a 3D laser scanner and these points are registered to the 3D model by the navigation software.
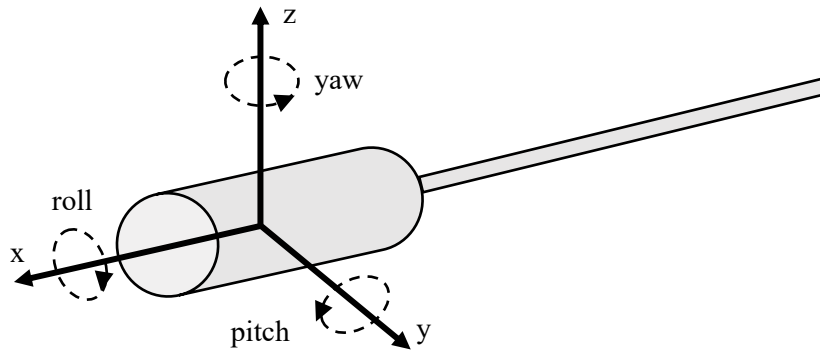
Figure 1.10 *Schematic overview of a 6DOF sensor. The three translations (x, y, z) and three orientations (pitch, yaw, roll) are shown.*

1.4.4.1 Mobility problem of the mandible

Although navigation is commonly used in maxillofacial surgery, its use in mandibular surgery is limited due to the complex registration procedure. In standard registration procedures, a sensor is fixed onto the patient's cranium to measure head movements. However, the mandible moves independently of the rest of the craniofacial skeleton, which acts as one solid structure [42]. Currently, two strategies are being employed to tackle this 'mobility' problem: either keeping the mandible in fixed position during preoperative imaging and surgery, or attaching a dynamic reference frame to the mandible that tracks mandibular movements during surgery [43, 44]. A more extensive explanation of these strategies can be found in Chapter 2. In oncologic surgery with tumors invading multiple structures in the oral cavity, the strategy where the mandible can move freely is preferred to enable good visibility during tumor resection. Therefore, in two prior studies in the NKI-AvL an EM sensor was fixed onto the mandibular bone to track its movements.

1.4.4.2 Previous research in the NKI-AvL

In a phantom study by Brouwer de Koning et al., point registration was evaluated *ex vivo* using notches on a dental splint, screws in the ipsilateral mandible (the side where the virtual tumor was located), screws in the contralateral mandible (the side where the virtual tumor was not located), and a combination of screws on the mandible and notches on the dental splint resulting in average target registration errors (TRE, see paragraph 2.3.5.1 for the definition and formula) of 0.83 mm, 1.28 mm, 2.62 mm, and 1.34 mm respectively [45]. Since TRE values of maximum 2.0 mm are considered as clinically acceptable for mandible reconstruction surgery according to literature and surgeons from our institute, the splint method, ipsilateral screws method, and combined method would be feasible [46]. However, these methods have drawbacks. The major drawback of using screws for registration is the invasiveness for the patient. Screws should either be implanted in the outpatient clinic before preoperative imaging is performed or during surgery. However, the latter method requires an additional CT scan during surgery on a hybrid OR containing a Cone Beam CT (CBCT) scanner. In the NKI-AvL, only one hybrid OR is available and most hospitals do not have a hybrid OR at all thus the application of this method is limited. Moreover, the additional scan leads to extra ionizing radiation for the patient and the clinical workflow is interrupted since most staff members need to leave the OR during scanning. Using notches on a dental splint is a noninvasive alternative. However, splints cannot be used in edentulous patients or in patients with tooth loosening. Moreover, the splint should fit perfectly on the teeth for accurate registration. Therefore, splints should be patient-specific, which requires separate designing and fabrication for every patient.

The screws method was also evaluated *in vivo* in a patient study in the NKI-AvL [30]. In this study, the cutting guide was attached to the mandible with four screws, an intraoperative CBCT scan was acquired, and the four screws were used for registration. The accuracy was validated using four anatomic landmarks and four landmarks on the cutting guide. The procedure was performed in eleven patients resulting in average TREs of 3.2 ± 1.1 mm for the anatomic landmarks and 2.6 ± 1.5 mm for the landmarks on the cutting guide. The total time to perform the navigation procedure, from sensor placement to validation, was on average 32 minutes. CBCT scanning added up to 16 minutes extra to the registration procedure and registration was the most time consuming step since this was often redone to improve the system's accuracy [30].

1.5 Thesis objectives and outline

To enable the use of electromagnetic navigation during mandible reconstruction surgery, accurate registration of the preoperative imaging data, including the virtual surgical plan, to the patient in the OR is required. Since existing mandible registration methods with screws or dental splints are either invasive for the patient or require a complex and patient-specific fabrication process, an alternative registration method is preferred. Therefore, the main goal of this thesis is:

> **Introduce and assess a simple, accurate, and noninvasive registration method to enable electromagnetic navigation of the mandible.**

To reach the described goal, secondary objectives are defined as listed below:

1. Provide an overview of existing registration methods for surgical navigation of the mandible (chapter 2)
2. Introduce a simple and noninvasive registration method for surgical navigation of the mandible (chapter 3)
3. Design a sensor applicator to fixate an EM sensor to the mandible to enable intraoperative tracking (chapter 4)
4. Determine the optimal approach for accurate mandible registration in a phantom study (chapter 5)
5. Evaluate the clinical feasibility of mandible registration in patients undergoing mandible reconstruction surgery (chapter 6)

NOTE: Chapters 2 and 5 are original manuscripts submitted for publication in a scientific journal. Therefore, these chapters contain overlapping information with other chapters in this thesis.

Chapter 2

Registration methods for surgical navigation of the mandible: a systematic review

A.F. de Geer, S.G. Brouwer de Koning, M.J.A. van Alphen, S. van der Mierden, C.L. Zuur, F.W.B. van Leeuwen, A.J. Loeve, R.L.P. van Veen, M.B. Karakullukcu

2.1 Introduction

The mandible plays an important role in mastication, speech, and swallowing function and represents the contour of the lower third of the face. Losses of mandibular continuity can result in limited range of motion, malocclusion, and proprioceptive problems. Therefore, an important aim during surgery of the mandible is to maintain or restore its shape and function. To enhance the surgeon's orientation within the surgical field and provide intraoperative guidance, computer-assisted surgery (CAS) techniques can be applied [1].

In CAS, a virtual three-dimensional (3D) model of the mandible is constructed from a Computed Tomography (CT) scan. Based on this model, a virtual surgical plan is made. Often, this plan is translated to the operating room (OR) by 3D printed patient-specific cutting guides [30]. However, these cutting guides are not ideal; preparation time can take up to several weeks before surgery, the guides are costly to produce, and there is no possibility to adjust the surgical plan shortly before or during surgery (e.g. in oncologic surgery when tumor growth occurred between preoperative planning and actual surgery) [30, 47]. As an alternative to cutting guides, surgical navigation can be used to translate the virtual surgical plan to the OR.

Surgical navigation provides real-time visualization of the position and orientation of surgical instruments in relation to the patient's anatomy. Two main methods exist for tracking of the patient and surgical instruments: optical tracking and electromagnetic (EM) tracking. Optical methods use a camera system for tracking, while EM methods use a magnetic field that induces currents in sensors on the surgical instruments and patient [48]. Essential for these tracking systems to work is accurate image-to-patient registration, i.e. registration of the preoperative imaging data (including the virtual surgical plan) with the intraoperative anatomy [42, 45]. For a complete overview of the steps of surgical navigation, see Figure 2.1.

Surgical navigation has been increasingly used in oral and maxillofacial surgery over the last 20 years [49]. In standard registration procedures, a tracker is fixed onto the patient's cranium to measure head movements [48]. However, the mandible moves independently of the rest of the craniomaxillofacial skeleton, which acts as one solid structure. Consequently, registration of the mandible with the preoperative CT scan is complex [42, 50]. As a result, navigation is not routinely applied in mandibular surgery in clinical practice. Moreover, studies researching the application of navigation in mandibular surgery often use inconsistent quantification methods for the registration accuracy or do not report the used registration method and/or accuracy values at all [51-55].

The aim of this systematic review is to provide an overview of the different registration methods for navigated mandibular surgery. This overview can help surgeons and technicians to gain insight in the available options, which can be useful when choosing a registration method for navigation in different applications of mandibular surgery. The main research question of this review is: Which registration methods are used for surgical navigation of the mandible? To answer this question, the following secondary research questions are addressed:

1. For which applications of mandibular surgery is navigation employed?
2. Which variants of navigation are used in mandibular surgery?
3. How is the mobility of the mandible accounted for in the reported registration methods?
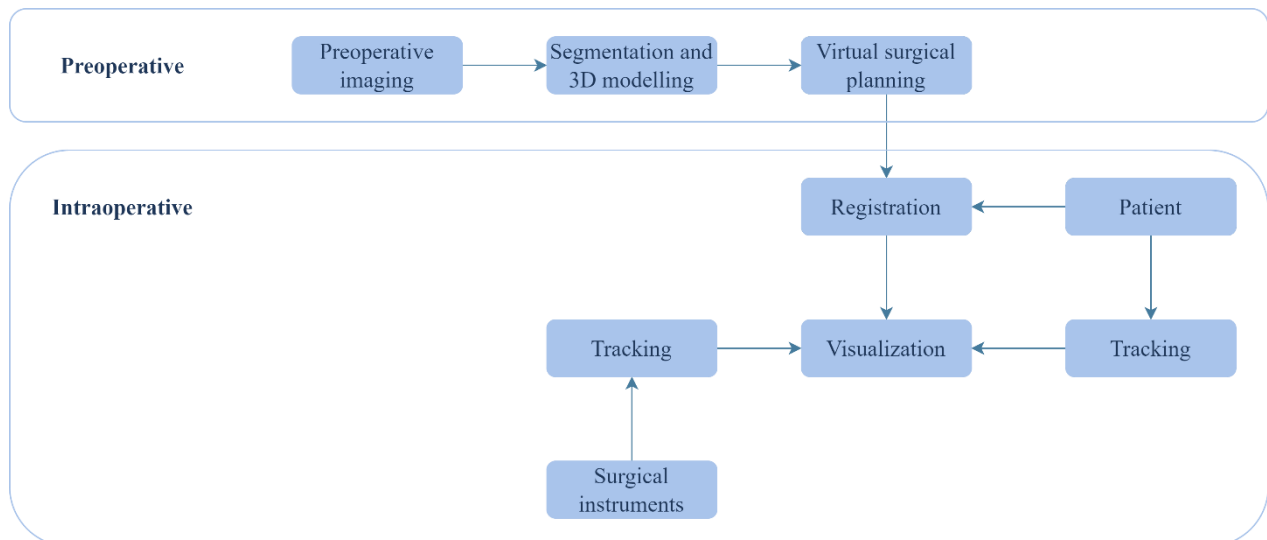4. What is the accuracy of the reported registration methods?

Figure 2.1 *Flowchart containing the steps of surgical navigation.*

2.2 Methods

This systematic review is written according to the Preferred Reporting Items for Systematic Reviews and Meta-Analyses (PRISMA) statement [56]. Risk of bias was not applicable and, therefore, bias assessment was not performed.

2.2.1 Database search

A systematic literature search was conducted using the Medline Ovid (Ovid MEDLINE ALL resource), Scopus and Embase.com databases on March 25, 2021. The search queries were built using both free terms and indexed terms for mandibular surgery, surgical navigation, and registration methods. The full search queries are provided in Appendix I.

2.2.2 Study selection

Identified articles were deduplicated in Endnote X9 (Clarivate Analytics, Philadelphia, United States) using the method described by Bramer et al. [57] and remaining references were screened manually for duplicates. References indexed as 'conference abstracts' in the databases were removed. Afterwards, the Endnote file was loaded into Rayyan for title and abstract assessment [58]. Two researchers (FG and SBK) independently assessed the articles based on title and abstract. In case of disagreement, the researchers discussed the article until consensus was reached. The inclusion criteria used for title and abstract screening were: 1) From the title or abstract it becomes clear that the study is about mandibular, orthognathic or maxillofacial surgery. 2) At least one navigation related term, such as 'navigation', 'augmented reality', 'guided surgery', 'computer-assisted surgery', 'image-guided surgery', 'registration' or 'tracking', is mentioned in the title or abstract. Articles about dental implant navigation were excluded as well as expert views, reviews, clinical guidelines, and editorial letters.

Full-text assessment was performed by FG; afterwards the in- or exclusion of articles was checked by SBK. The inclusion criteria for full-text assessment were: 1) The article is about surgical navigation of the mandible. 2) The registration method, used for image-to-patient registration, is reported. 3) In articles that report on surgical navigation in areas additional to the mandible, the registration method used for the mandible is explicitly mentioned. Phantom studies, animal studies, cadaver studies, technical reports, case reports, case series, cohort studies, and clinical trials were included. Articles were excluded with the following reasons: 1) The article is not about surgical navigation of the mandible. 2) The registration method is not reported or it is not reported how the researchers accounted for mandibular mobility. 3) In articles that describe surgical navigation in areas additional to the mandible, the used registration

method for the mandible is not explicitly mentioned. 4) No full-text is available. 5) No Dutch or English translation is available.

2.2.3 Data extraction

Data extraction was performed by FG using a predefined data-extraction Excel sheet. Baseline features such as study focus, surgery type, and number of subjects were recorded for each article. Moreover, the navigated procedure, mandibular mobility, tracking method, used (commercial) navigation system, registration method, registration time, registration markers, marker location, registration accuracy metrics, and surgical outcome metrics were extracted. In addition, a short explanation of the registration procedure was written for each article.

2.3 Results

2.3.1 Search results

The search yielded a total of 2952 articles, of which 1259 articles remained after duplicate and conference abstract removal (Figure 2.2). During title and abstract screening, 1029 articles were excluded. The full-text version of six articles could not be retrieved, one article was withdrawn from the publisher and 23 full-text articles were excluded based on language, leaving 200 articles eligible for assessment. During full-text assessment, 119 articles were excluded based on the predefined exclusion criteria (Figure 2.2). Some articles described the use of surgical navigation in the mandibular region and seemed to meet the inclusion criteria [59-72]. However, these articles were excluded because the authors did not report how the mandibular mobility was accounted for during the registration. Finally, 81 articles were included for analysis. Seven types of studies were identified in the articles: one study with a healthy volunteer [73], two simulation studies [74, 75], 24 case reports (≤ 2 patients) [42-44, 46, 54, 55, 76-93], 24 patient studies (≥ 3 patients) [1, 30, 94-115], 19 phantom studies [33, 41, 45, 47, 50, 116-129], three (animal) cadaver studies [130-132], and three animal studies [133-135]. Five articles used a combination of study types: a cadaver and patient study [136], a phantom and patient study [137], a cadaver and animal study [138], a phantom and volunteer study [139], and a combined phantom, volunteer and case study [140].

2.3.2 Applications of surgical navigation

Navigation is currently being utilized in different fields of mandibular surgery. In *oncologic surgery*, navigation is used to guide tumor resection and/or bone reconstruction [1, 42, 46, 83, 85, 92, 98, 101, 104, 106, 107, 110, 111, 136]. Often, the osteotomies and bone reconstruction are planned preoperatively based on CT and Magnetic Resonance Imaging (MRI) data. During surgery, navigation is used to determine the location of the osteotomies in the resection phase and the positioning of bone segments in the reconstruction phase.

In *orthognathic surgery,* small misalignments can lead to aesthetic and functional problems [51]. Therefore, surgical navigation is used to guide osteotomies and to reposition bone segments. Orthognathic procedures that use navigational technology include bimaxillary surgery [78, 79, 129], sagittal split ramus osteotomy [137], high oblique sagittal split osteotomy [95], intraoral vertical ramus gonioplasty [112], condyle resection [54, 88, 97, 109], mandibular angle reduction surgery [108, 113-115, 118, 120], condyle repositioning after Le Fort I osteotomy [102], and temporo-mandibular joint replacement [103].

In *foreign body removal surgery* of the mandible or pterygomandibular space, removal is complex when the foreign body is close to critical structures, such as the inferior alveolar nerve [43, 44, 55, 76, 77, 80, 81, 83, 84, 86, 89, 101]. In these cases, surgical navigation is used to determine the exact location of the
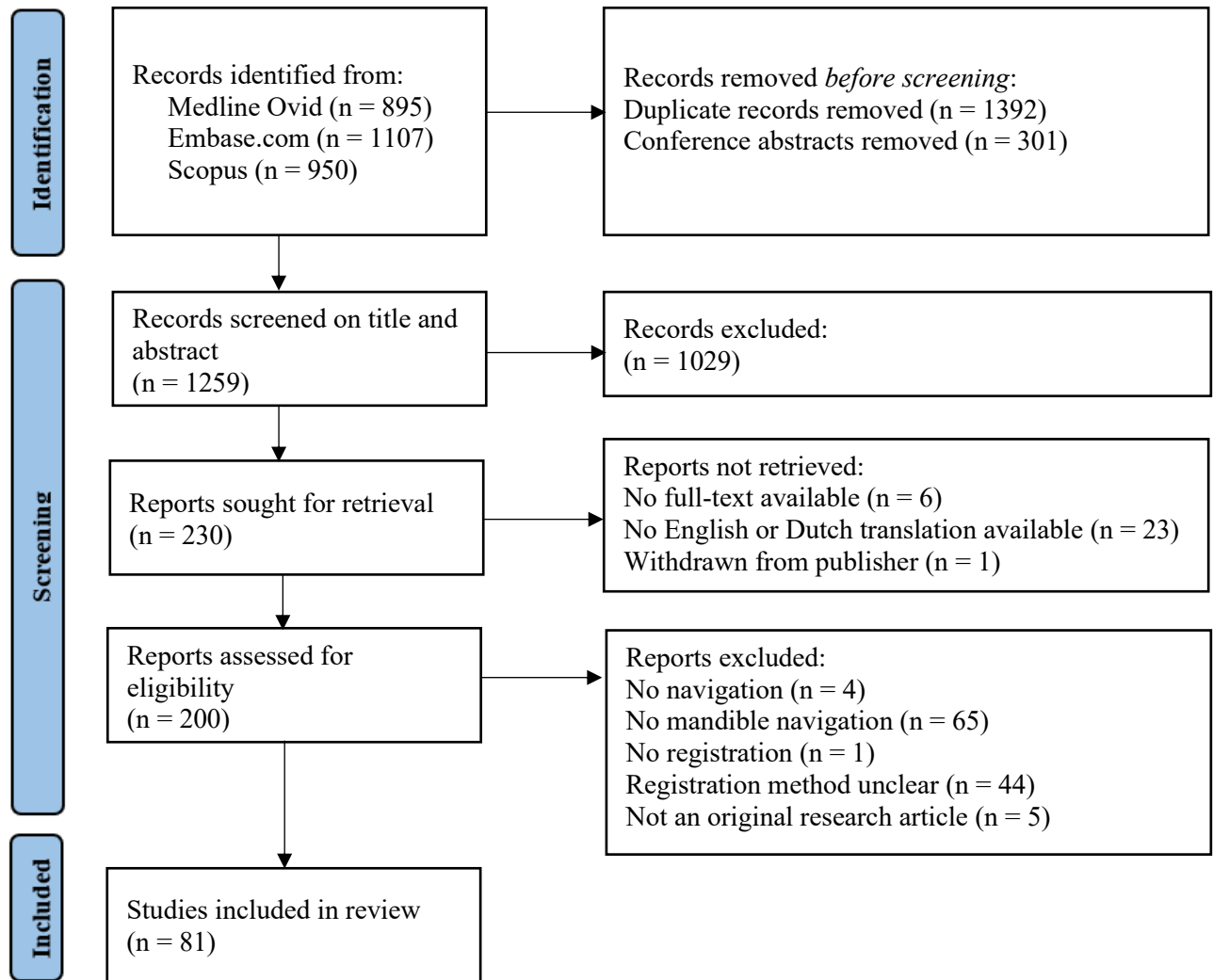
Figure 2.2 *PRISMA flowchart for the conducted literature search and article selection process.*

foreign body and to guide removal, while reducing the risk of secondary injury caused by nerve or blood vessel damage.

Finally navigation is used for *cyst removal* [87, 90], *guidance during osteosynthesis* [117], *removal of osteosynthesis material* [99], and *secondary mandibular reconstruction* [91].

2.3.3 Variants of surgical navigation

Three different variants of surgical navigation were used in the included articles: traditional navigation, augmented reality based navigation, and robotic navigation. Most articles used traditional navigation surgery, where surgical instruments and the patient's anatomy are visualized on a monitor in the OR [1, 30, 33, 41-45, 47, 50, 54, 55, 76-104, 106-112, 116, 117, 119, 121, 122, 125, 127, 131-134, 136-138]. The surgeon looks at the monitor for guidance during surgery. However, the need to observe the monitor negatively affects the eye-hand coordination of the surgeon [126].

To tackle this problem, together with recent progress in hardware, augmented reality (AR) has emerged as a new technology to guide the surgeon during complex operative procedures [46, 73-75, 105, 113-115, 118, 120, 126, 128, 135, 139, 140]. In AR, computer generated 3D images are superimposed onto the surgical area. Because of the co-display of the virtual surgical plan and real-time situation, the surgeon is able to utilize and interact with the components of both worlds simultaneously [73].

Navigation can also be performed robotically [120, 123, 124, 129, 130]. Surgeries of the mandible, especially mandible reconstruction surgery, can last eight hours or even longer [123]. Furthermore, surgeons often operate through the patient's mouth cavity resulting in a limited workspace [124]. Robot arms can help the surgeon to maintain the right position during surgical procedures and facilitate working in a narrow area [123]. Navigated robot arms can assist surgeons in various tasks such as drilling, sawing, and positioning of bone segments according to a virtual surgical plan [123, 129, 130]. Currently, research is conducted with autonomous robot systems, where the robot is the main operator of the surgery instead of being merely the assistant of the surgeon [123]. In these systems, a camera works as the surgeon's eyes, the robot works as the surgeon's hands, and a tracking system connects them working as the surgeon's brain [124].

2.3.4 Mandibular mobility problems

The mandible moves independently from the other craniofacial bones, which makes image-to-patient registration difficult [42]. Literature revealed that two strategies are currently being employed to tackle this 'mobility' problem: either keeping the mandible in the same position during preoperative imaging and surgery (41 articles), or attaching a dynamic reference frame (DRF) to the mandible that tracks the mandibular movements during surgery (41 articles) [43, 44]. For an overview which strategy was used in specific articles, see Table 2.1.

In the first approach, the mandible is fixed in a specific position during preoperative imaging and during surgery; the mandible is kept occluded against the maxilla, either with a dental splint or by intermaxillary fixation (IMF) with wires. Since the mandible now acts like a solid structure with the maxilla, common registration methods that are used in craniofacial surgery can be applied.

In the second approach, the mandible can move freely during surgery. By attaching a DRF to the mandible, e.g. a DRF with reflecting spheres or an EM tracked sensor, its movements are tracked. This method enables the surgeon to move the mandible during surgery.

2.3.5 Registration methods

Different methods can be used for image-to-patient registration. In the included articles, four main registration methods were used: point registration, surface registration, hybrid registration, and computer vision based registration. In the next paragraphs, these methods are explained alongside with their accuracy.

2.3.5.1 Registration accuracy

Registration accuracy is usually assessed in terms of the 'fiducial registration error' (FRE) or 'target registration error' (TRE) (Figure 2.3) [141]. The FRE, or 'image-to-tracker' error, is a measure of how closely the preoperative CT scan is registered to the patient [33, 47, 136]. The FRE is defined as the distance between the pinpointed registration points on the patient and the virtual registration points on the preoperative CT scan, after registration. The FRE is often calculated by the navigation system software. According to Maurer et al. [142], this distance (between n registration points) can be calculated as the root mean squared error (RMSE):

$$FRE = \sqrt{\frac{1}{N} \sum_{n=1}^{N}(x_{patient,n} - x_{ct,n})^2 + (y_{patient,n} - y_{ct,n})^2 + (z_{patient,n} - z_{ct,n})^2} \qquad 2.1$$

The TRE is a measure of how closely the location of virtual predefined target points (other than the registration points) correspond to their actual intraoperative location after registration [131, 141]. Usually, the TRE is measured with a tracked probe by pinpointing different landmarks on the mandible and comparing them to their locations in the preoperative CT scan [119, 131, 137]. For every target

point (*n*), the TRE can be calculated as the Euclidean distance (ED) between the location of the point on the patient and the point in the preoperative CT scan [142]:

$$TRE_n = \sqrt{(x_{patient,n} - x_{ct,n})^2 + (y_{patient,n} - y_{ct,n})^2 + (z_{patient,n} - z_{ct,n})^2} \qquad 2.2$$

The overall TRE (i.e. for multiple target points in an area of interest) can be calculated as the RMSE or the mean of the individual TREs [30, 45, 128].
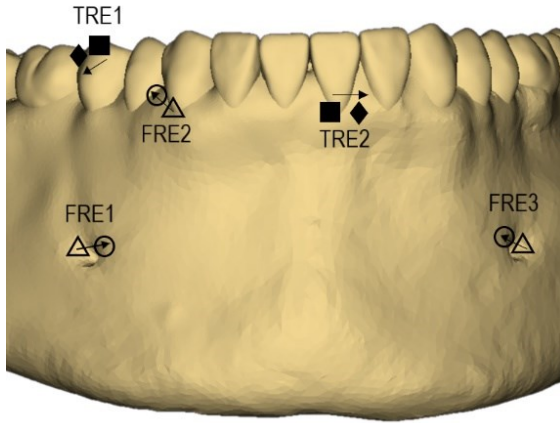

Figure 2.3 *Two types of errors to describe the accuracy of image-to-patient registration. The fiducial registration error (FRE) measured at each registration point is the distance between the position of the registration point on the patient (circle) and its counterpart on the virtual surgical plan (triangle), after registration. The target registration error (TRE) measured at a target point, other than the registration points, is the distance after registration between the position of the target point on the patient (check) and its counterpart on the virtual surgical plan (square).*

2.3.5.2 Point registration

In point registration, or point-to-point registration, a minimum of three points is required to register the preoperative imaging data with the patient [41]. Before surgery, specific points in the virtual surgical plan are chosen and their coordinates in 3D space are saved. During surgery, the surgeon touches these predefined points on the patient with a tracked probe. The coordinates of the virtual points are then matched to the coordinates of the actual points to complete the registration process [45]. Both anatomic landmarks and artificial markers can be used for point registration.

In the former method, registration is performed with anatomic landmarks that are clearly visible on both the preoperative imaging data and the patient during surgery. Often, tooth cusps or the mental or mandibular foramina are used as landmarks (Figure 2.4a) [47, 102, 119, 127]. Reported FREs and TREs ranged from 0 – 1.50 mm and 0.20 – 2.10 mm, depending on the tracking method, *ex vivo* or *in vivo* usage and the mandibular mobility (Table 2.1).

Alternatively, artificial markers can be attached to the patient for registration purpose, e.g. bone screws (Figure 2.4b). Alveolar bone screws can be placed at the outpatient clinic before surgery [88, 97, 100, 107, 109]. Next, preoperative CT scanning is performed and the locations of the screws are saved in the virtual surgical plan. During surgery, the screws are touched with a tracked probe to obtain their intraoperative positions and registration is performed automatically by the navigation software. Another way to use bone screws is by implanting them during surgery instead of in the outpatient clinic [30]. The exact location of the screws can be determined by performing a Cone Beam CT scan (CBCT) during

surgery. Reported FREs and TREs for using artificial bone markers ranged from 0 – 1.20 mm and 0 – 3.20 mm (Table 2.1).

A third way of using artificial markers is by incorporating them in a dental splint (Figure 2.4c). Markers, e.g. gutta-percha markers, notches or screws, can be attached to a splint preoperatively and the preoperative CT scan is acquired while the patient is wearing the splint [45, 101, 116]. Registration is performed the same way as with the earlier described artificial bone markers. Different types of splints can be used, either maxillomandibular splints that fixate the mandible against the maxilla or splints that are only attached to the mandible enabling mandibular movements during surgery [80, 137]. Moreover, maxillomandibular splints can put the mandible in an 'open' or in an 'occluded' position against the maxilla. In open splints, the polygon between the markers is often bigger than in closed splints, resulting in a better registration [50]. Reported FREs and TREs for using splint markers ranged from 0 – 1.00 mm and 0 – 1.47 mm (Table 2.1).

2.3.5.3 Surface registration
Surface registration is a marker-free registration method, using a series of points on anatomical surfaces, such as the facial skin contour (Figure 2.4d). Either an infrared laser surface scanner or a tracked probe can be used to capture the surface contours [83, 86]. Mostly, the periorbital and frontal facial areas are used for surface scanning [91, 92]. Reported FREs were < 1.00 mm and TREs ranged from 1.90 – 2.10 mm (Table 2.1).

Another potential area to apply surface registration is the mandibular bone surface itself, after removal of soft tissue (Figure 2.4e). In cases with facial swelling, trauma or incomplete imaging of the soft tissues, this can be an alternative to facial surface scanning [82]. Only two studies described the use of this method to perform registration. However, in the first study, the registration attempts failed due to an incongruence of the surfaces of the mandible [82]. The used laser scanner could only make a single scan and parts of the mandible were always covered with soft tissue. The other study used a tracked probe to sweep the surface of the mandible, resulting in a successful registration with a TRE of 1.00 mm (Table 2.1) [46].

2.3.5.4 Hybrid registration
Hybrid registration uses a combination of point registration and surface registration. Some articles started with point registration and used surface registration for optimization [42, 94, 96, 122]. For example, Badiali et al. [94] used point registration with the aim of obtaining a TRE < 3.0 mm, and continued with surface registration to obtain a final TRE ≤ 0.5 mm. Other articles started with surface registration and used point registration for refinement [55, 76, 86, 87]. For hybrid registration, the reported FREs were < 1.00 mm and TREs ranged from 0.10 – 4.00 mm (Table 2.1).

2.3.5.5 Computer vision based registration
In articles using augmented reality as navigation method, computer vision based registration methods were often used. These registration methods included automatic contour detection (marker-free) and automatic marker detection (marker-based).

Several articles used automatic contour detection methods to register the preoperative imaging data to the patient (Figure 2.4f) [73-75, 123, 124, 128, 139, 140]. Preoperatively, a two-dimensional (2D) contour model, from the lower teeth or mandible, is constructed from 3D imaging data. During surgery, the contour model is automatically matched with real-time images, obtained by stereo cameras or a single monochrome or color camera, and overlaid onto the surgical site [123]. The matching procedure is often based on a shape-based method for 2D-3D matching developed by Ulrich et al. [143], refined by an Iterative Closest Point (ICP) algorithm [74, 75, 140]. In these articles, registration accuracy was

reported in terms of TRE or overlay error, defined as the difference between the projected scene and actual scene [75]. The reported TREs ranged from 0.30 – 0.89 mm. The overlay error for image registration ranged from 0.34 – 0.75 mm and for image overlay from 0.23 – 1.01 mm (Table 2.1).

Another commonly used registration method in AR applications is registration by automatic marker detection (Figure 2.4g) [105, 113-115, 118, 120, 135]. In this method, AR software is used for the recognition of specific patterns (often black squares or a QR code) on a marker plate using a single camera or stereo cameras. When the software recognizes the pattern, automatic registration is performed and the marker plate is tracked in real-time. The marker plate is fixed to a dental splint as a fulcrum in order to keep the mandible and the marker in a permanent relationship. The reported TREs ranged from 0.95 – 1.89 mm (Table 2.1).

2.4 Discussion

The mandible plays a vital role in various functions. Hence, it is important to maintain or restore its shape and function after surgery [1]. Surgical navigation can be used to enhance the surgeon´s orientation within the surgical field and provide intraoperative guidance. To translate the virtual surgical plan to the intraoperative situation, accurate image-to-patient registration is vital [50]. However, due to the mobile character of the mandible with regard to the other craniofacial bones, registration is complex [42, 50]. As a result, surgical navigation is rarely used in the mandibular region in clinical practice. The aim of this systematic review was to provide an overview of the different registration methods that are used for navigated mandibular surgery.

In the studied articles, two different methods for accounting for the mandibular mobility were identified: either the mandible is kept in a fixed position, or the mandible can move freely and its movements are tracked. Casap et al. [42] used both approaches in the same patient and concluded that tracking mandibular movements results in a more precise registration than fixing the mandible against the maxilla. This is due to the fact that fixation needs to eliminate every possible movement of the mandible since even slight changes in mandible position negatively impact the navigation accuracy. Moreover, the ability to move the mandible is an advantage since the surgical working field can be enlarged by changing the mandible's position [42]. Especially in oncologic surgery with tumors involving multiple structures in the oral cavity, this is preferred to enable good visibility and accurate tumor resection.

Registration methods for navigated mandibular surgery can be divided into four main categories: point registration, surface registration, hybrid registration, and computer vision based registration. Every method has its limitations and strengths; this should be kept in mind when choosing a specific method. There is always a tradeoff between accuracy, registration time, usability, and invasiveness for the patient. For example, point registration with bone screws is often more accurate than with anatomic landmarks since the latter method is user dependent [119]. If a surgeon is asked to pinpoint the same anatomic landmark multiple times, the exact location varies slightly every time. In addition, in edentulous patients or in patients where the foramina are not visible during surgery it can be difficult to find three anatomic landmarks [30]. However, implanting bone screws during the outpatient clinic is invasive for the patient and, therefore, usually not the first choice. Implanting bone screws during surgery is also not preferred since a hybrid OR with a CBCT scanner is required to obtain the 'preoperative' imaging with screws so they can be used for registration [30]. This lengthens OR time and leads to extra ionizing radiation for the patient. Surface registration using points on the facial skin is more easy compared to using the mandibular bone surface, because with the latter method soft tissue attached to the bone needs to be removed first [82]. However, facial scanning results in a less accurate registration than bone matching. For hybrid registration multiple time consuming steps are required, which makes it a less user-friendly method. Registration with markers on dental splints is noninvasive
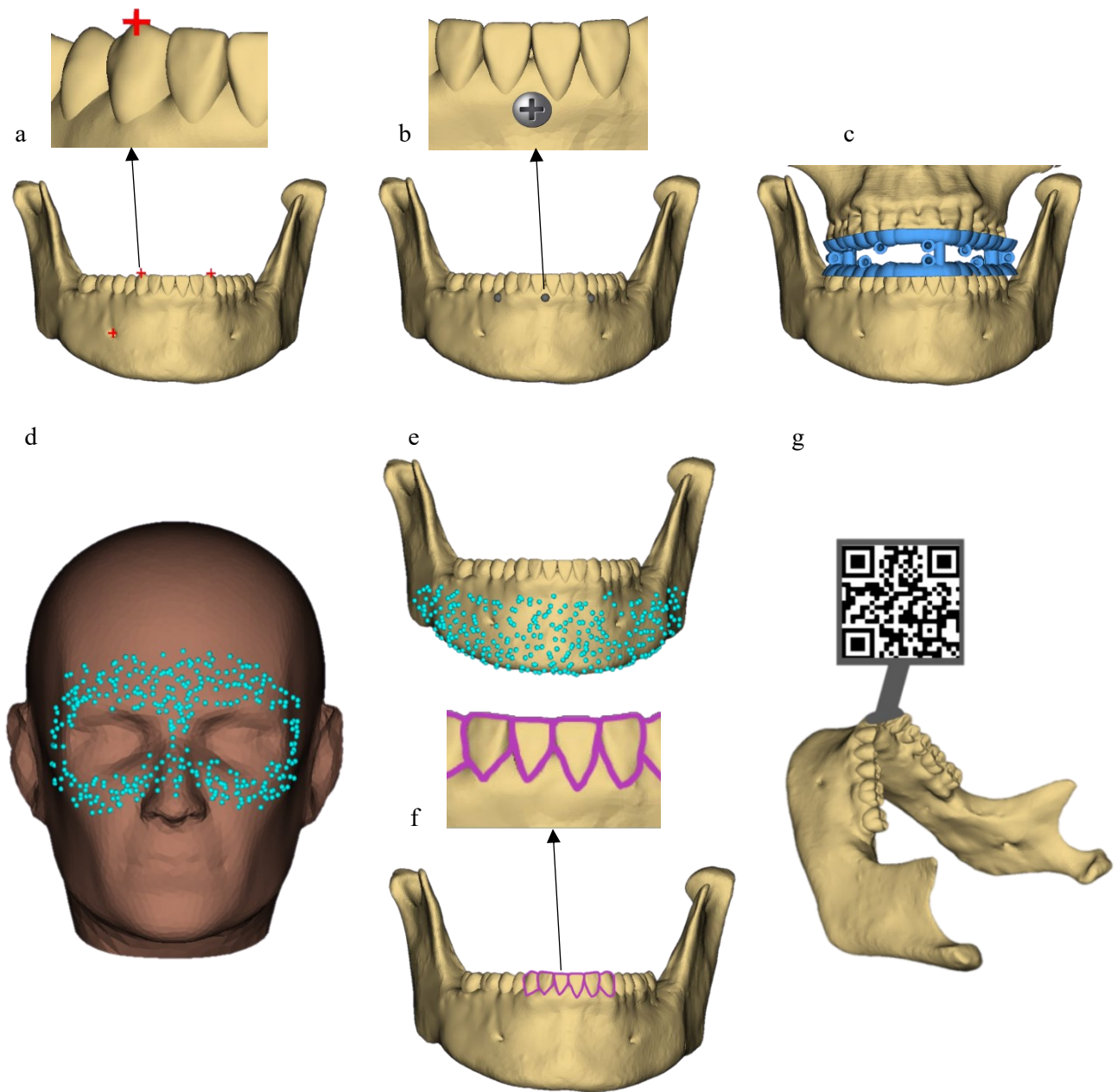
Figure 2.4 *Visualization of the different image-to-patient registration methods for surgical navigation of the mandible: a) point registration using anatomic landmarks, b) point registration using implanted bone screws, c) point registration using notches on a dental splint, d) surface registration using points on the facial skin contour, e) surface registration using points on the mandibular bone surface, f) computer vision based registration with automatic teeth contour detection, g) computer vision based registration with automatic marker detection.*

Table 2.1. Overview of different image-to-patient registration methods and reported accuracy ex vivo (phantom studies) and in vivo (patient, healthy volunteer, animal and cadaver studies) and total number of patients that were included in the articles for each registration method. The minimum and maximum mean values, which are reported in the articles, are reported in this table together with the corresponding standard deviation. If multiple experiments were performed in an article, e.g. experiments with different splints or number of registration points, the best results are reported in this table. The TRE values only include the TREs measured with target points on the mandible.

Registration method	Markers	Tracking method	Mandibular mobility	Registration time	Accuracy ex vivo mean (SD) in mm	Accuracy in vivo mean (SD) in mm	Total number of patients in articles	References
Point registration	Anatomic	EM	Mobile	Not reported	TRE: 2.10 (0.88)	Not reported	5	[95, 131, 138]
		Optic	Fixed	Not reported	Not reported	FRE: <1.00 TRE: 0.20 – 0.50	13	[104, 130]
			Mobile	Not reported	FRE: 1.50[a] TRE: 1.70 – 1.93	FRE: 0.70 (0.30) – 0.80	12	[43, 47, 102, 119, 127, 136, 137]
	Fiducial markers on bone	EM	Mobile	2-3 minutes	FRE: 0.40 (0.30)[b] – 0.73[b] TRE: 1.28[c] – 2.62[c]	FRE: 1.20 (1.10)[b] TRE: 2.60 (1.50)[c] – 3.20 (1.10)[c]	11	[61, 62, 87]
		Optic	Fixed	12 minutes	Not reported	FRE: 0.73 (0.14) – 1.04 TRE: ≤ 1.00	69	[77, 97, 107, 108, 117, 134]
			Mobile	Not reported	FRE: < 1.00 TRE: 0.86 – 1.76	TRE: ≤ 1.00	12	[41, 88, 93, 100, 109, 119, 125, 126, 133, 137]
	Fiducial markers on splint	EM	Mobile	Not reported	FRE: 0.36[b] TRE: 0.83[c]	TRE: 1.90[b]	1	[45, 79]
		Optic	Fixed	3-10 minutes	FRE: < 1.00 TRE: 0.50 – 1.47[b]	FRE: 0.31 – 1.00 TRE: 0.40 – 0.94[b]	31	[50, 54, 78, 80, 81, 84, 90, 101, 103, 112, 116, 121, 129]
			Mobile	Not reported	TRE: 0.98	TRE: < 0.50	9	[42, 89, 138]
Surface registration	Skin surface contour	Optic	Fixed	4-20 minutes	Not reported	FRE: < 1.00 TRE: 1.90 – 2.10	51	[44, 83, 85, 90-92, 98, 99, 106, 110, 111, 132]
			Mobile	Not reported	Not reported	FRE: < 0.70	4	[1]
	Bone surface	Optic	Mobile	Not reported	Not reported	TRE: 1.00	3	[46, 82]
Hybrid registration		EM	Fixed	10 minutes	Not reported	Not reported	3	[55, 86, 87]
		Optic	Fixed	Not reported	Not reported	FRE: < 1.00 TRE: 0.10 – 4.00	16	[42, 76, 94, 96]
			Mobile	Not reported	FRE: < 1.00	Not reported	0	[122]
Computer vision based registration	Contour matching	Optic	Mobile	3 seconds	TRE: 0.42 – 0.89[b] Overlay error: Image registration: 0.34 – 0.75 Image overlay: 0.23 – 1.01	TRE: 0.30[b]	1	[73-75, 123, 124, 128, 139, 140]
	Marker detection	Optic	Mobile	Not reported	TRE: 0.95 (0.14) – 1.89 (0.51)	Not reported	76	[105, 113-115, 118, 120, 135]

SD = standard deviation, EM = electromagnetic, FRE = fiducial registration error, TRE = target registration error, [a] median error, [b] root mean squared error, [c] Euclidean distance.

but splints are patient-specific, which requires separate fabrication for every single patient [116]. Moreover, to enable accurate registration, the splints should fit perfectly onto the teeth. This demands for skilled people and special equipment for fabrication [50, 120]. Furthermore, splints cannot be used in edentulous patients or patients with tooth loosening [50, 120]. The same applies for automatic teeth contour registration, although this is a quick and user-friendly method for surgeons. Another quick registration method is automatic marker detection. This method, however, requires complex and expensive software and is often unfavorable because of the bulky marker, which limits the surgical working space [123].

Apart from to the choice of registration method, users should also decide on which tracking method to use. EM tracking is often less accurate than optical tracking due to field distortions because of ferromagnetic materials in the vicinity of the EM field in the OR, e.g. the patient table [95]. However, for optical tracking a continuous line-of-sight between the optical camera and the tracked tools and tracked area is required, which limits the surgeon's movements and is, therefore, challenging in small working areas such as the oral cavity [30, 131]. In addition, EM trackers are usually much smaller in size compared to optical trackers.

Although this review provides an overview of different registration methods, the results should be interpreted carefully due to several reasons. First, the majority of the studied articles are phantom studies or case reports. From the number of included articles (81) it would seem that navigation is widely used in mandibular surgery. However, in only 26 articles navigation was used in three or more patients. This indicates that navigation in mandibular surgery is still under development.

Unfortunately, it was not possible to quantitatively compare the registration methods based on the reported accuracies. The majority of the articles described the used registration method, but did not report registration accuracy in terms of FRE [41, 42, 50, 78, 79, 90, 93, 94, 96, 99, 116, 119, 131, 137], TRE [1, 33, 43, 44, 47, 74-76, 98, 101, 103, 105, 107, 108, 112, 113, 115, 121-124, 126, 135, 136] or both [54, 55, 77, 80, 82-89, 91, 92, 95, 97, 100, 102, 104, 109-111, 117, 127, 129, 132, 138]. Another essential point is the way how the TRE is measured. In some studies the TRE was measured using anatomic landmarks [73, 78, 79, 90, 93, 94, 127, 130, 133, 134], while in other studies the TRE was measured using artificial markers [41, 45, 50, 114, 116, 118-120, 125, 128, 131, 139, 140] or using a combination of both [30, 42, 137]. Often, artificial markers yield a lower TRE as a result of more objective marker identification [30]. Furthermore, different formulas to calculate the FRE and TRE were used in the articles. Most articles reported the mean FRE and mean TRE, but some articles calculated the FRE or TRE in terms of RMSE or ED (Table 2.1). Due to these reasons, the reported accuracy of the described registration methods cannot be compared one-to-one. This should be taken in mind when interpreting the reported registration accuracy values.

This review does not report the surgical outcomes of the navigated procedures. Many studies reported the surgical outcomes in terms of 'image-to-image' error, surgical precision, osteotomy accuracy or reconstruction accuracy [1, 33, 47, 78, 79, 85, 91, 92, 94, 95, 102-108, 110-112, 114, 115, 121, 122, 124-126, 129, 131-134, 136-138]. To calculate these metrics, often a postoperative CT scan was registered with the preoperative CT scan (including the virtual surgical plan), and osteotomy planes or landmark positions were compared. Until recently, there was no golden standard for reporting accuracy of CAS in mandibular surgery [144]. Therefore, various distance and angular deviation metrics are used, which makes it impossible to compare the different studies [145]. In addition, beneficial surgical outcomes are not solely the result of an accurate registration. Several other factors can influence the surgical outcome, such as the surgeon's eye-hand coordination and the used sawing or drilling equipment. Due to these reasons, it was decided not to include surgical outcomes in this review.

Given the high technological complexity that comes with surgical navigation of the mandible, it can be challenging to find an optimal balance between the usability, registration time, accuracy, and invasiveness of a registration method. Future studies should focus on developing registration methods with an optimal balance between these metrics. In addition, the existing registration methods should be compared within the same study to enable quantitative comparisons between the accuracies of the methods. Also, there is a need for studies testing the applicability of the registration methods in larger patient studies since the majority of the included articles in this review are phantom studies and case reports. In future studies, we recommend to report the registration accuracy in terms of both FRE and TRE. In our opinion, the TRE of individual target points should be calculated as the ED and the overall TRE of a specific area of interest should be calculated as the RMSE of the individual TREs since large individual errors are penalized more severely in RMSE calculation compared to mean calculation.

Chapter 3

Introduction to hybrid registration for mandible navigation

In this chapter, a noninvasive registration method for mandible navigation is explained as introduction to Chapters 4, 5, and 6. In addition, the used navigation system is explained.

3.1 Navigation system

In this thesis, surgical navigation is performed using 3D Slicer software (https://www.slicer.org) in combination with the Aurora V2 electromagnetic (EM) tracking system (Northern Digital Inc., Waterloo, Canada) consisting of a sensor interface unit (SIU), sensor control unit (SCU), field generator (FG), and a host computer. A 6 degrees-of-freedom (DOF) EM sensor is used for tracking of the mandible and a 6DOF EM surgical probe is used by the surgeon to perform the registration procedure (Figure 3.1) [146]. 3D Slicer is an open-source software platform for research applications in medical imaging [147]. Surgical navigation is performed with the extension 'SlicerIGT', which provides a toolkit for image-guided and navigated interventions [148]. The PLUS Toolkit (https://plustoolkit.github.io/) is used to synchronize the data streams from the EM sensor and the EM probe and to send them to 3D Slicer in real-time via a network communication protocol called 'OpenIGTLink' (http://www.openigtlink.org/) [149, 150]. An overview of the communication between the software and hardware components is visualized in Figure 3.2.

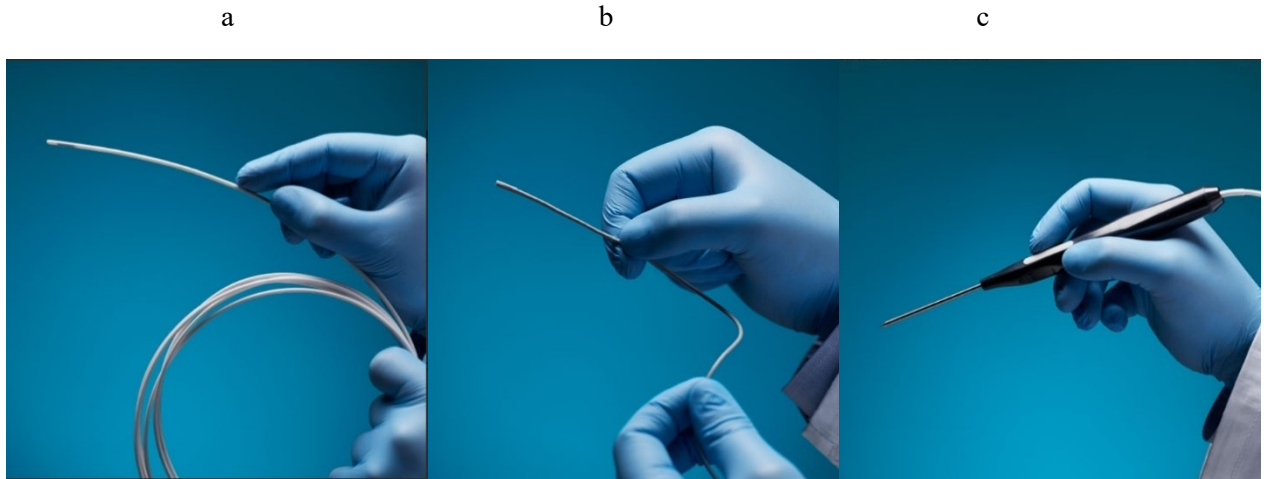a   b   c

Figure 3.1 *a) Aurora 6DOF sensor 'flex tube', b) Aurora 6DOF sensor 'cable tool', c) Aurora 6DOF surgical probe [146].*
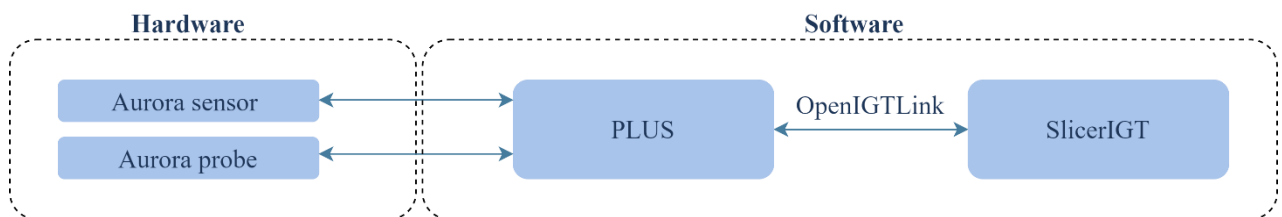

Figure 3.2 *Communication between hardware and software components of the used navigation system for mandible navigation in the NKI-AvL.*

3.2 Registration

Image-to-patient registration is used to align the preoperative imaging data, including the virtual surgical plan, with the patient in the operating room (OR). The location and orientation of the patient is determined by the electromagnetic tracking system (EMTS) using a reference EM sensor that is attached to the mandible. Currents from the reference sensor are detected by the FG, resulting in the transformation $^{EMTS}T_{Ref}$. The aim of image-to-patient registration is to find the correspondence between points on the patient in EMTS coordinates (^{Ref}p) and corresponding points in the CT scan (^{CT}p). This is obtained with Equation 3.1:

$$^{CT}p = {}^{CT}T_{EMTS} * {}^{EMTS}T_{Ref} * {}^{Ref}p \qquad\qquad 3.1$$

To obtain $^{CT}T_{EMTS}$, mutual information from the patient and the preoperative CT scan is required. This transformation can be calculated through registration of corresponding points on the patient and the CT scan. In this thesis, a hybrid registration method is employed consisting of two steps: 1) point registration; performed for initialization using three anatomic landmarks on the mandible ($^{CTinit}T_{EMTS}$) and 2) surface registration; performed for optimization using the surgically exposed mandibular bone surface after removal of soft tissue ($^{CT}T_{CTinit}$). Combined, these registrations result in Equation 3.2:

$$^{CT}T_{EMTS} = {}^{CT}T_{CTinit} * {}^{CTinit}T_{EMTS} \qquad\qquad 3.2$$

The registration points on the patient, needed for initial and final registration, are collected with the tip of the surgical probe. Currents from the probe are detected by the FG, resulting in transformation $^{EMTS}T_{Probe}$. The relation between the location and orientation of the tip of the probe and the reference sensor on the mandible ($^{Ref}T_{Probe}$) is calculated with Equation 3.3:

$$^{Ref}T_{Probe} = {}^{EMTS}T_{Ref}^{-1} * {}^{EMTS}T_{Probe} \qquad\qquad 3.3$$

Equation 3.4 shows the transformation of a point on the patient pinpointed with the tip of the probe ($^{Probe}p$) to the same point in the preoperative scan (^{CT}p) by combining Equations 3.1 to 3.3:

$$^{CT}p = {}^{CT}T_{EMTS} * {}^{EMTS}T_{Ref} * {}^{Ref}T_{Probe} * {}^{Probe}p \qquad\qquad 3.4$$

An overview of the transformations used in the registration procedure is shown in Figure 3.3.
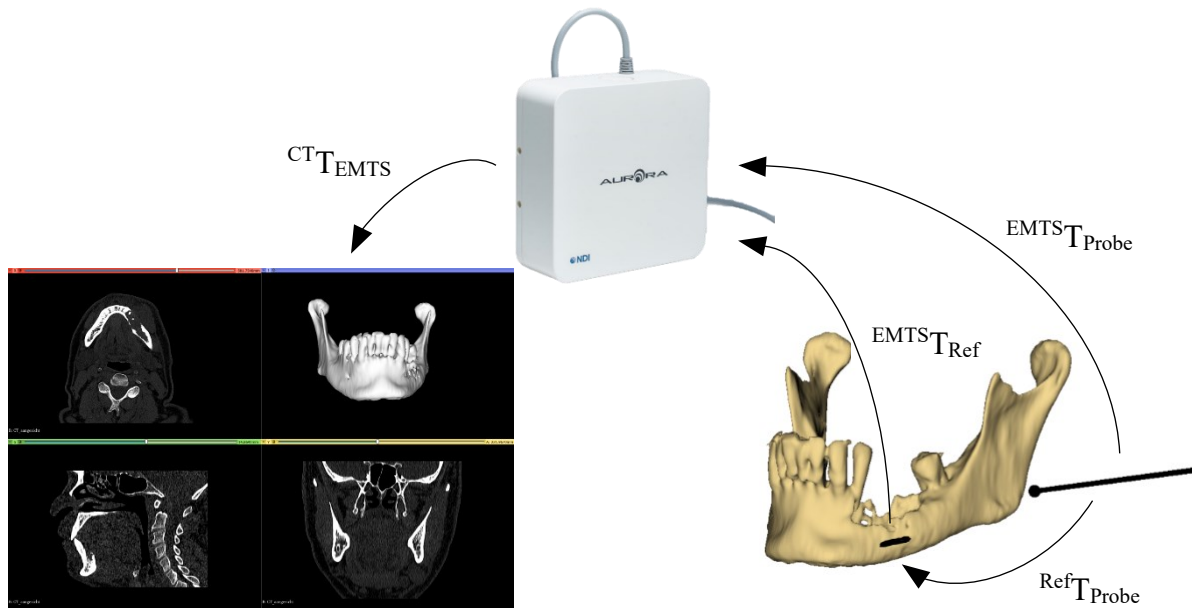

Figure 3.3 *Overview of the required transformations in the registration procedure performed in this thesis.*

3.3 Navigational workflow

The navigational workflow, used in this thesis, consists of several preoperative, intraoperative, and postoperative steps (Figure 3.4).

Preoperatively, virtual surgical planning is performed with the available CT scan of the mandible*. A 3D model is constructed from the CT scan by segmenting the bone with intensity based thresholding. Three anatomic landmarks on the mandible are chosen that will be used for registration during surgery. Also, landmarks are chosen that will be used for validation during surgery. The coordinates of these registration and validation landmarks on the CT scan are saved in 3D Slicer.

Intraoperatively, the software and hardware components are set up and a 6DOF EM sensor is fixated to the mandible with a sensor applicator and screws (Chapter 4). First, the FG is positioned against the back of the head (Figure 3.5). Then, the sensor is fixated onto a part of the mandible that is removed during surgery to prevent screw holes in the remaining bone. After sensor fixation, the surgical probe and the sensor are connected with the SIU. The software program 'NDI Track' (Northern Digital Inc, Waterloo, Canada) is used to check whether the sensor and probe are positioned within the EM field and to check their tracking accuracy (the error provided by NDI Track should be < 0.2). NDI Track is shut down, and the 'PLUSServer' from the PLUS Toolkit is activated to collect the information from the sensor and the probe in real-time. 3D Slicer is initiated and the tracking information from the PLUSServer is loaded into 3D Slicer using 'OpenIGTLink' from the SlicerIGT extension. Now, initial registration can be performed; the surgeon pinpoints the three registration landmarks with the probe and their locations are saved in 3D Slicer. These points are rigidly registered with their corresponding virtual locations in the preoperative CT scan with the 'Fiducial Registration Wizard' module. The CT scan, including the virtual surgical plan, is now roughly aligned with the patient ($^{CTinit}T_{EMTS}$). Next, the initial registration is optimized by performing a surface registration. The probe is swept over the surgically exposed mandibular bone surface to capture surface points (the number of points varies in Chapters 5 and 6). These points are rigidly registered with the 3D model using the 'Fiducials-Model Registration' module in 3D Slicer by applying an Iterative Closest Point (ICP) algorithm with 100 iterations ($^{CT}T_{CTinit}$). Finally, validation measurements are performed.

Postoperatively, the registration accuracy is calculated from the validation measurements**.

When navigation is used to position a navigated cutting guide, the determination of the locations and orientations of the osteotomy planes should also be included in the virtual surgical planning procedure.

*** When navigation is used to perform osteotomies or to guide the surgeon in another way during surgery, the registration accuracy should be determined intraoperatively, directly after registration. In this thesis, navigation was used to perform and assess (a new) registration (method), not to perform osteotomies or to provide guidance for the surgeon. Therefore, the accuracy could be determined postoperatively.*

Preoperative

Acquisition of preoperative imaging

↓

Segmentation and 3D modelling

↓

Choose anatomic landmarks and validation points

Intraoperative

FG positioning and sensor placement

↓

Connect sensor and probe, check tracking accuracy in NDI Track

↓

Start PLUS server

↓

Start 3D Slicer, load tracking information via OpenIGTLink

↓

Point registration

↓

Surface registration

↓

Validation measurements

Postoperative

Calculate registration accuracy

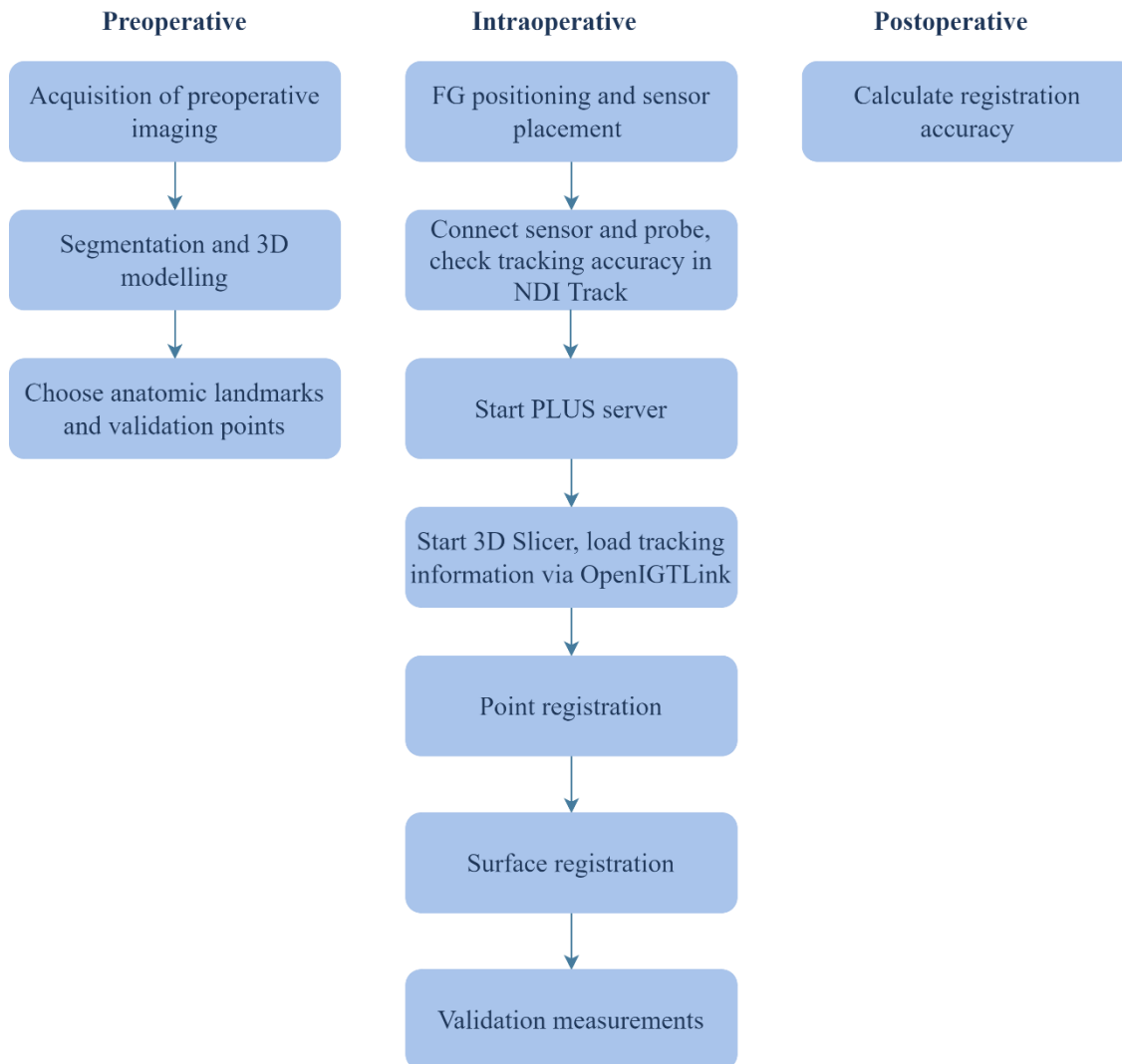*Figure 3.4* *Overview of preoperative, intraoperative, and postoperative steps of the surgical navigation procedure conducted in this thesis. 3D = three-dimensional, FG = field generator, NDI = Northern Digital Inc.*
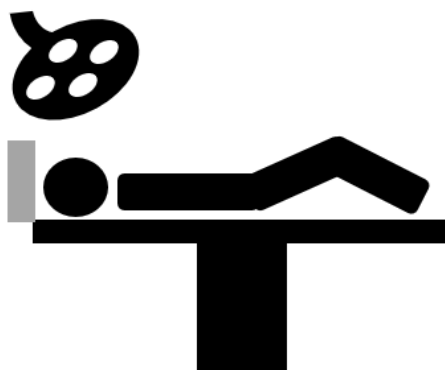

Figure 3.5 *Schematic overview of the position of the field generator (in grey) during surgical navigation of the mandible.*

Chapter 4

Design of a sensor applicator for mandibular tracking

4.1 Problem definition

To enable surgical navigation of the mandible, a 6 degrees-of-freedom (DOF) electromagnetic (EM) sensor should be attached to the mandible to track its movements. In previous research by Brouwer de Koning et al., a three-dimensional (3D) printed sensor applicator was used to fixate a reusable 1.4 mm diameter x 200 mm long Aurora sensor 'flex tube' (Northern Digital Inc., Waterloo, Canada) to the mandible during navigated surgery (Figure 4.1a) [30]. In this study, the applicator was attached to the bone with two 2.0 mm diameter x 9.0 mm long titanium screws (KLS Martin, Tuttlingen, Germany) (Figure 4.1b). Subsequently, the sensor was folded into the applicator. After surgery, the applicator was thrown away and the flex tube was cleaned, disinfected, and sterilized for reuse.

In the described applicator, the sensor can move both by a roll rotation and a translation in the x direction (Figure 1.10) resulting in inaccurate navigation. Moreover, the cable of the sensor is fragile and often breaks after 3 to 6 use cycles. Therefore, another 6DOF EM sensor is preferred for usage during surgery; the 2.5 mm diameter x 200 mm long Aurora 'cable tool' (Northern Digital Inc., Waterloo, Canada). This sensor is thicker and more robust compared to the flex tube and has the same tracking accuracy (Figure 3.1b); it is already being used by another department of the NKI-AvL for navigation during liver surgery. The cable tool can only be used once since the tip of the tool contains a lumen disabling appropriate cleaning. If the tip of the tool is glued into an applicator or a device that prohibits contact of the tip with the patient, this device is cleanable and could be reused. Such a device is already being used during navigated liver ablations in the NKI-AvL.

For the cable tool, a new applicator had to be designed that prevents movement in all directions. This applicator was designed quickly since we wanted to use the applicator as soon as possible. Therefore, the design process itself was limited.

a   b

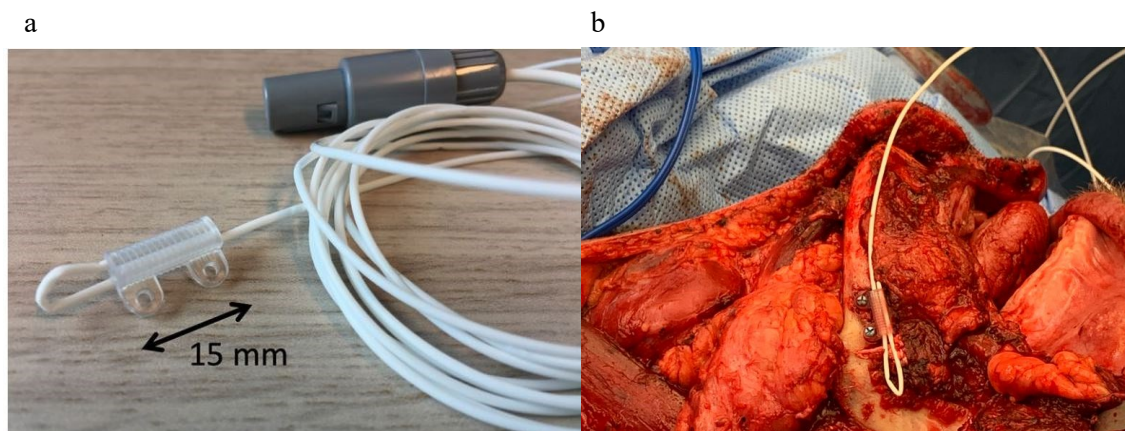*Figure 4.1* a) Current sensor applicator with sensor attached, b) sensor attached to the mandible during surgery in the NKI-AvL [30].

4.2 Design requirements

The proposed sensor applicator should fulfil the requirements listed in Table 4.1. This list was created in consultation with a head and neck surgeon and an employee of the department of Clinical Physics and Medical Devices in the NKI-AvL.

Table 4.1 *List of requirements for an applicator that fixates a 6DOF EM sensor to the mandible during navigated surgery.*

Category	Number	Requirement	Importance
Usability	1	Small in size (max. 20 x 15 x 15 mm) in order to fit onto the mandibular bone surface	Moderate
	2	Attachable/detachable in 5 minutes without damaging the sensor	Moderate
Materials	3	Non-ferromagnetic to prevent EM field distortion	High
	4	Biocompatible and sterilizable with STERRAD or autoclave*	High
	5	Should not break during attachment, usage, and detachment	Moderate
	6	Preferably printable with Formlabs Form 3B 3D printer since this printer is already available in the NKI-AVL	Low
Design	7	Does not contain lumens or sharp edges that can lead to improper disinfection and sterilization	High
	8	Has no sharp edges that can potentially damage gloves or sterile covers	Moderate
	9	Enables reuse of the cable tool	Moderate
Result	10	Fixates the sensor in all 6DOFs	High

* In the NKI-AvL two types of sterilization are available: STERRAD sterilization, which is performed in-house, or (steam) autoclave sterilization, which is performed at an external company.

4.3 Design concepts

Three design concepts were developed and 3D computer-assisted design (CAD) models were created. These concepts are introduced below and were evaluated in a Harris profile (Table 4.2). In each concept, the applicator is attached to the bone with two screws since the surgeons are already familiar with this method from the current applicator and this method provides robust fixation.

Design concept 1: Two part stud-and-tube applicator

This sensor applicator consists of two parts: a disposable base block with two screw holes and a reusable sensor block in which the sensor is glued. The sensor block is attached to the base block with a stud-and-tube interference fit (Figure 4.2).
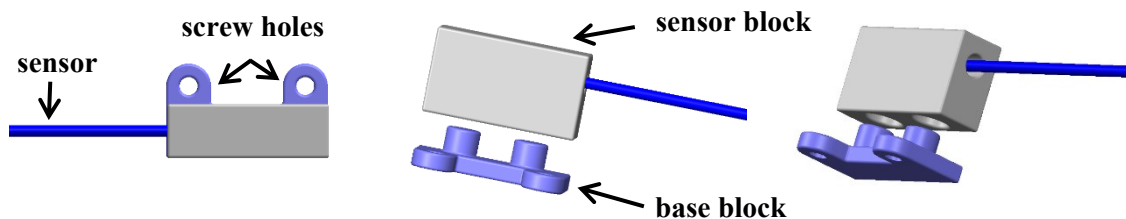

Figure 4.2 *CAD model of design concept 1: two part stud-and-tube applicator.*

Design concept 2: Block applicator

This sensor applicator consists of a single part; the sensor is glued into the applicator (Figure 4.3). This applicator is reusable.
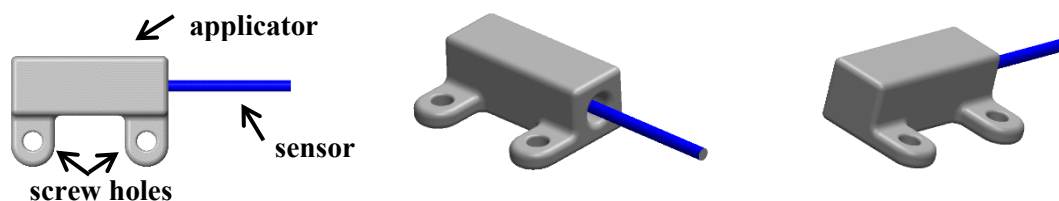

Figure 4.3 *CAD model of design concept 2: block applicator.*

Design concept 3: Clamp applicator

This sensor applicator consists of a single part; the sensor is clamped into the applicator by tightening the fixation screws (Figure 4.4). This applicator (including the sensor) is disposable.
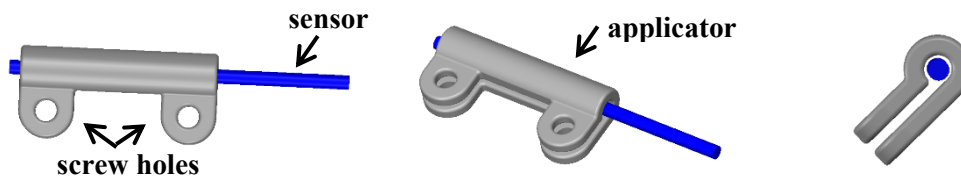

Figure 4.4 CAD model of design concept 3: clamp applicator.

Table 4.2 *Harris profile of three design concepts.*

Requirement	Design concept 1				Design concept 2				Design concept 3			
Score	-2	-1	+1	+2	-2	-1	+1	+2	-2	-1	+1	+2
1. Small in size			■					■				■
2. Easy in use, no sensor damage				■				■				■
3. Non-ferromagnetic				■				■				■
4. Biocompatible and sterilizable				■				■				■
5. Should not break during usage		■	■			■	■			■	■	
6. Printable with Form3B			■					■				■
7. No lumens		■						■				■
8. No sharp edges				■				■				■
9. Cable tool can be reused				■		■					■	
10. No movement of sensor				■				■			■	

Based on the Harris profile, design concept 1 scored 15 points, design concept 2 scored 19 points, and design concept 3 scored 14 points. Therefore, design concept 2 was chosen for further development.

4.4 Final design

Drawings of the final design of the sensor applicator with dimensions are shown in Figure 4.5. It is a simple design and the attachment method to the bone is similar to the currently used applicator by using two 2.0 mm diameter x 9.0 mm long titanium screws. The edges of the applicator are rounded to minimize the risk that dirt and bacteria will remain after the cleaning and sterilization process and to prevent rupture of gloves or sterile covers during surgery.
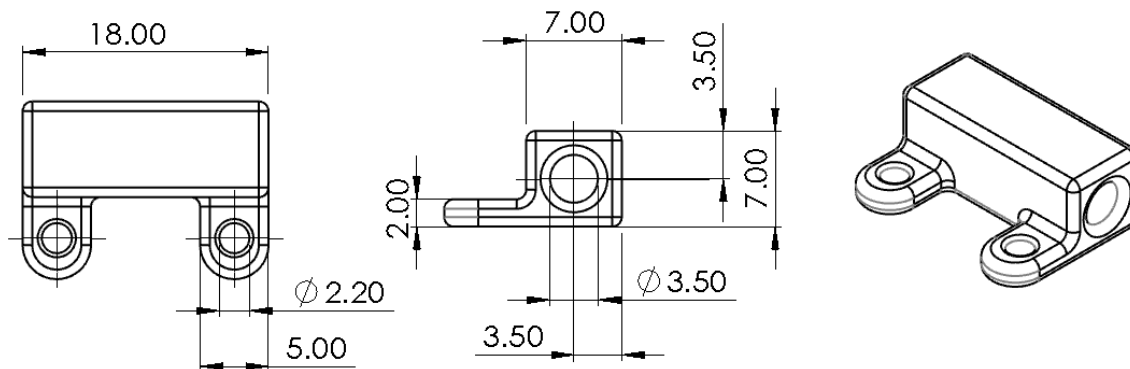

Figure 4.5 Design drawings of the sensor applicator with dimensions in mm; the edges are rounded, the tolerance for all dimensions except the screw holes is 0.10 mm, the screw holes should have a clearance fit (H7/h6) .

4.5 Materials and manufacturing process

The applicator can be manufactured in-house with the Formlabs Form3B printer using BioMed Clear Resin. This is a biocompatible USP Class VI certified material that is suitable for medical applications that require wear resistance over time and has been developed in compliance with EN ISO 13485:2016 and EN ISO 14971:2012 [151]. BioMed Clear Resin is compatible with chemical disinfection with 70% Isopropyl Alcohol for 5 minutes and with common sterilization methods (Table 4.3).

The cable of the Aurora cable tool is made from silicone rubber. Therefore, the glue should be both adhesive to the 3D printed material and the silicone of the sensor. Two possibly suitable silicone based glues are available in the NKI-AvL; NuSil (Nusil Technology LLC, Carpinteria, California, USA) and Elastosil E41 (Wacker Chemie AG, München, Germany). NuSil is being used by the department of facial prosthetics in the NKI-AvL for the manufacturing of nasal and ear prostheses. This is a biocompatible glue. Elastosil is used by the department of Surgical Oncology in the NKI-AvL for the manufacturing of 3D printed devices for surgery and its applicability was already tested for the purpose of gluing the Aurora cable tool into a 3D printed device from BioMed Clear Resin. Therefore, it is expected that Elastosil will be appropriate for the gluing of our applicator as well. Elastosil is non-biocompatible.

Table 4.3 Sterilization compatibility of BioMed Clear Resin, information retrieved from [151].

Sterilization method	Instructions
E-beam	35 kGy E-beam radiation
Ethylene Oxide	100% Ethylene oxide at 55 °C for 180 minutes
Gamma	29.4-31.2 kGy gamma radiation
Steam sterilization	Autoclave at 134 °C for 20 minutes, autoclave at 121 °C for 30 minutes

4.6 Next steps

A prototype of the applicator was 3D printed with (non-sterilizable) Clear V4 Resin, since BioMed Clear Resin was not yet available in the NKI-AvL. The Aurora cable tool was glued into the applicator with Elastosil. This prototype was used for the phantom experiments in Chapters 5 and 6.

The next step is to obtain approval for use of the new applicator from the Central Sterilization Department (CSD) of the NKI-AvL (see Appendix II for the application form). The department of Surgical Oncology has previously requested approval from the CSD for a 3D printed device for surgery that uses the same materials (BioMed Clear Resin, Aurora Cable Tool, Elastosil glue). Therefore, it was decided to wait for their approval before submitting our application form to the CSD. If the CSD approves the new applicator, BioMed Clear Resin should be purchased and a prototype should be manufactured. The 3D printing process will be as recommended by Formlabs [151]. After printing, the sensor will be glued into the applicator.

The prototype should be evaluated in terms of sterilization compatibility and usability. Since the cable of the Aurora cable tool cannot withstand temperatures higher than 70 °C, autoclave sterilization is not suitable. Therefore, STERRAD sterilization should be used since temperatures do not exceed 50 °C in this process. STERRAD is a chemical sterilization method exploiting the synergism between hydrogen-peroxide and low temperature gas plasma (an excited or ionized gas) to destroy microorganisms. After sterilization, no toxic residues remain on the sterilized items [152]. The suitability of STERRAD sterilization for the materials from which the proposed applicator is manufactured, should be evaluated by the CSD. Next, usability tests should be performed. The applicator should be screwed onto a

mandible phantom ten times (arbitrarily chosen) to evaluate if the material does not break when tightening the screws. The 3D printed material can become brittle when repeated sterilization occurs. Therefore, the attachment of the applicator to the mandible should be tested *ex vivo* with a 'test applicator' before applicators are manufactured for *in vivo* usage in patients during surgery. If the material breaks during *ex vivo* testing, the sensor applicator should be manufactured from a different material. A more robust alternative to 3D printing with BioMed Clear Resin would be 3D printing with (non-ferromagnetic) titanium or injection moulding with a biocompatible plastic.

Chapter 5

Evaluating the optimal approach for hybrid registration of the mandible: a phantom study

A.F. de Geer, M.J.A van Alphen, C.L. Zuur, A.J. Loeve, R.L.P. van Veen, M.B. Karakullukcu

5.1 Introduction

During mandible reconstruction surgery, computer-assisted surgery (CAS) techniques are routinely applied [153]. Preoperatively, a three-dimensional (3D) model of the mandible is constructed from a Computed Tomography (CT) scan. Next, the positions and orientations of the osteotomies are planned virtually to ensure adequate tumor margins and an accurate fit of the bone segments needed for reconstruction. During surgery, the virtual surgical plan is translated to the patient using 3D printed patient-specific cutting guides [29, 31]. However, these cutting guides are not ideal. The most important shortcoming is their lack of adaptability: if the intraoperative situation is different than expected, the surgical plan cannot be adapted. Moreover, the design and fabrication process of such cutting guides is costly and often takes several weeks. In the meantime, tumor progression can occur in which case the produced cutting guides cannot be used because the virtually planned margins will be inadequate [30, 47].

A possible solution to overcome these problems is to use universal, navigated cutting guides that can be adapted for any patient [33]. The preoperative planning is similar to the current workflow. However, during surgery, the cutting guides are positioned on the bone using surgical navigation. This enables the surgeon to change the surgical plan shortly before or even during surgery. To enable navigation, accurate alignment of the preoperative CT scan, including the virtual surgical plan, with the patient in the operating room (OR) is required, i.e. image-to-patient registration [42].

Two main registration methods exist for navigated (maxillofacial) surgery: point registration and surface registration [40]. In point registration, at least three distinct points are required to register the preoperative CT scan with the patient [41]. The surgeon pinpoints these points on the patient with a tracked probe and their coordinates are matched with the corresponding points on the CT scan. Both anatomic landmarks and artificial markers can be used as registration points. In neurosurgery, artificial markers implanted in the cranium are commonly used [154]. Surface registration is a marker-free method using a series of points on anatomical surfaces such as the facial skin contour. In surgery of the sinonasal cavity, the periorbital and frontal facial skin areas are often used for registration; the surgeon captures 200-300 surface points with an infrared laser surface scanner or a tracked probe that are registered to the 3D model [155, 156].

Although navigation is commonly used in maxillofacial surgery, its use in mandibular surgery is limited since the registration procedure is complex due to the mobile character of the mandible [42]. During navigation, the mandible should either be kept in a fixed position or its movements should be tracked. The first method is known to be prone to errors since even minor movements of the mandible decrease the navigation accuracy [42]. The latter method is currently being used for dental implant surgery [157-159]. These navigation systems use optical tracking with a large patient tracker that requires a continuous line-of-sight. This continuous line-of-sight, however, is difficult to guarantee during oncologic surgery with large tumors invading the oral cavity since the surgical working space is limited. In electromagnetic navigation (EM), patient trackers are smaller and no line-of-sight is required. EM tracking is currently being researched by others for its use in orthognathic surgery [160, 161].

In two prior studies, our research group investigated EM based navigation of the mandible using different point registration methods; registration with screws inserted in the alveolar bone or with notches on a dental splint [30, 45]. However, these registration methods were either invasive or required a complex and time consuming fabrication process preoperatively. In the current study, a simple, noninvasive registration method using a hybrid technique is proposed and evaluated, consisting of two phases: 1) point registration; performed for initialization by using anatomic landmarks on the mandible, i.e. teeth or mental foramen, and 2) surface registration; performed for optimization using the surgically

exposed bone surface of the mandible after removal of soft tissue. Using phantom experiments, the feasibility of this hybrid registration technique for EM navigated surgery of the mandible was assessed. Various configurations were investigated to determine the optimal approach for accurate registration. Target registration error (TRE) values of < 2.0 mm were considered as clinically acceptable [46].

5.2 Methods

5.2.1 Phantoms

Three mandible phantoms (one dentate mandible, two (partially) edentulous mandibles with atypical anatomy based on CT scans from patients treated in our institute) were 3D printed using a Form3B printer using Clear V4 resin (Formlabs, Sommerville, Massachusetts, USA). Reference notches were added at two intended osteotomy locations; for the dentate phantom two frequently occurring locations were chosen, for the edentulous phantoms, the actual intended osteotomy locations at time of surgery were used (Figure 5.1). The notches were designed to fit an EM trackable probe (Northern Digital Inc., Waterloo, Canada); the inner surfaces of the notches were cone shaped with a maximum diameter of 3.0 mm that equals the largest diameter of the probe. A CT scan was acquired for each phantom with 0.60 mm slice thickness (Siemens Somatom Confidence, Siemens Healthineers, Erlangen, Germany).

5.2.2 Navigation system

An EM tracking system (Aurora V2, Northern Digital Inc., Waterloo, Canada) in combination with 3D Slicer software (https://www.slicer.org/) was used to perform the navigation. 3D Slicer is an open-source software platform for research applications in medical imaging [147]. 3D Slicer was connected to the EM tracking system by using 'PLUS' (https://plustoolkit.github.io/) and 'OpenIGTLink' (https://openigtlink.org/) [149, 150]. The 'SlicerIGT' extension was used to perform the registration and validation procedure [148].

To track the position of the mandible during the experiments, a 6 degrees-of-freedom (DOF) EM tracked sensor (Aurora cable tool, Northern Digital Inc., Waterloo, Canada) was used. To attach the sensor to the phantoms, an applicator was developed and 3D printed with the Form3B printer, again using Clear V4 resin. The sensor was glued (Elastosil, Wacker Chemie AG, München, Germany) into the applicator and the applicator was attached to the phantoms with two 1.5 mm diameter x 5.0 mm long titanium screws (Drill-Free maxDrive, KLS Martin, Tuttlingen, Germany) (Figure 5.2). During surgery, the sensor is attached to bone that is removed to prevent damage from the screw holes in the remaining mandible. Therefore, to simulate intraoperative use, the sensor was attached to the phantoms between the osteotomy planes. The phantoms were positioned such that the distance between the sensor and the EM field generator was approximately 25 cm, similar to intraoperative use.

5.2.3 Workflow

For each phantom, a 3D model was constructed from the CT scan in 3D Slicer by segmentation with thresholding. Next, three anatomic landmarks, visible on both the CT scan and the phantom were chosen and their coordinates on the CT scan were saved. The registration procedure consisted of two steps: initial registration with the anatomic landmarks (point registration) and final registration with mandible surface points (surface registration). The initial registration points were pinpointed on the phantom using an EM tracked probe. The coordinates of these points were matched with their CT coordinates by a rigid transformation using the 'Fiducial Registration Wizard' module in 3D Slicer. Next, the probe was swept over the phantom surface to capture surface points (the number of points varied in the experiments). These points were rigidly registered with the 3D model using the 'Fiducials-Model Registration' module, by applying an Iterative Closest Point (ICP) algorithm with 100 iterations.

a

Plane 1

Plane 2

b

Plane 1

Plane 2

c

Plane 1

Plane 2
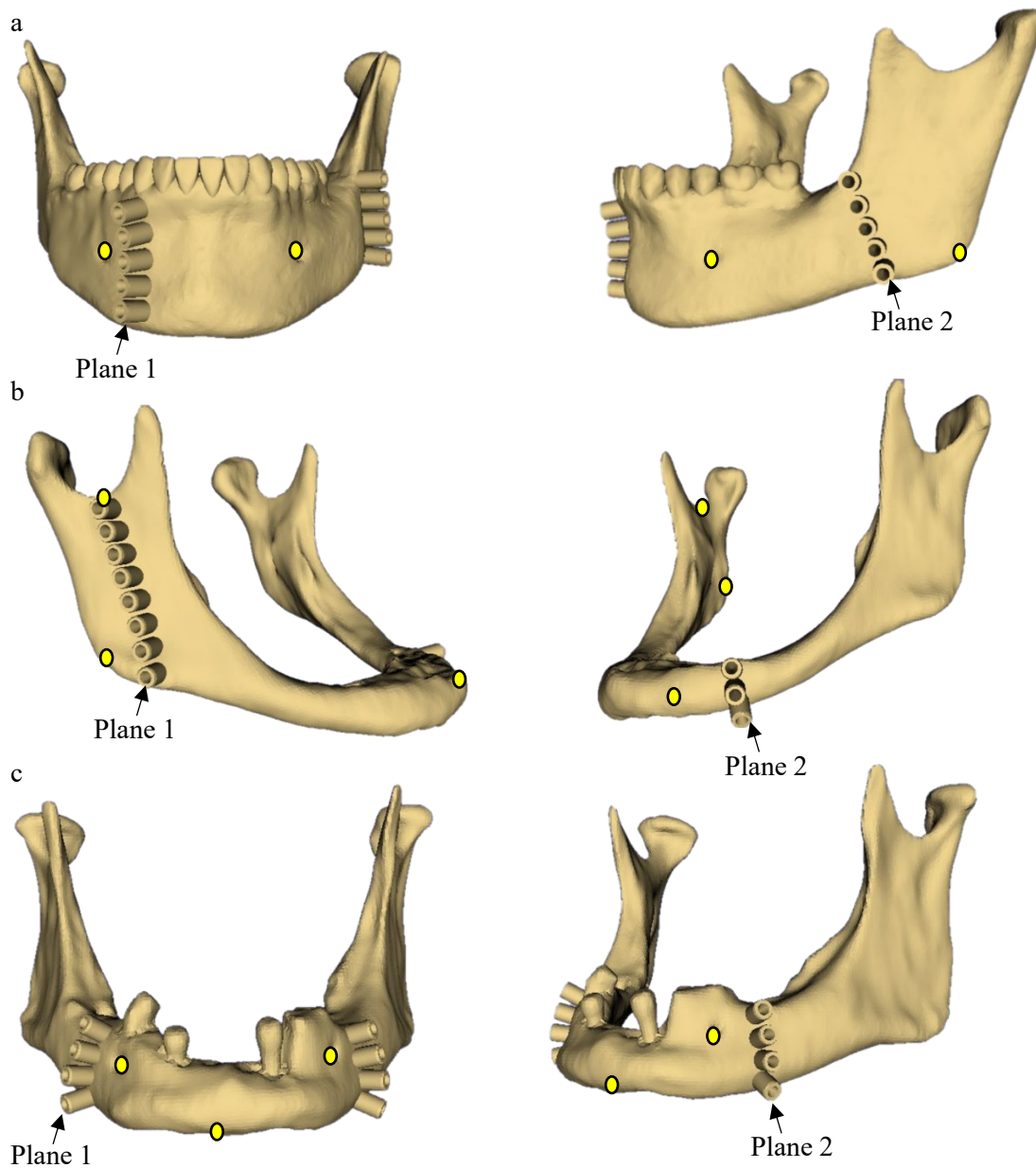
Figure 5.1 Three mandible phantoms that were used for the experiments. The three anatomic landmarks that were used for initial point registration are annotated on each phantom. For each phantom, two views are shown to enable a view of both osteotomy planes with reference notches. a) phantom A, b) phantom B, c) phantom C.

a   b

Figure 5.2 Sensor positioned on phantom A during a) Experiments 1-3, b) Experiments 4-5.

5.2.4 Registration accuracy

For each experiment, registration accuracy was calculated after initial point registration and after surface registration. The registration accuracy was assessed in terms of 'fiducial registration error' (FRE) and 'target registration error' (TRE) [141, 142].

The FRE is a measure of how accurately the phantom is registered with the CT scan. The FRE is defined as the root mean squared distance between the pinpointed registration points on the phantom (in physical space) and the virtual registration points on the CT scan (in image space), after registration. The FRE was calculated and shown by 3D Slicer after point registration and surface registration.

The TRE is a measure of how closely the location of virtual predefined target points (other than the registration points) correspond to their actual intraoperative location after registration. The notches on the osteotomy planes were used as target points to calculate the TRE. Prior to the experiments, the locations of the notches were marked on the CT scan. After eac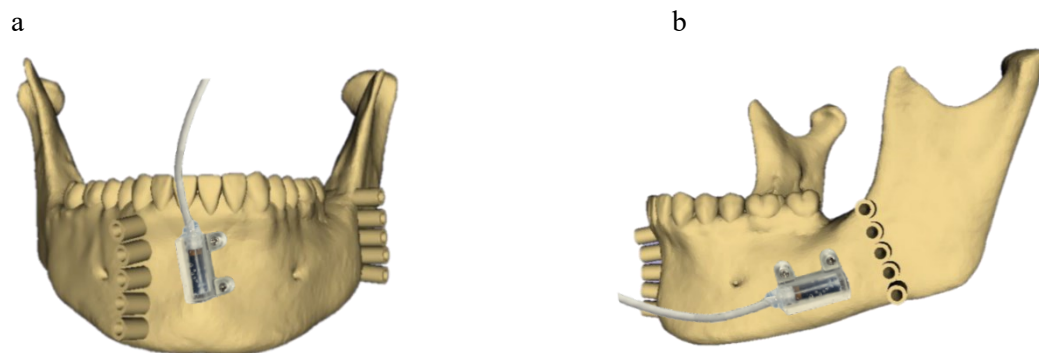h registration step (point registration and surface registration), the notches were pinpointed on the phantom with the tracked probe. For every notch (n), the distance between the coordinates on the CT data and the corresponding point on the phantom was calculated in terms of Euclidean distance (ED):

$$TRE_n = \sqrt{(x_{phantom,n} - x_{ct,n})^2 + (y_{phantom,n} - y_{ct,n})^2 + (z_{phantom,n} - z_{ct,n})^2} \qquad 5.1$$

The overall TRE, for both osteotomy planes together and for each plane separately, was calculated as the root mean squared error (RMSE) of the individual TREs:

$$TRE_{overall} = \sqrt{\frac{1}{N} \sum_{n=1}^{N}(TRE_n)^2} \qquad 5.2$$

5.2.5 Experiments

The dentate phantom (A) was used for Experiments 1-4, for Experiment 5 both the dentate phantom and the (partially) edentulous phantoms (B and C) were used. All experiments were repeated 10 times by one researcher. Experiments 1-4 were performed in a metal-free environment to minimize EM field distortions. Experiment 5 was performed in an intraoperative environment on a standard patient table.

The area of the mandibular bone surface that can be prepared free from tissue depends on the tumor location, tumor size, and individual anatomy of the patient. Therefore, in *Experiment 1*, four different surface areas with a varying number of surface points were tested. The goal of this experiment was to simulate four different surface area configurations that would be exposed during various clinical situations and determine the registration accuracy. First, point registration was performed with three anatomic landmarks (mental foramen left and right, mandibular angle left, Figure 5.1). Next, four different surface area locations were tested (areas A to D), as shown in Figure 5.3. Area A resembled the surface that needs to be prepared free from tissue to attach the cutting guide during mandible reconstruction surgery (70 points; 35 around each osteotomy plane). For area B, extra points were added on the surface where the reconstruction plate would be attached (120 points; 60 around each osteotomy plane). For area C, additional points were added between the osteotomy planes (200 points). Area D resembled exposing the inferior border of the mandible (100 points).

In *Experiment 2*, using area B, the number of surface points was varied to determine how many surface points are required for an accurate registration, either in a line configuration or randomly located within the specified area. After point registration, similar to Experiment 1, surface registration was performed with 30, 60, and 120 surface points in line configuration, and 60, 120, and 240 points randomly located

within area B (Figure 5.4). For pragmatic reasons, only a partial overlap between the number of points was tested since 240 points on a line would have been very dense.

In *Experiment 3*, the effect of the initial point registration on the final registration accuracy was determined. During surgery, anatomic landmarks on the mandible are often difficult to pinpoint exactly, which can result in large initial registration errors. To simulate this, instead of pinpointing exactly on the anatomic landmarks on the phantom, the tracked probe was pinpointed at a range of 10 mm from the landmarks. Next, surface registration was performed with area B using 120 points in line configuration.

In *Experiment 4*, the effect of the sensor location (on the mandible) on the registration accuracy was determined. The sensor was placed at a different position and orientation compared to Experiments 1, 2, and 3 (Figure 5.2). Area B and 120 points in line configuration were used for surface registration.

In *Experiment 5*, the registration procedure was tested in the OR on a standard patient table to determine the influence of the metal in the table. For this experiment, the dentate phantom (A) was used, but also the (partially) edentulous phantoms (B and C) to determine whether the current registration method works for different individual anatomies and different osteotomy locations (Figure 5.1). For each phantom, the sensor was attached between the osteotomy planes. Surface registration was performed with area B using 120 points in line configuration for phantom A and 90 points in line configuration for the phantoms B and C (since less mandibular surface was available due to atypical anatomy).
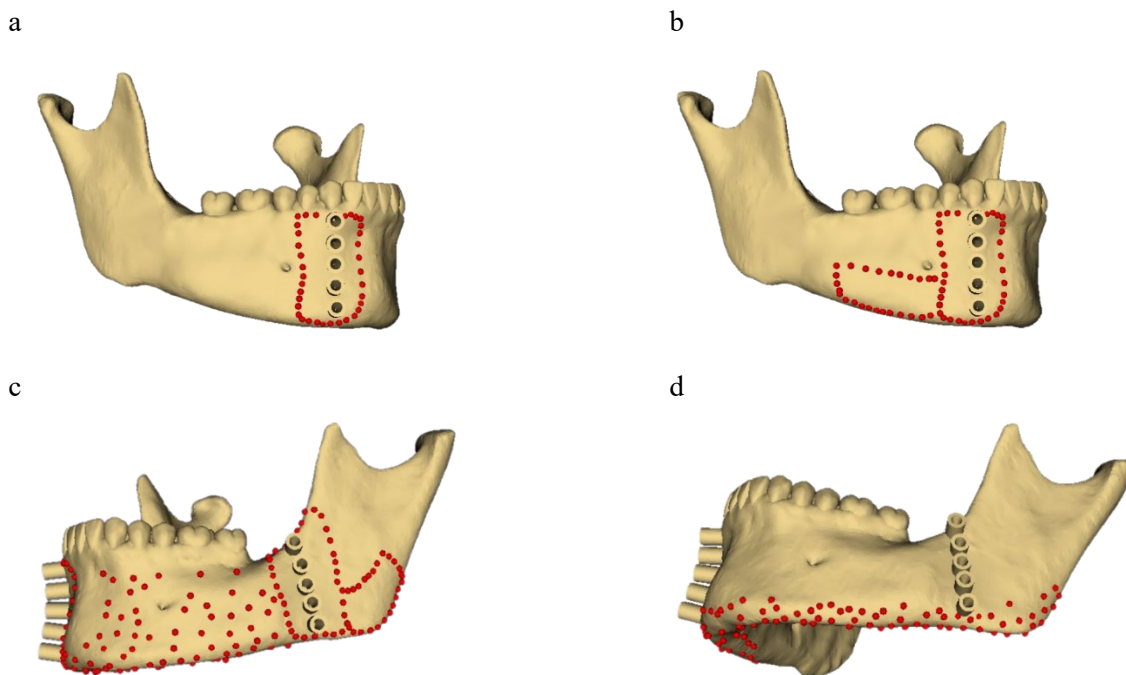
a

b

c

d

Figure 5.3 Surface areas for Experiment 1; the red points indicate the used points for surface registration. a) area A, b) area B, c) area C, d) area D.
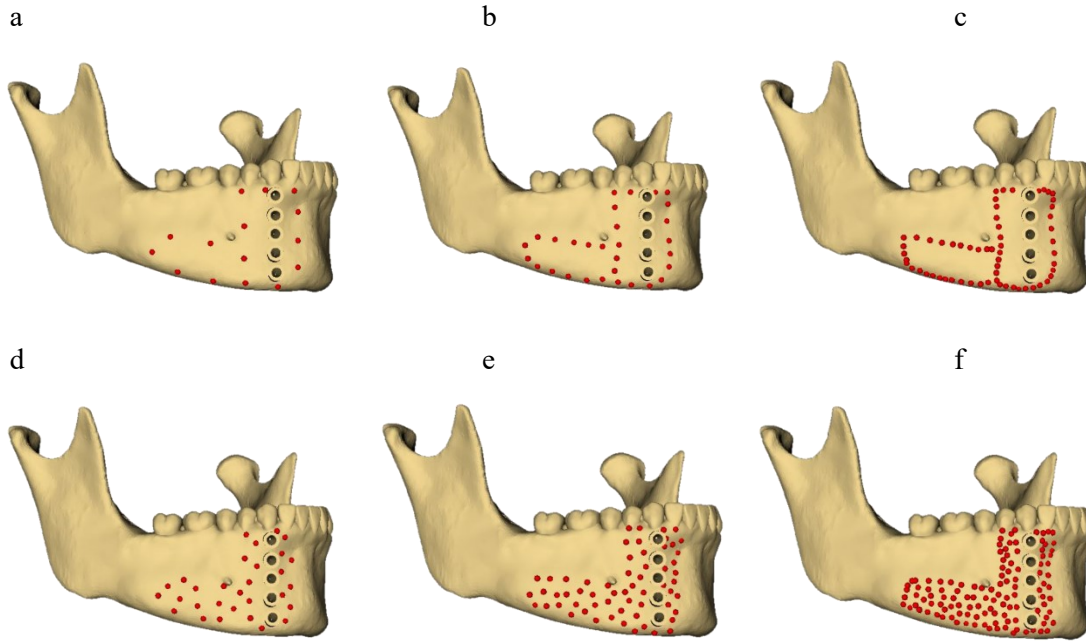
Figure 5.4 *Surface point configurations for Experiment 2; the red points indicate the used points for surface registration (the points used for one osteotomy plane are shown). a) 30 points in line configuration, b) 60 points in line configuration, c) 120 points in line configuration, d) 60 points in random configuration, e) 120 points in random configuration, f) 240 points in random configuration.*

5.3 Results

In *Experiment 1*, determining the registration accuracy of different surface area configurations that simulate clinical situations, the mean *FRE* was 0.22 ± 0.04 mm, 0.28 ± 0.05 mm, 0.31 ± 0.06 mm, and 0.39 ± 0.07 mm for area A, area B, area C, and area D respectively. The mean overall *TRE* values ranged from $0.98 – 1.21$ mm (Table 5.1).

In *Experiment 2*, determining the effect of different numbers and configurations of surface points on the registration accuracy, the mean *FRE* was 0.22 ± 0.03 mm, 0.22 ± 0.03 mm, and 0.23 ± 0.01 mm for 30, 60, and 120 points in a line configuration and 0.28 ± 0.04 mm, 0.26 ± 0.04 mm, and 0.25 ± 0.04 mm for 60, 120, and 240 points randomly located within the specified surface area. The mean overall *TRE* values ranged from $0.98 – 1.05$ mm (Table 5.2).

In *Experiment 3*, determining the effect of the initial registration accuracy on the final registration accuracy, the mean *FRE$_{initial}$* (after point registration) was 4.96 ± 1.71 mm and the mean final *FRE* (after surface registration) was 0.32 ± 0.09 mm. The mean overall *TRE$_{initial}$* values ranged from $3.98 – 15.01$ mm, the mean overall final *TRE* values ranged from $0.89 – 1.48$ (Table 5.3). Figure 5 shows the correlation between *TRE$_{initial}$* and final *TRE* for all experiments.

In *Experiment 4*, determining the effect of the sensor location on the registration accuracy, the mean *FRE* was 0.32 ± 0.03 mm. The mean overall *TRE* values ranged from $0.85 – 1.32$ mm (Table 5.4).

In *Experiment 5*, determining the registration accuracy in the OR with different patient anatomies and osteotomy plane locations, the mean *FRE* values were respectively 0.28 ± 0.04, 0.43 ± 0.08, and 0.28 ± 0.07 mm for phantom A, phantom B, and phantom C. The mean overall *TRE* values ranged from $0.93 – 1.50$ mm (Table 5.5).

No statistical analysis was performed since all the measured *TRE* values fell within the clinically acceptable range.

Table 5.1 *Registration accuracies for Experiment 1. The overall TRE is given and the TRE for each osteotomy plane. Values are given as mean ± SD (range) in mm.*

	Area A (n=10)	Area B (n=10)	Area C (n=10)	Area D (n=10)
Overall	1.03 ± 0.20	1.00 ± 0.15	0.98 ± 0.20	1.21 ± 0.29
	(0.75 – 1.43)	(0.77 – 1.27)	(0.60 – 1.23)	(0.72 – 1.59)
Plane 1	0.78 ± 0.31	0.84 ± 0.26	0.86 ± 0.42	0.96 ± 0.34
	(0.41 – 1.29)	(0.56 – 1.44)	(0.30 – 1.45)	(0.47 – 1.72)
Plane 2	1.20 ± 0.18	1.11 ± 0.23	1.04 ± 0.17	1.39 ± 0.39
	(0.98 – 1.65)	(0.74 – 1.50)	(0.79 – 1.36)	(0.74 – 1.86)

Table 5.2 *Registration accuracies for Experiment 2. The overall TRE is given and the TRE for each osteotomy plane. Values are given as mean ± SD (range) in mm.*

	30 points line (n=10)	60 points line (n=10)	120 points line (n=10)	60 points random (n=10)	120 points random (n=10)	240 points random (n=10)
Overall	1.05 ± 0.26	1.00 ± 0.15	0.98 ± 0.20	1.03 ± 0.14	1.04 ± 0.18	1.01 ± 0.20
	(0.64 – 1.35)	(0.81 – 1.22)	(0.64 – 1.29)	(0.78 – 1.21)	(0.76 – 1.34)	(0.69 – 1.49)
Plane 1	0.76 ± 0.39	0.68 ± 0.18	0.66 ± 0.40	0.61 ± 0.17	0.69 ± 0.21	0.66 ± 0.31
	(0.25 – 1.68)	(0.43 – 0.97)	(0.29 – 1.67)	(0.39 – 0.88)	(0.44 – 1.00)	(0.30 – 1.12)
Plane 2	1.20 ± 0.41	1.21 ± 0.29	1.15 ± 0.32	1.32 ± 0.22	1.26 ± 0.34	1.23 ± 0.27
	(0.57 – 1.76)	(0.73 – 1.61)	(0.69 – 1.65)	(1.03 – 1.64)	(0.90 – 1.82)	(0.87 – 1.78)

Table 5.3 *Registration accuracies for Experiment 3. The overall TRE is given and the TRE for each osteotomy plane. Values are given as mean ± SD (range) in mm.*

	TRE after initial registration (n=10)	TRE after final registration (n=10)
Overall	7.82 ± 3.61	1.19 ± 0.20
	(3.98 – 15.01)	(0.89 – 1.48)
Plane 1	8.35 ± 4.44	0.99 ± 0.37
	(2.21 – 17.76)	(0.29 – 1.54)
Plane 2	7.00 ± 3.23	1.32 ± 0.19
	(3.75 – 12.82	(1.08 – 1.64)

Table 5.4 *Registration accuracies for Experiment 4. The overall TRE is given and the TRE for each osteotomy plane. Values are given as mean ± SD (range) in mm.*

	Different sensor location (n=10)
Overall	1.09 ± 0.15
	(0.85 – 1.32)
Plane 1	1.04 ± 0.35
	(0.62 – 1.65)
Plane 2	1.10 ± 0.15
	(0.88 – 1.29)

Table 5.5 *Registration accuracies for Experiment 5. The overall TRE is given and the TRE for each osteotomy plane. Values are given as mean ± SD (range) in mm.*

	Phantom A (n=10)	Phantom B (n=10)	Phantom C (n=10)
Overall	0.96 ± 0.22	0.93 ± 0.26	1.50 ± 0.28
	(0.65 – 1.38)	(0.55 – 1.25)	(1.09 – 1.99)
Plane 1	0.79 ± 0.25	0.91 ± 0.32	1.68 ± 0.40
	(0.42 – 1.07)	(0.36 – 1.29)	(1.12 – 2.38)
Plane 2	1.09 ± 0.30	0.95 ± 0.20	1.28 ± 0.21
	(0.81 – 1.78)	(0.67 – 1.35)	(1.02 – 1.65)

Table 5.6 *Registration accuracy for phantom A using separate registrations for both osteotomy planes. The overall TRE is given and the TRE for each osteotomy plane. Values are given as mean ± SD (range) in mm.*

	Phantom A (n=10)
Overall	0.86 ± 0.28
	(0.59 – 1.33)
Plane 1	0.86 ± 0.47
	(0.43 – 1.78)
Plane 2	0.80 ± 0.26
	(0.57 – 1.31)
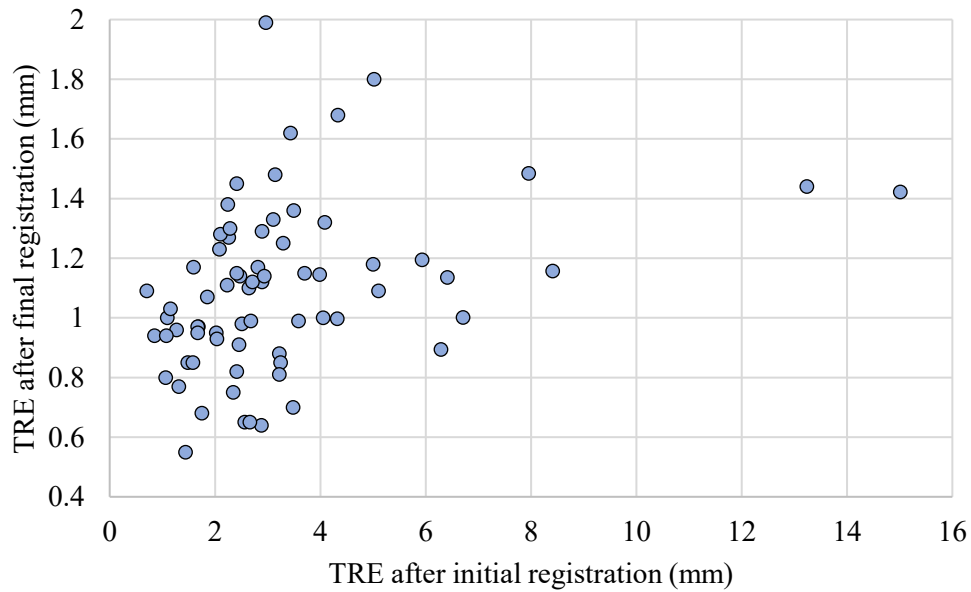
Figure 5.5 *Correlation between initial TRE (target registration error) after point registration and final TRE after surface registration. Results from all experiments (n=70) are shown (from Experiment 1, the measurements with area B are used, from Experiment 2 the measurements with 120 points in line configuration are used).*

5.4 Discussion

In this phantom study, the feasibility of a noninvasive hybrid registration technique, combining point- and surface registration, for navigated mandibular surgery was assessed. The results showed that hybrid registration is an accurate registration method with a mean TRE < 2.0 mm in all experiments. This meets the requirements of clinical practice for mandible reconstruction surgery according to literature and surgeons from our institute [46]. Moreover, the results suggest that the accuracy of this method is hardly affected by different patient anatomies and osteotomy plane locations.

Registration accuracy did not improve by using a larger surface area with more registration points, more registration points within the same surface area, different surface point configurations, a different sensor position, or when initial point registration was more accurate, showing the robustness of this approach. During oncologic mandible reconstruction surgery, the mandible needs to be prepared free from soft tissue and periosteum to attach the cutting guides (before resection) and the reconstruction plate (during reconstruction). Ideally, only this surface is used for registration, obviating the necessity of exposing extra bone. For sensor placement, surgeons can use any accessible location on the segment that will be extirpated since its position and orientation doesn't affect the registration accuracy. Similarly, the results suggest that the final registration accuracy is hardly affected by the accuracy of the initial point registration (Figure 5.5). Therefore, less distinct landmarks such as the mandibular angle or the incisura can be used, which can be useful in edentulous patients with few distinct landmarks.

Although the mean overall accuracy (of both osteotomy planes together) in all experiments was ≤ 1.50 mm, differences were noticed between the two osteotomy planes for phantoms A and C. For phantom A, in almost all measurements the registration was more accurate in the frontal plane (0.79 ± 0.25 mm) than in the lateral plane (1.09 ± 0.30 mm). For phantom C, the accuracy was higher in the left osteotomy plane (1.28 ± 0.21 mm) compared to the right plane (1.68 ± 0.40 mm). These differences may have been caused by several reasons, such as segmentation errors or tracking errors due to EM field distortions. Since it is known that registration points should be placed over a large area around the surgical site but also as close to the surgical site as possible to increase the accuracy, an additional experiment was performed with phantom A with separate registrations for each osteotomy plane [162, 163]. In this additional experiment, initial point registration and the collection of surface points was performed similarly to the other experiments. However, the surface registration was split into two separate registrations; first, the surface points around the frontal osteotomy plane were used for registration and the accuracy of this plane was validated by pinpointing the notches. Next, the registration transform was reset and the surface points around the lateral osteotomy plane were used for registration and accuracy of this plane was assessed. This method resulted in comparable accuracy for both planes with mean TRE values around 0.85 mm (Table 5.6). However, during surgery this method of two separate registrations may add 10 minutes extra to the registration procedure since registration needs to be performed twice and consequently the accuracy needs to be verified two times. Moreover, the two cutting guides cannot be positioned at the same time since they require different registrations.

Even though the overall TRE in phantom C was below 2.0 mm, thus clinically acceptable, it was noted that the TRE was almost 1.5 times higher than in phantoms A and B (1.50 ± 0.28 mm versus 0.96 ± 0.22 mm and 0.93 ± 0.26 mm respectively). This difference may have been caused by the location of the osteotomy planes and/or individual patient anatomy. The osteotomy planes were located anteriorly on the mandible, next to the two mental foramen. Therefore, the surface points used for registration were located on a relatively flat part of the body of the mandible. Hence, this surface had less varying and less unique features than the surfaces used in phantoms A and B, where surface points were not only located on the mandibular body but also on the mandibular angle and ramus. The ICP algorithm, used for surface registration, is known to be easily trapped into a local minimum [164]. This may have

happened in phantom C, explaining the higher TRE values compared to the other phantoms. However, as the obtained TRE values for phantom C still meet the requirements for clinical practice, this difference was not considered clinically relevant.

Although the results of this study are promising, there are some limitations to keep in mind when interpreting the results. Although the notches on the phantoms were designed to fit the tracked probe, some pivoting of the probe was possible due to minor 3D printing inaccuracies. The variability in pinpointing the notches with the probe was determined by pinpointing the notches ten times and calculating the mean deviation, which was 0.23 mm. Another fact to keep in mind is that all experiments were performed by the same person to eliminate inter-observer/operator variability. However, during surgery, not always the same surgeon performs the navigation procedure. Therefore, multiple surgeons need to be trained to perform the registration procedure. Furthermore, 'clean' phantoms were used in this study to simulate the exposed bone surface, while during surgery residual soft tissue specimens may remain on the bone, which could affect the registration accuracy. Lastly, although the intraoperative environment was simulated in Experiment 5 by using a standard patient table, during surgery there will probably more distortion of the EM field due to other metal in the OR such as instrument tables.

To our knowledge, this is the first study assessing a combination of point registration, using anatomic landmarks, and surface registration, using the surgically exposed bone surface, as a hybrid registration method for EM navigation of the mandible. Until now, three studies used the mandibular bone surface for registration during optical navigation of the mandible, either as standalone method or as part of a hybrid technique. However, in a study by Marmulla et al. (2007) the registration failed due to an incongruence of the mandibular surface [82]. Sun et al. (2020) achieved a successful registration in three patients with a TRE of 1.0 mm and Lubbers et al. (2010) achieved a deviation of less than 1 mm in a phantom study [46, 122]. Some studies did use a hybrid registration method for EM navigated mandibular surgery, just using the facial skin surface instead of the exposed mandibular bone [55, 86, 87]. In these studies, surface registration was used for initialization and point registration for optimization. Accuracies were not reported.

Compared to other registration methods, such as point registration with bone screws or a dental splint, the proposed hybrid method has several advantages. First, it obviates the need for implanting invasive bone screws. Screws can be implanted preoperatively in the outpatient clinic before preoperative CT scanning is performed or during surgery. However, the latter requires intraoperative Cone Beam CT scanning (to obtain a 'preoperative' CT scan with the screws visible) which lengthens OR time and leads to extra ionizing radiation for the patient. Alternatively, artificial markers can be attached to a noninvasive dental splint. However, splints are patient-specific and require separate fabrication for every patient for which skilled people and special equipment are needed. In addition, splints cannot be used in edentulous patients or patients with tooth loosening. The proposed hybrid registration method is both simple, since standard preoperative imaging data can be used, and noninvasive, since only anatomic points and surfaces are used and no artificial markers are required. Therefore, this technique has greater potential for implementation into clinical practice.

Pilot tests by the authors in a clinical setting during oncologic mandible reconstruction surgery (with registration performed on surgically exposed bone, before the cutting guide was attached) showed that registration can be performed within 15 minutes and visual validation (pinpointing multiple anatomic landmarks on the patient after registration and simultaneously looking at the monitor to see were the probe is located at the 3D model) confirmed the accuracy. However, further testing should be performed to objectively and quantitatively assess the accuracy and to validate the current findings in clinical setting.

5.5 Conclusion

This study assessed the feasibility of a noninvasive hybrid registration method for EM navigated mandibular surgery. This method consists of two phases: 1) point registration; performed for initialization by using anatomic landmarks on the mandible, and 2) surface registration; performed for optimization using the surgically exposed bone surface of the mandible after removal of soft tissue. In phantom experiments, accurate registration was obtained with mean TRE < 2.0 mm, which meets the practical clinical requirements for mandible reconstruction surgery. A small surface area, marked by limited surface points, was sufficient for accurate registration. Moreover, anatomical variations of the mandible, different osteotomy plane locations, initial point registration accuracy, and sensor location had no observable effect on the TRE, demonstrating the robustness of this approach. Future studies should test this method in clinical setting during surgery.

Chapter 6

Hybrid registration of the mandible in
patients undergoing mandible
reconstruction surgery:
a clinical feasibility study

6.1 Introduction

6.1.1 General introduction

To enable surgical navigation of the mandible, the preoperative imaging data, including the virtual surgical plan, must be registered with the intraoperative anatomy of the patient. Various registration methods exist, but there is always a tradeoff between the usability for the surgeon, invasiveness for the patient, registration time, and registration accuracy (Chapter 2). In Chapter 3, a simple, noninvasive hybrid registration method has been introduced that consists of two steps: 1) point registration for initialization, and 2) surface registration, using the surgically exposed mandibular bone surface, for optimization. In phantom experiments (Chapter 5), accurate registration was obtained with a mean target registration error (TRE) of < 2.0 mm, which meets the practical clinical requirements for mandible reconstruction surgery.

In this chapter, the clinical feasibility of hybrid registration for electromagnetic (EM) navigation of the mandible is assessed in four patients undergoing mandible reconstruction surgery. This study considers both the navigational workflow during surgery and the accuracy of the registration in terms of fiducial registration error (FRE) and TRE (see paragraph 2.3.5.1 for definitions and formulas). Intraoperatively, it can be difficult to obtain reliable TRE values (compared to measurements in phantom setting as in Chapter 5) since the mandible lacks clear anatomic landmarks that the surgeon can pinpoint. Therefore, an alternative, more objective method is proposed in this study for simple and basic assessment of the registration accuracy. This method uses a cloud of surface points, collected by sweeping a tracked probe over the exposed mandibular surface after registration (Figure 6.1). Point clouds are one of the most primitive and fundamental surface representations [165]. Therefore, the idea of using a point cloud for assessment of the registration accuracy is that the obtained point cloud is a representation of the surface of the mandible.
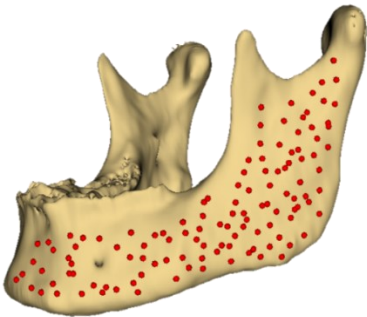
Figure 6.1. Example of a cloud of surface points on the mandible.

6.1.2 Hausdorff distance

The Hausdorff distance is a metric used to measure how far two subsets of a metric space are from each other. Considering the distance between two points a and b as $d(a, b) = \|a - b\|$, the distance between the point a in the validation point cloud (A) and the nearest neighboring point on the surface of the 3D model (B) is defined as [166]:

$$d(a, B) = \min_{b \in B} d(a, b) \qquad\qquad 6.1$$

This distance (*d*) is calculated for every point of the validation point cloud. The Hausdorff distance is defined as the maximum of these distances [166]:

$$d_{Hausdorff}(A, B) = \max_{a \in A} d(a, B) \qquad\qquad 6.2$$

The Hausdorff distance is known to be sensitive to outliers, since one or a few points with a large error will result in a large Hausdorff distance even if all other points perfectly match [166]. When capturing the validation point cloud, the surgeon sweeps over the mandibular surface with a tracked probe. Since the surface is not always smooth, it can happen that the probe slips and loses contact for a moment. Validation points collected when the probe is not in contact with the surface are considered as outliers. Therefore, instead of taking the maximum distance over all point-to-plane distances, the top 5% of the maximum distances are removed and the 95% Hausdorff distance is calculated.

If the registration is accurate (TRE < 2.0 mm), it is hypothesized that the 95% Hausdorff distance is small (< 2.0 mm) since the points from the point cloud are located on the mandibular bone surface. If the registration is not accurate (TRE > 2.0 mm), for example due to EM field distortions, it is hypothesized that the 95% Hausdorff distance is larger (> 2.0 mm). To verify this hypothesis and to investigate whether the 95% Hausdorff distance can be used as basic method to assess the registration accuracy, a phantom experiment was performed.

6.1.3 Study objectives

This study has two objectives:

1. Perform a phantom experiment to assess whether the 95% Hausdorff distance, calculated from a cloud of surface points obtained after registration, is a valid method for simple and basic assessment of the registration accuracy during EM navigation of the mandible.
2. Evaluate the clinical feasibility of hybrid registration of the mandible in patients undergoing mandible reconstruction surgery in terms of both the navigational workflow and registration accuracy.

6.2 Methods

6.2.1 Navigation system

The Aurora V2 electromagnetic (EM) tracking system (Northern Digital Inc., Waterloo, Canada) combined with 3D Slicer software (https://www.slicer.org/) was used for the navigation procedure (see paragraph 3.1). The field generator (FG) was positioned 25 cm from the mandible phantom in the phantom experiment and against the back of the head of the patient in the patient study (Figure 3.5). A 6 degrees-of-freedom (DOF) EM probe and a 6DOF EM flex tube sensor were used for registration and tracking purposes (Figure 3.1).

6.2.2 Phantom experiment

A three-dimensional (3D) printed mandible phantom with validation notches on the osteotomy planes was used for the experiment (the phantom was designed and 3D printed similar to the phantoms used in Chapter 5). The experiment was performed in a metal-free environment. Point registration was performed with three anatomic landmarks (right mandibular angle, both mental foramen) and surface registration with 120 points located around and in between the two osteotomy planes. After registration, the notches were pinpointed with the probe as validation landmarks and the TRE was calculated, the same as in Chapter 5. The TRE was regarded as the ground truth; a small TRE (< 2.0 mm) reflected an accurate registration. The probe was swept over the phantom's surface to capture a validation point cloud (120 points). For every point in the validation point cloud, the distance to the closest point on the surface of the mandibular 3D model was calculated using the 'Fiducials to Model' module in 3D Slicer. A table containing the point-to-plane distances was exported to Microsoft Excel 2019 and the 95% Hausdorff distance was calculated.

To simulate small errors that can occur during registration and can influence the registration accuracy, a translation of -2, -1, 1, and 2 mm in the left right (LR), posterior anterior (PA) or inferior superior (IS)

direction or a rotation of -2, -1, 1, and 2 degrees around the LR, PA or IS axis (Figure 6.2) was applied to the validation points (i.e. the points used to calculate the TRE and the point cloud) and the TRE and 95% Hausdorff distance were calculated again.
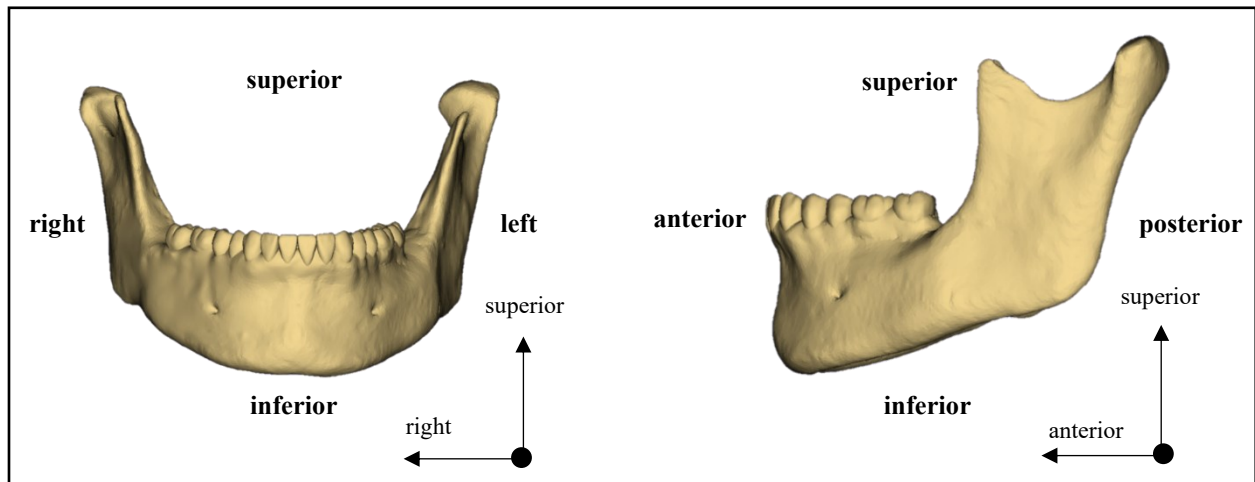

Figure 6.2 *Orientation of the mandible in the RAS coordinate system.*

6.2.3 Patient study

6.2.3.1 Patients

Patients that were planned for a segmental or hemi-mandibulectomy at the NKI-AvL from January 2021 until December 2021 were included. These patients were treated for benign or malignant tumors invading the mandible. This study was approved by the hospital's Medical Ethics Committee (NL60004.031.17/N17TOT) and institutional research ethics board. All patients gave their written informed consent for participation prior to surgery.

Preoperatively, all patients underwent a conventional diagnostic CT scan (Siemens Somatom Confidence, 1.0 mm slice thickness, 0.39 x 0.39 pixel spacing). The treatment plans were discussed by a team of head and neck surgeons and a technical physician in the NKI-AvL, and patient-specific cutting guides were designed and 3D printed (see 'current workflow' in Figure 1.7).

6.2.3.2 Workflow

Preoperatively, a 3D model of the mandible was constructed from the preoperative CT scan by segmentation with intensity based thresholding. Three anatomic landmarks were chosen for initial point registration. The coordinates of these landmarks on the CT scan were saved in 3D Slicer. In addition, the coordinates of three to six anatomic landmarks were saved as validation points as well as the coordinates of the end points of the saw slots of the cutting guide in the virtual surgical plan.

Intraoperatively, the navigation procedure started when the mandibular bone was exposed, soft tissue was removed, and the surgeon was ready to attach the cutting guide. The EM sensor was fixated to a part of the bone that was planned for resection; the sensor was folded into a 3D printed applicator and the applicator was screwed onto the bone with two 2.0 mm diameter x 9.0 mm long titanium screws (KLS Martin, Tuttlingen, Germany) (Figure 4.1). After connecting the software and hardware (see paragraph 3.3), the registration procedure was initiated. Initial point registration was performed with three anatomic landmarks. Surface registration was performed by sweeping the probe over the exposed mandibular bone surface and collecting between 100-200 surface points. Validation of the accuracy of the registration was performed in four ways: 1) with a visual check, 2) with anatomic landmarks, 3) with a cloud of surface points, and 4) with artificial landmarks on the cutting guide (end points of the saw slots). Visual validation was performed by the surgeon by moving the probe over the mandible and

simultaneously looking at the monitor to see where the probe was positioned in the 3D model. Next, the anatomic landmarks that were chosen for validation were pinpointed with the probe and their coordinates were saved in 3D Slicer. Then, the probe was swept over the mandibular bone surface to capture 100-200 validation surface points. Finally, the cutting guide was attached to the mandible, the ends of the saw slots were pinpointed with the probe and their coordinates were saved. The sensor was removed from the mandible and the standard surgical procedure was continued.

At the begin and end of every step of the workflow (sensor placement, point registration, surface registration, and validation), the time was written down to determine the duration of each step and to calculate the total time needed for the navigation.

6.2.3.4 Registration accuracy

The registration accuracy was evaluated in terms of FRE and TRE (see paragraph 2.3.5.1 for definitions and formulas); the FRE was calculated and shown by 3D Slicer and the TRE values for both the anatomic landmarks, $TRE_{anatomic}$, and the cutting guide landmarks, $TRE_{cuttingguide}$, were calculated postoperatively. In addition, the 95% Hausdorff distance was calculated using the same method as during the phantom experiment.

6.3 Results

6.3.1 Phantom experiment

Original registration resulted in a TRE and 95% Hausdorff distance of 1.13 mm and 0.57 mm respectively. The correlation between the TRE and 95% Hausdorff distance is shown in a Bland-Altman plot in Figure 6.3. For mean accuracy values of < 2.0 mm, the difference between the TRE and 95% Hausdorff distance was between 0 and 1 mm. A table containing the exact TRE and 95% Hausdorff distance values obtained during the experiment can be found in Appendix III.
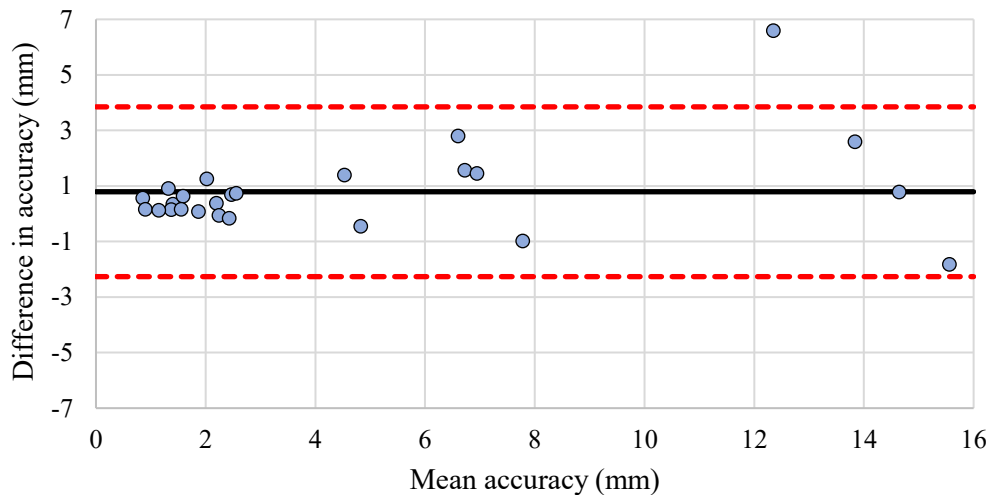
Figure 6.3 *Bland-Altman plot showing the correlation between the TRE and 95% Hausdorff distance. On the x axis, the mean accuracy (i.e. the mean of the TRE and 95% Hausdorff distance) is shown for the original registration and after applying a translation of -2, -1, 1, and 2 mm in the LR, PA, or IS direction and a rotation of -2, -1, 1, and 2 degrees around the LR, PA, or IS axis to the validation points. On the y axis, the difference in accuracy between the TRE and 95% Hausdorff distance is shown for the original registration and after applying the transformations. The average difference between the TRE and 95% Hausdorff distance is plotted as a solid black line, the 95% confidence intervals are plotted as dashed red lines.*

6.3.2 Patient study

A total of nine patients were included between January 2021 and December 2021. In five patients, the navigation was not or only partially performed due to technical failure caused by a broken sensor (1 patient), errors in the navigation software (2 patients), or a rotated or shifted sensor before the validation measurements could be performed (2 patients). These patients were excluded from further analysis. Four patients remained for analysis; their characteristics are summarized in Table 6.1.

Table 6.1 *Patient characteristics of the included patients, tumor staging according to the Union for International Cancer Control guidelines [13].*

Patient	Gender	Age	Mandibulectomy	Reconstruction	Tumor staging and tumor location
1	M	53	Hemi	FFF	cT4N2bM0 retromolar trigone left
2	F	65	Segmental	FFF	cT2N0M0 alveolar process left
3	M	64	Segmental	FFF	cT4aN2bM0 alveolar process left
4	M	55	Hemi	FFF	cT1N0M0 retromolar trigone right

M = male, F = female, FFF = free fibula flap.

The total time needed to perform the navigation was (mean ± SD) 18.8 ± 7 minutes (Figure 6.4). An overview of the registration accuracies for each patient can be found in Tables 6.2 and 6.3. The (mean ± SD) FRE, 95% Hausdorff distance, overall $TRE_{anatomic}$, and overall $TRE_{cuttingguide}$ were respectively 0.59 ± 0.25 mm, 1.79 ± 1.20 mm, 3.37 ± 1.91 mm, and 2.27 ± 0.91 mm. For each included patient, the details of the navigation procedure are provided below.
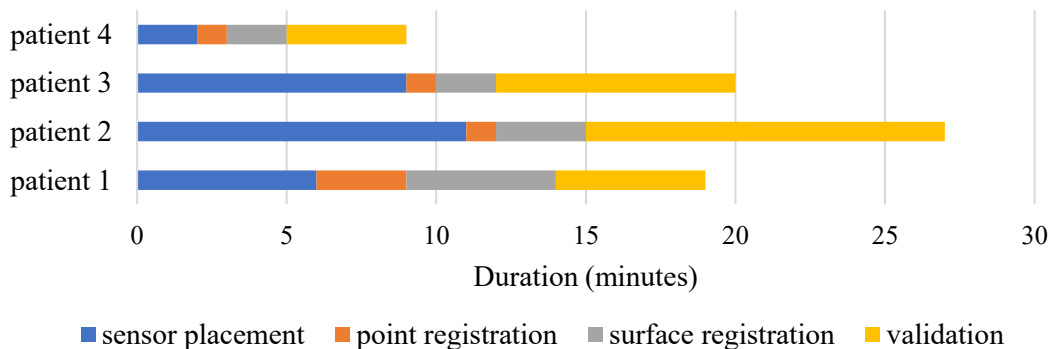
Figure 6.4 *Surgical delay due to navigation procedure.*

Patient 1

The anatomic landmarks used for registration and validation are shown in Figure 6.5. Visually, the registration seemed accurate over the whole surface of the mandible. During point cloud validation on the posterior part of the mandible, the sensor rotated in the sensor applicator making the validation points on the ramus invalid. Therefore, for analysis, only the points on the anterior part of the mandible were taken into account. Since the sensor had rotated, the registration was no longer valid and no validation with cutting guide landmarks could be performed in this patient.

Patient 2

To prevent movement of the sensor in the sensor applicator, the sensor was glued into the applicator with sterile tissue glue (DermaBond, Ethicon Inc., Norderstedt, Germany) before fixation to the bone with screws. The anatomic and cutting guide landmarks used for registration and validation are shown in Figure 6.6. Visually, the registration seemed accurate over the whole surface of the mandible.

Figure 6.5 *3D model of the mandible of patient 1 with the intraoperative position of the sensor indicated in black and the initial registration points (R) and anatomic validation points (Va) annotated.*
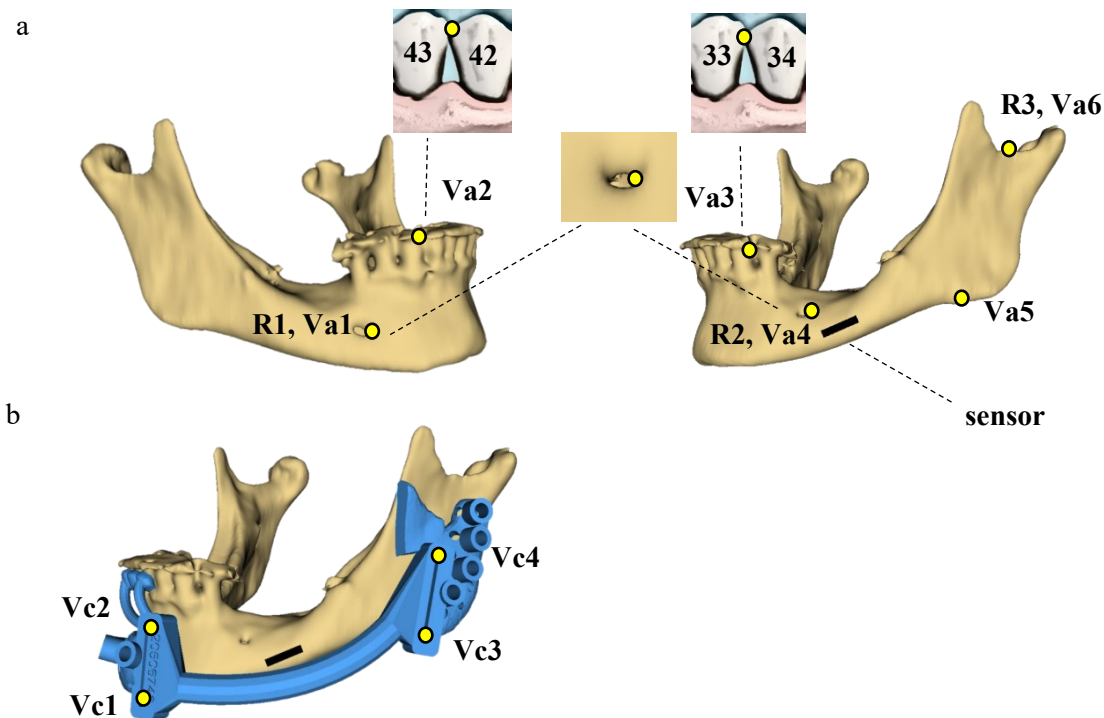
Figure 6.6 *3D model of the mandible of patient 2 with the intraoperative position of the sensor indicated in black. a) the mandible with the initial registration points (R) and anatomic validation points (Va), b) the mandible with the planned position of the cutting guide and cutting guide validation points (Vc).*

Patient 3

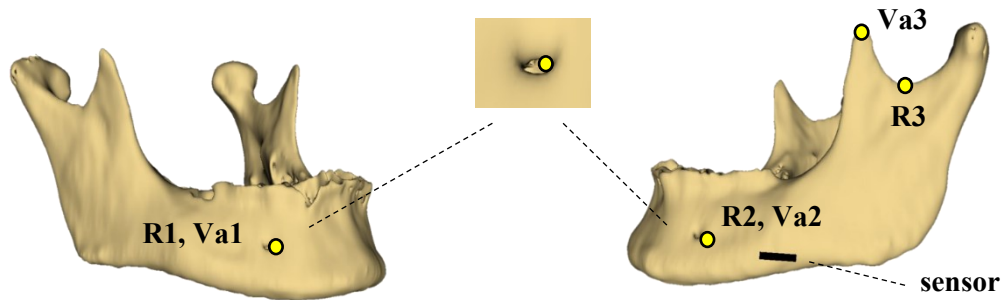Similar to patient 2, the sensor was glued into the applicator before fixation to the bone. The anatomic landmarks used for registration and validation are shown in Figure 6.7. Visually, the registration seemed accurate on the anterior side of the mandible, but shifted on the ramus; in the 3D model, the probe was hovering in air instead of making contact with the bone.

The cutting guide had to be cut in two separate parts because the guide did not fit on the mandibular surface because of the bulky tumor (Figure 6.8). Consequently, the virtually planned position of the cutting guide was impossible to determine on the patient. Therefore, it was decided not to perform validation measurements with the cutting guide as the position of the saw slots could have differed from the virtual surgical plan.

Figure 6.7 *3D model of the mandible of patient 3 with the intraoperative position of the sensor indicated in black and the initial registration points (R) and anatomic validation points (Va) annotated.*
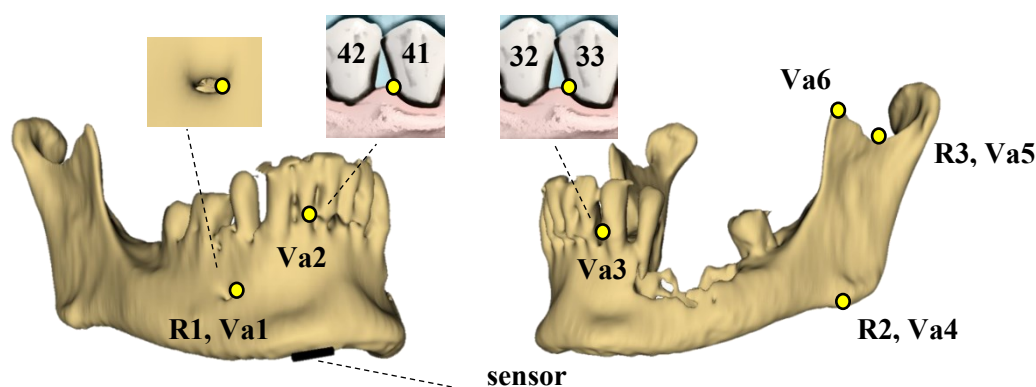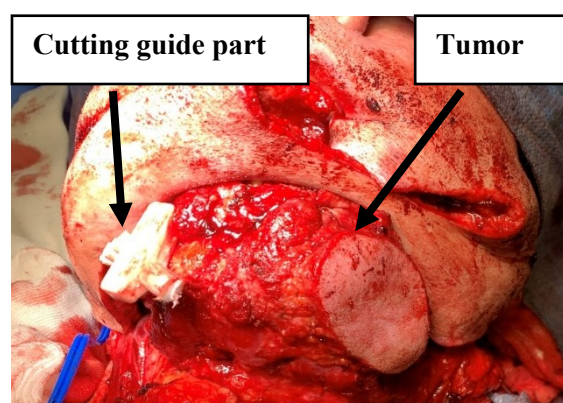

Figure 6.8 *Bulky tumor of patient 3 involving the mandible, soft tissue, and facial skin necessitating to cut the cutting guide in two parts for separate attachment.*

Patient 4

Similar to patients 2 and 3, the sensor was glued into the applicator before fixation to the bone. The anatomic and cutting guide landmarks used for registration and validation are shown in Figure 6.9. Visually, the registration did not seem accurate; when the surgeon was pointing an anatomic landmark with the probe, the tip of the probe was positioned on a different location in the 3D model.

Postoperatively, when looking more closely to location of the registration points in the 3D model and the CT scan, it was noted that the points were located on surface of the 3D model, but inside the bone (under the surface) in the CT scan. This raised the thought that the 3D model was too small. Therefore, an alternative 3D model was constructed from the CT scan using a different threshold for segmentation resulting in a slightly larger model. The surface points were registered to this model and the transformation matrix of the registration was applied to the validation points (anatomic-, point cloud- and cutting guide points). Visually, the registration seemed accurate over the whole surface of the mandible.

Figure 6.9 *3D model of the mandible of patient 4 with the intraoperative position of the sensor indicated in black. a) the mandible with the initial registration poi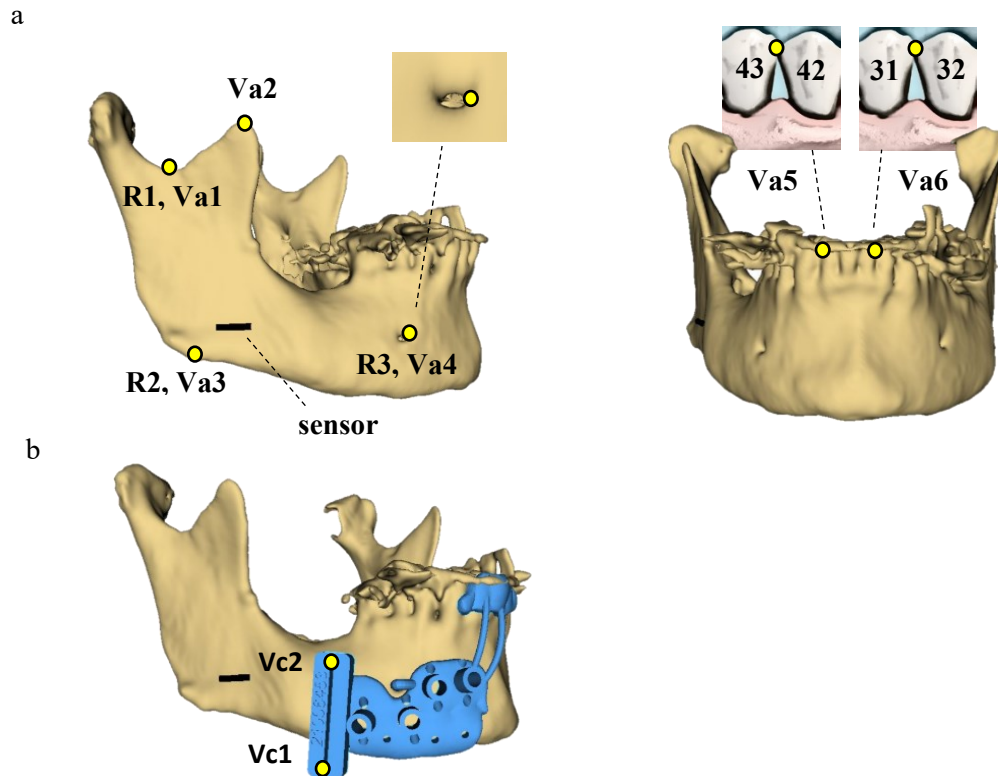nts (R) and anatomic validation points (Va), b) the mandible with the planned position of the cutting guide and cutting guide validation points (Vc).*

Table 6.2 *Registration accuracy of the analyzed patients in terms of FRE and 95% Hausdorff distance. All values are given in mm.*

	FRE	95% HD
Patient 1	0.23	0.56*
Patient 2	0.70	1.50
Patient 3	0.80	3.43
*Patient 4***	0.62	1.68
Mean ± SD	**0.59 ± 0.25**	**1.79 ± 1.20**

FRE = fiducial registration error, HD = Hausdorff distance. Only the points on the anterior mandible were used in the calculation.** Only the values of the postoperative registration with the alternative 3D model (adapted threshold) are shown in this table.*

Table 6.3 *Registration accuracy of the analyzed patients in terms of TRE using anatomic landmarks and cutting guide landmarks. All values are given in mm.*

	Patient 1		Patient 2		Patient 3		Patient 4*	
	$TRE_{anatomic}$	$TRE_{cuttingguide}$	$TRE_{anatomic}$	$TRE_{cuttingguide}$	$TRE_{anatomic}$	$TRE_{cuttingguide}$	$TRE_{anatomic}$	$TRE_{cuttingguide}$
Point 1	1.58	NA	1.76	2.40	2.45	NA	1.07	1.56
Point 2	1.03	NA	2.87	3.34	2.70	NA	2.96	1.68
Point 3	1.71	NA	1.90	0.71	8.93	NA	6.99	NA
Point 4	NA	NA	2.64	2.01	6.43	NA	2.30	NA
Point 5	NA	NA	2.97	NA	6.18	NA	1.04	NA
Point 6	NA	NA	3.02	NA	6.36	NA	2.53	NA
RMSE	**1.47**	NA	**2.58**	**2.91**	**5.96**	NA	**3.45**	**1.62**

NA = not applicable, TRE = target registration error, RMSE = root mean squared error. Only the values of the postoperative registration with the alternative 3D model (adapted threshold) are shown in this table.*

6.4 Discussion

In this study, a novel method for simple and basic assessment of the registration accuracy during surgical navigation of the mandible was proposed and evaluated in a phantom experiment. Furthermore, this study assessed the clinical feasibility of hybrid registration, using the surgically exposed mandibular bone surface, for electromagnetic navigation of the mandible. The navigational workflow and accuracy values of four patients undergoing mandible reconstruction surgery were described.

The results of the phantom experiment showed that for mean accuracy values (i.e. the mean of the TRE and 95% Hausdorff distance) of < 2.0 mm, the difference between the TRE and 95% Hausdorff distance was between 0 and 1 mm. This indicates that a small 95% Hausdorff distance (< 2.0 mm) correlates with a small TRE (< 2.0 mm). Based on these results, we conclude that the 95% Hausdorff distance can be used for simple and basic assessment of the registration accuracy.

Regarding the patient study, the standard surgical workflow was prolonged with (mean ± SD) 18.8 ± 7 minutes due to the navigation procedure. The registration procedure, including point- and surface registration, could be performed within 4.5 ± 2 minutes. Sensor placement (7.0 ± 4 minutes) and validation measurements (7.3 ± 4 minutes) were the most time consuming steps. Sensor attachment itself can be performed quickly, however, the location of the sensor should be chosen carefully in order that the cutting guide can be attached without damaging the sensor. The accuracy of the registration was assessed in terms of FRE, $TRE_{anatomic}$, $TRE_{cuttingguide}$, and the 95% Hausdorff distance which were respectively (mean ± SD) 0.59 ± 0.25 mm, 3.37 ± 1.91 mm, 2.27 ± 0.91 mm, and 1.79 ± 1.20 mm. As TRE values of < 2.0 mm are considered as clinically acceptable, there is still room for improvement of the registration.

In patient 3, the $TRE_{anatomic}$ and the 95% Hausdorff distance values were noticeably larger compared to the other patients. Visually, the registration seemed accurate on the anterior mandible, but shifted on ramus. Postoperatively, when looking more closely to the locations surface registration points after registration, it was noted that the points on the ramus were located under the surface of the mandible (in the bone instead of on the surface of the bone) and on the medial surface of the mandible (instead of on the lateral surface). Moreover, on the ramus, the points of the validation point cloud were hovering in the air. In this patient, a large stainless steel retractor was used to enable the surgeon to access the ramus with the probe, keeping soft tissue away. This retractor was positioned within the EM field during the navigation procedure. Metal instruments are known to cause distortions of the EM field that can lead to inaccuracies during registration and/or navigation [35, 36]. We hypothesize that the EM field was distorted by the metal retractor, causing inaccurate registration in this patient. A phantom experiment could be performed to verify this hypothesis. In this experiment, registration and validation should be performed with a mandible phantom both with and without the metal retractor positioned in the EM field near the ramus. If proving to be the cause of the deviations, this problem might be prevented in the future by using titanium retractors that are non-ferromagnetic.

In patient 4, the $TRE_{anatomic}$ was below 3.0 mm for all points except for the point on the mandibular angle (point 3 in Figure 6.9, TRE 6.99 mm). Visually, the registration seemed accurate and this observation was supported by the 95% Hausdorff distance and $TRE_{cuttingguide}$ values, which were below 2.0 mm. The mandibular angle is not a distinct anatomic landmark since it covers a large area. Preoperatively, the registration and validation points are discussed with the surgeon by showing the 3D model and the location of the points on the CT scan. Intraoperatively, before pinpointing the validation points, these points are showed again. However, it could have happened that the surgeon pinpointed a wrong point on the mandibular angle. This may have caused the large TRE value. In future navigation procedures,

during validation measurements, more attention should be paid by the researcher to make sure that the surgeon pinpoints the same landmarks as discussed preoperatively.

A relevant finding of this study is that the registration may be highly dependent on the accuracy of the segmentation of the bone from the CT scan. In patient 4, registration was not accurate during measurements in the OR. However, when performing the registration with a slightly larger 3D model (adapted segmentation threshold) postoperatively, higher accuracy was achieved. In this study, thresholding was performed semi-automatically in 3D Slicer based on intensity. In 3D Slicer, an automatic threshold was set by the software and the researcher manually adapted this threshold until the segmentation seemed accurate (i.e. including only bone, no other tissues). Postoperatively, when looking more closely to the original segmentation of patient 4, it was noticed that some parts of the mandible were under segmented. Therefore, for future patients, more attention should be paid to the segmentation procedure during preoperative planning. The researcher has to carefully examine the entire segmentation to see whether parts are under- or over segmented and should apply manual adjustments when necessary.

The results of the patient study should be interpreted carefully due to several reasons. The registration and validation measurements were performed by three different surgeons, using different surface areas and number of surface registration points due to the different individual patient anatomies. In addition, the number of validation points differed for the individual patients. After patient 1, we changed the number of anatomic validation points from three to six in the protocol to obtain more validation points. Also, cutting guide landmarks varied from two points in patients with a hemi-mandibulectomy (since only one cut was necessary) to four points in patients with a segmental mandibulectomy (since two cuts were necessary). Moreover, in patient 1 and 3, no cutting guide validation points could be used since the sensor had moved or the cutting guide had to be cut in separate parts. Another aspect to keep in mind when interpreting the results are the used validation methods. During surgery with commercial navigation systems, validation of the registration accuracy is performed in two ways: with the FRE value (shown by the system) and with visual validation. The FRE and visual validation, however, only give an impression of the registration accuracy. In the current study, FRE values of < 1.0 mm were obtained while the TRE values were > 2.0 mm. Thus, the FRE was not correlated with the TRE. Other validation methods were used as well in the current study: 1) point-to-point validation with 3 to 6 anatomic landmarks, 2) point-to-point validation with 2 to 4 cutting guide landmarks, and 3) point-to-plane validation with 100 to 200 points collected with the probe by sweeping the mandibular bone surface. These methods, however, also have limitations. Validation with anatomic landmarks is known to be user dependent since most anatomic landmarks on the mandible are not very distinct [30, 119]. The mental foramen, for example, has a diameter of several millimeters in most patients. Although the surgeon is asked to point the mental foramen at a specific point, e.g. at three o'clock, it is difficult for the surgeon to position the probe on this specific point exactly. Artificial landmarks on the cutting guide are easier for the surgeon to pinpoint but the exact position of the cutting guide on the patient is unknown which is a limitation. For validation, the coordinates of the points pinpointed with the probe are compared with the coordinates of the points on the virtual surgical plan. However, a study by Brouwer de Koning et al. (2020), evaluating the intraoperative position of the cutting guide compared to the planned position of the cutting guide, revealed that the intraoperative position of the cutting guide differed from the planned position with 1.1 ± 0.8 (mean $\pm$ SD) mm for the posterior osteotomy plane and 0.8 ± 0.1 (mean $\pm$ SD) mm for the anterior plane [31]. This should be kept in mind when interpreting the $TRE_{cuttingguide}$ values. Identification of the intraoperative position of the cutting guide is possible when a Cone Beam CT scan (CBCT) is acquired intraoperatively. However, this was not performed in the current study since an intraoperative CBCT scan leads to extra radiation for the patient and disrupts the surgical workflow as most personnel is required to leave the OR during scanning. With the current point cloud method, the exact locations of the points on the 3D model remain unknown. Since we are especially interested in the

registration accuracy at specific locations on the mandible (i.e. the virtual osteotomy planes), this method is not ideal. However, it can give an overall indication of the registration accuracy since an accurate registration (TRE < 2.0 mm) yields small Hausdorff distance values (< 2.0 mm) in most cases.

Since only four patients were included in this study, more patients should be included in the future before any conclusions can be drawn. The current results imply that hybrid registration introduces extra surgery time of (mean ± SD) $18.8 ± 7$ minutes when implemented into the standard surgical workflow of mandible reconstruction surgery. Registration accuracy values of maximum 2.0 mm are regarded as clinically acceptable by the surgeons in our institute. For patients 1, 2, and 4, the 95% Hausdorff distance values were below 2.0 mm, which suggests that the registration was accurate. Contrarily, the $TRE_{anatomic}$ and $TRE_{cuttingguide}$ values were larger, up to 3.45 mm. However, one should keep in mind that pinpointing anatomic landmarks is user subjective and the location of the cutting guide can differ from the virtual surgical plan. These factors make that the measured $TRE_{anatomic}$ and $TRE_{cuttingguide}$ values might be smaller or larger than the true $TRE_{anatomic}$ and $TRE_{cuttingguide}$ values. Compared to another patient study performed in our institute by Brouwer de Koning et al., using point registration with screws inserted in the mandible, our accuracy results are quite similar [30]. In that study, navigation was performed in eleven patients during mandible reconstruction surgery. Mean ± SD values for $TRE_{anatomic}$ and $TRE_{cuttingguide}$ were respectively $3.2 ± 1.1$ mm and $2.6 ± 1.5$ mm (compared to $3.4 ± 1.9$ mm and $2.3 ± 0.9$ mm in our study). Since registration with screws is invasive (see Chapters 1 and 2) and the performance is rather similar, hybrid registration is the preferred method for implementation into clinical practice. Moreover, we believe that the registration accuracy can be further improved in future patients by optimizing the current method, e.g. using a more accurate segmentation for preoperative modelling and using titanium retractors during surgery.

6.5 Conclusion

In this study, a novel method for determining the registration accuracy was introduced; the 95% Hausdorff distance. Phantom experiments showed that this metric can be used for simple and basic assessment of the registration accuracy during EM navigation of the mandible. In addition, the clinical feasibility of hybrid registration consisting of a point registration, using three anatomic landmarks, for initialization, and a surface registration, using the surgically exposed mandibular bone surface, for optimization, was assessed in four patients undergoing mandible reconstruction surgery. The navigation procedure could be incorporated into the standard surgical workflow and the registration itself could be performed quickly. Although promising, the obtained TRE values did not yet meet the clinical requirements for mandible reconstruction surgery. Therefore, the current workflow should be further optimized to achieve higher registration accuracy in future patients.

Chapter 7

Conclusion and future perspectives

7.1 Overall conclusion

The currently used three-dimensional (3D) printed patient-specific cutting guides for mandible reconstruction surgery do not allow for alterations of the surgical plan if the intraoperative situation is different than expected, e.g. due to tumor progression. This problem can be solved by using universal, navigated cutting guides that are adapted for each patient. To enable surgical navigation of the mandible, the preoperative imaging data, including the virtual surgical plan, should be registered to the patient in the operating room (OR). Registration methods that were used in previous research in the NKI-AvL were either invasive or required complex and time consuming preoperative steps. Therefore, the main goal of this thesis was to introduce and asses a simple, accurate, and noninvasive registration method for electromagnetic (EM) navigation of the mandible.

A hybrid registration method was introduced consisting of two steps: 1) point registration; performed for initialization using three anatomic landmarks on the mandible, and 2) surface registration; performed for optimization using the surgically exposed mandibular bone surface after removal of soft tissue. This method was assessed in both a phantom study and a clinical feasibility study with four patients undergoing mandible reconstruction surgery. The registration accuracy was assessed in terms of the fiducial registration error (FRE) and target registration error (TRE). TRE values of maximum 2.0 mm were considered as clinically acceptable.

In the phantom study, clinically acceptable TRE values were obtained in every experiment. The results suggest that only a small surface area, marked by limited surface points, is required for accurate registration. Additionally, hybrid registration seems to be applicable for different patient anatomies and osteotomy plane locations.

In the patient study, the navigation procedure could be incorporated into the standard surgical workflow and the registration itself could be performed quickly. The obtained TRE values (3.4 mm for anatomic landmarks and 2.3 mm for cutting guide landmarks) indicate that the registration procedure should be further optimized before implementation into clinical practice is possible.

7.2 Future perspectives

Ultimately, we want to use EM navigation in mandible reconstruction surgery to position a universal cutting guide according to a preoperatively defined virtual surgical plan. The research in this thesis focused on image-to-patient registration of the mandible, which is a precondition for surgical navigation. Future research should focus on further optimization and assessment of hybrid registration of the mandible, researching the applicability of hybrid registration to the fibula, and the development and validation of universal navigated cutting guides for the mandible and fibula.

7.2.1 Hybrid registration

The results of the patient study (Chapter 6) indicate that several factors might have compromised the registration accuracy. Using a more accurate bone segmentation for 3D model construction, using surgical instruments made from non-ferromagnetic materials during the navigation procedure, and gaining more insight in the variability of pinpointing anatomic landmarks might enable us to obtain better registration accuracy values. Therefore, this should be studied in future research.

In this thesis, hybrid registration was only evaluated for mandible navigation. When surgical navigation will be used to replace the patient-specific cutting guides during mandible reconstruction surgery, a method to translate the virtual surgical plan to the fibula is also required. Therefore, the applicability of hybrid registration to the fibula should be assessed in future research. Contrarily to the mandible, the fibula is a long, triangular shaped bone with little unique surface features. Consequently, there is a higher chance that the points used for surface registration will fit on the fibular surface in multiple ways.

Therefore, we hypothesize that the registration will generally be less accurate for the fibula compared to the mandible, especially in the longitudinal direction. Nevertheless, this is not necessarily a problem as long as the dimensions and the shape of the bone segments are according to the virtual surgical plan. Future research should start with a phantom study to determine the optimal approach for fibula navigation (similarly as was done for the mandible in this thesis). Next, a patient study should be initiated where the results obtained from the phantom study are confirmed in a clinical environment.

Besides mandible reconstruction surgery, the utilization of hybrid registration can be extended to other types of mandibular surgery, e.g. orthognathic surgery, foreign body removal, and trauma surgery. In addition, hybrid registration might be useful during navigated surgery of other parts of the body, e.g. during resection of malignant bone tumors of the pelvis, sacrum or tibia, or corrective surgery of the radius [167, 168].

7.2.2 Navigated mandible reconstruction surgery

A prototype of a navigated mandibular cutting guide has already been developed and tested in a proof-of-concept phantom study by our research group. The results of this study were promising with mean deviations between the planned and performed osteotomies of 1.1 ± 0.6 mm, $1.8 \pm 1.4°$ (yaw) and $1.6 \pm 1.3°$ (roll) [33]. The next step is to design and build a prototype for a navigated fibular cutting guide. Then, mandible reconstruction surgery (mandible resection, fibula resection, and reconstruction) can be simulated in a phantom study as a proof-of-concept. In this study, the osteotomies should be performed with both the currently used patient-specific cutting guides (golden standard) and the navigated cutting guides to determine and compare the reconstruction accuracy obtained with both methods. If the accuracy values are similar, the prototypes of the navigated cutting guides should be further developed for clinical use.

The main advantage of using navigated cutting guides compared to patient-specific cutting guides is the ability to adjust the surgical plan intraoperatively. A (semi-)automatic planning software is required to enable these adjustments since the currently used (manual) planning software does not allow for rapid alterations of the virtual surgical plan. The software should be able to rapidly generate a new reconstruction plan based om the altered positions of the mandibular osteotomy planes. A prototype of such software has already been developed and evaluated by our research group [169]. However, the overall performance of the software was inferior compared to manual planning. Thus, future research should focus on further optimization of this software.

Finally, the *in vivo* accuracy of navigated mandible reconstruction surgery should be assessed in a cadaver- and a patient study using the (semi-)automatic planning software and the clinical versions of the cutting guides. If proven to be as accurate as the patient-specific cutting guides and incorporable into the surgical workflow, the navigated cutting guides may be used as standard surgical method in the NKI-AvL.

References

References

[1]   Abbate V, Orabona GDA, Solari D, Bonavolonta P, Iaconetta G, Califano L (2017) Mandibular Surgical Navigation: An Innovative Guiding Method. J Craniofac Surg 28:2122-2126 https://dx.doi.org/10.1097/SCS.0000000000003816

[2]   Breeland G, Aktar A, Patel BC, *Anatomy, Head and Neck, Mandible*, Treasure Island (FL): StatPearls Publishing, 2021. [Online]. Available: https://pubmed.ncbi.nlm.nih.gov/30335325/.

[3]   Gray H, *Anatomy of the Human Body*, Philadephia: Lea & Febiger, 1918. [Online]. Available: https://www.bartleby.com/br/107.html.

[4]   Basit H, Tariq MA, Siccardi MA, *Anatomy, Head and Neck, Mastication Muscles*, Treasure Island (FL): StatPearls Publishing, 2021. [Online]. Available: https://pubmed.ncbi.nlm.nih.gov/31082071/.

[5]   "Human mandible." Encyclopaedia Brittanica. https://www.britannica.com/science/mandible (accessed December 9, 2021).

[6]   Haggerty CJ, Laughlin RM, *Atlas of operative oral and maxillofacial surgery*, Ames, Iowa: John Wiley & Sons Inc., 2015. [Online]. Available: https://onlinelibrary.wiley.com/doi/book/10.1002/9781118993729.

[7]   IKNL. "Incidentie hoofd-halskanker." https://iknl.nl/kankersoorten/hoofd-halskanker/registratie/incidentie (accessed September 23, 2021).

[8]   Sung H, Ferlay J, Siegel RL, Laversanne M, Soerjomataram I, Jemal A, Bray F (2021) Global Cancer Statistics 2020: GLOBOCAN Estimates of Incidence and Mortality Worldwide for 36 Cancers in 185 Countries. CA: A Cancer Journal for Clinicians 71:209-249 https://dx.doi.org/10.3322/caac.21660

[9]   Watters C, Brar S, Pepper T, "Oral Mucosa Cancer," StatPearls, 2021. [Online]. Available: https://www.ncbi.nlm.nih.gov/books/NBK565867/

[10]   Lubek JE, Magliocca KR (2017) Evaluation of the Bone Margin in Oral Squamous Cell Carcinoma. Oral Maxillofac Surg Clin North Am 29:281-292 https://dx.doi.org/10.1016/j.coms.2017.03.005

[11]   Van Cann EM, Koole R, Oyen WJ, de Rooy JW, de Wilde PC, Slootweg PJ, Schipper M, Merkx MA, Stoelinga PJ (2008) Assessment of mandibular invasion of squamous cell carcinoma by various modes of imaging: constructing a diagnostic algorithm. Int J Oral Maxillofac Surg 37:535-541 https://dx.doi.org/10.1016/j.ijom.2008.02.009

[12]   Bernier J, Cooper JS, Pajak TF, van Glabbeke M, Bourhis J, Forastiere A, Ozsahin EM, Jacobs JR, Jassem J, Ang K-K, Lefèbvre JL (2005) Defining risk levels in locally advanced head and neck cancers: A comparative analysis of concurrent postoperative radiation plus chemotherapy trials of the EORTC (#22931) and RTOG (# 9501). Head & Neck 27:843-850 https://dx.doi.org/10.1002/hed.20279

[13]   Brierley JD, Gospodarowicz MK, Wittekind C, *TNM Classification of Malignant Tumours 8th edition*. John Wiley & Sons, Ltd, 2017.

[14]   Kuriakose MA, Trivedi NP, *Surgical Management of Oral Squamous Cell Carcinoma*, Kuriakose MA, ed., Cham: Springer International Publishing, 2017, pp. 147-187. [Online]. Available: https://dx.doi.org/10.1007/978-3-319-14917-2_6.

[15]   Hamman J, Howe CL, Borgstrom M, Baker A, Wang SJ, Bearelly S (2022) Impact of Close Margins in Head and Neck Mucosal Squamous Cell Carcinoma: A Systematic Review. Laryngoscope 132:307-321 https://dx.doi.org/10.1002/lary.29690

[16]   Mitchell DA, Kanatas A, Murphy C, Chengot P, Smith AB, Ong TK (2018) Margins and survival in oral cancer. Br J Oral Maxillofac Surg 56:820-829 https://dx.doi.org/10.1016/j.bjoms.2018.06.021

[17] Sutton DN, Brown JS, Rogers SN, Vaughan ED, Woolgar JA (2003) The prognostic implications of the surgical margin in oral squamous cell carcinoma. Int J Oral Maxillofac Surg 32:30-34 https://dx.doi.org/10.1054/ijom.2002.0313

[18] Butler CE, Fine NA, *Principles of cancer reconstructive surgery*, New York: Springer, 2008. [Online]. Available: https://link.springer.com/book/10.1007/978-0-387-49504-0.

[19] Pogrel MA, Podlesh S, Anthony JP, Alexander J (1997) A comparison of vascularized and nonvascularized bone grafts for reconstruction of mandibular continuity defects. J Oral Maxillofac Surg 55:1200-1206 https://dx.doi.org/10.1016/s0278-2391(97)90165-8

[20] Boyd JB, Mulholland RS, Davidson J, Gullane PJ, Rotstein LE, Brown DH, Freeman JE, Irish JC (1995) The free flap and plate in oromandibular reconstruction: long-term review and indications. Plast Reconstr Surg 95:1018-1028 https://dx.doi.org/10.1097/00006534-199505000-00010

[21] Bauer E, Mazul A, Zenga J, Graboyes EM, Jackson R, Puram SV, Doering M, Pipkorn P (2021) Complications After Soft Tissue With Plate vs Bony Mandibular Reconstruction: A Systematic Review and Meta-analysis. Otolaryngol Head Neck Surg 164:501-511 https://dx.doi.org/10.1177/0194599820949223

[22] De Santis G, Pinelli M, Gargano F, Baccarani A, "Aesthetic and Functional Innovations in Jaw Reconstruction with Free Fibula Flap," in *Innovations in Plastic and Aesthetic Surgery*, Eisenmann-Klein M and Neuhann-Lorenz C Eds. Berlin, Heidelberg: Springer Berlin Heidelberg, 2008, pp. 193-203.

[23] Gupton M, Munjal A, Kang M, "Anatomy, Bony Pelvis and Lower Limb, Fibula," *StatPearls* Treasure Island (FL): StatPearls Publishing, 2021. [Online]. Available: https://pubmed.ncbi.nlm.nih.gov/29261984/

[24] Ma H, Van Dessel J, Bila M, Sun Y, Politis C, Jacobs R (2021) Application of Three-Dimensional Printed Customized Surgical Plates for Mandibular Reconstruction: Report of Consecutive Cases and Long-Term Postoperative Evaluation. J Craniofac Surg 32:e663-e667 https://dx.doi.org/10.1097/scs.0000000000007835

[25] Pucci R, Weyh A, Smotherman C, Valentini V, Bunnell A, Fernandes R (2020) Accuracy of virtual planned surgery versus conventional free-hand surgery for reconstruction of the mandible with osteocutaneous free flaps. Int J Oral Maxillofac Surg 49:1153-1161 https://dx.doi.org/10.1016/j.ijom.2020.02.018

[26] Weyh AM, Quimby A, Fernandes RP (2020) Three-Dimensional Computer-Assisted Surgical Planning and Manufacturing in Complex Mandibular Reconstruction. Atlas Oral Maxillofac Surg Clin North Am 28:145-150 https://dx.doi.org/10.1016/j.cxom.2020.05.007

[27] Barr ML, Haveles CS, Rezzadeh KS, Nolan IT, Castro R, Lee JC, Steinbacher D, Pfaff MJ (2020) Virtual Surgical Planning for Mandibular Reconstruction With the Fibula Free Flap: A Systematic Review and Meta-analysis. Ann Plast Surg 84:117-122 https://dx.doi.org/10.1097/sap.0000000000002006

[28] Bak M, Jacobson AS, Buchbinder D, Urken ML (2010) Contemporary reconstruction of the mandible. Oral Oncol 46:71-76 https://dx.doi.org/10.1016/j.oraloncology.2009.11.006

[29] Powcharoen W, Yang WF, Yan Li K, Zhu W, Su YX (2019) Computer-Assisted versus Conventional Freehand Mandibular Reconstruction with Fibula Free Flap: A Systematic Review and Meta-Analysis. Plast Reconstr Surg 144:1417-1428 http://dx.doi.org/10.1097/prs.0000000000006261

[30] Brouwer de Koning SG, Geldof F, van Veen RLP, van Alphen MJA, Karssemakers LHE, Nijkamp J, Schreuder WH, Ruers TJM, Karakullukcu MB (2021) Electromagnetic surgical navigation in patients undergoing mandibular surgery. Sci Rep 11:4657 https://dx.doi.org/10.1038/s41598-021-84129-5

References

[31] Brouwer de Koning SG, Ter Braak TP, Geldof F, van Veen RLP, van Alphen MJA, Karssemakers LHE, Schreuder WH, Karakullukcu MB (2021) Evaluating the accuracy of resection planes in mandibular surgery using a preoperative, intraoperative, and postoperative approach. Int J Oral Maxillofac Surg 50:287-293 https://dx.doi.org/10.1016/j.ijom.2020.06.013

[32] Lohuis PJFM. "Reconstructieve chirurgie bij commando's." https://www.facial-plastic-surgery.nl/reconstructieve-chirurgie/commandos/ (accessed December 12, 2021).

[33] Ter Braak TP, Brouwer de Koning SG, van Alphen MJA, van der Heijden F, Schreuder WH, van Veen RLP, Karakullukcu MB (2020) A surgical navigated cutting guide for mandibular osteotomies: accuracy and reproducibility of an image-guided mandibular osteotomy. Int J CARS 15:1719-1725 https://dx.doi.org/10.1007/s11548-020-02234-8

[34] Franz AM, Haidegger T, Birkfellner W, Cleary K, Peters TM, Maier-Hein L (2014) Electromagnetic Tracking in Medicine—A Review of Technology, Validation, and Applications. IEEE Trans Med Imaging 33:1702-1725 https://dx.doi.org/10.1109/TMI.2014.2321777

[35] Koivukangas T, Katisko JPA, Koivukangas JP (2013) Technical accuracy of optical and the electromagnetic tracking systems. SpringerPlus 2:90 https://dx.doi.org/10.1186/2193-1801-2-90

[36] Yaniv Z, Wilson E, Lindisch D, Cleary K (2009) Electromagnetic tracking in the clinical environment. Medical Physics 36:876-892 https://dx.doi.org/10.1118/1.3075829

[37] "Aurora Electromagnetic Tracking system." Northern Digital Inc. https://www.ndigital.com/products/aurora/ (accessed November 9, 2021).

[38] "Aurora Sensors." Northern Digital Inc. https://www.ndigital.com/products/aurora/aurora-sensors/ (accessed November 18, 2021).

[39] Hill DLG, Fitzpatrick JM, Maurer CR, "Image registration," *Handbook of Medical Imaging, Volume 2. Medical Image Processing and Analysis*, Fitzpatrick JM and Sonka M, Eds.: SPIE Press, 2000.

[40] Sukegawa S, Kanno T, Furuki Y (2018) Application of computer-assisted navigation systems in oral and maxillofacial surgery. Jpn Dent Sci Rev 54:139-149 https://dx.doi.org/10.1016/j.jdsr.2018.03.005

[41] Hwang YE, Kang SH, Kim HK (2019) Errors according to the number of registered markers used in navigation-assisted surgery of the mandible. Head Face Med 15:6 https://dx.doi.org/10.1186/s13005-019-0190-z

[42] Casap N, Wexler A, Eliashar R (2008) Computerized navigation for surgery of the lower jaw: comparison of 2 navigation systems. J Oral Maxillofac Surg 66:1467-1475 https://dx.doi.org/10.1016/j.joms.2006.06.272

[43] Chen S, Liu YH, Gao X, Yang CY, Li Z (2020) Computer-assisted navigation for removal of the foreign body in the lower jaw with a mandible reference frame: A case report. Medicine 99:e18875 https://dx.doi.org/10.1097/MD.0000000000018875

[44] Li P, Li Z, Tian W, Tang W (2015) A strategy for removal of foreign body in mandible with navigation system. Int J Oral Maxillofac Surg 44:885-888 https://dx.doi.org/10.1016/j.ijom.2015.01.021

[45] Brouwer de Koning SG, Riksen JJM, Ter Braak TP, van Alphen MJA, van der Heijden F, Schreuder WH, Karssemakers LHE, Karakullukcu MB, van Veen RLP (2020) Utilization of a 3D printed dental splint for registration during electromagnetically navigated mandibular surgery. Int J CARS 15:1997-2003 https://dx.doi.org/10.1007/s11548-020-02271-3

[46] Sun Q, Mai Y, Yang R, Ji T, Jiang X, Chen X (2020) Fast and accurate online calibration of optical see-through head-mounted display for AR-based surgical navigation using Microsoft HoloLens. Int J CARS 15:1907-1919 https://dx.doi.org/10.1007/s11548-020-02246-4

[47] Bernstein JM, Daly MJ, Chan H, Qiu J, Goldstein D, Muhanna N, de Almeida JR, Irish JC (2017) Accuracy and reproducibility of virtual cutting guides and 3D-navigation for osteotomies of the mandible and maxilla. PLoS ONE 12:e0173111 https://dx.doi.org/10.1371/journal.pone.0173111

[48] Liu TJ, Ko AT, Tang YB, Lai HS, Chien HF, Hsieh TM (2016) Clinical Application of Different Surgical Navigation Systems in Complex Craniomaxillofacial Surgery: The Use of Multisurface 3-Dimensional Images and a 2-Plane Reference System. Ann Plast Surg 76:411-419 https://dx.doi.org/10.1097/sap.0000000000000429

[49] Azarmehr I, Stokbro K, Bell RB, Thygesen T (2017) Surgical Navigation: A Systematic Review of Indications, Treatments, and Outcomes in Oral and Maxillofacial Surgery. J Oral Maxillofac Surg 75:1987-2005 https://dx.doi.org/10.1016/j.joms.2017.01.004

[50] Bettschart C, Kruse A, Matthews F, Zemann W, Obwegeser JA, Gratz KW, Lubbers HT (2012) Point-to-point registration with mandibulo-maxillary splint in open and closed jaw position. Evaluation of registration accuracy for computer-aided surgery of the mandible. J Craniomaxillofac Surg 40:592-598 https://dx.doi.org/10.1016/j.jcms.2011.10.016

[51] Chen C, Sun N, Jiang C, Sun J (2021) Randomized Controlled Clinical Trial to Assess the Utility of Computer-Aided Intraoperative Navigation in Bimaxillary Orthognathic Surgery. J Craniofac Surg 02:02 https://dx.doi.org/10.1097/SCS.0000000000007512

[52] Lin L, Fan B, Yu Z, Xu L, Yuan J, Wu J, Wei M (2019) Application of computer-assisted navigation in mandibular angle osteotomy. J Int Med Res 47:3160-3170 https://dx.doi.org/10.1177/0300060519850722

[53] Han B, Wang X, Li Z, Yi B, Liang C, Wang X (2018) Hemimandibular Hyperplasia Correction by Simultaneous Orthognathic Surgery and Condylectomy Under Digital Guidance. J Oral Maxillofac Surg 76:1563.e1561-1563.e1518 https://dx.doi.org/10.1016/j.joms.2018.03.006

[54] Lo J, Xia JJ, Zwahlen RA, Cheung LK (2010) Surgical navigation in correction of hemimandibular hyperplasia: a new treatment strategy. J Oral Maxillofac Surg 68:1444-1450 https://dx.doi.org/10.1016/j.joms.2009.11.008

[55] Sukegawa S, Kanno T, Shibata A, Matsumoto K, Sukegawa-Takahashi Y, Sakaida K, Furuki Y (2017) Use of an intraoperative navigation system for retrieving a broken dental instrument in the mandible: a case report. J Med Case Rep 11:14 https://dx.doi.org/10.1186/s13256-016-1182-2

[56] Page MJ, McKenzie JE, Bossuyt PM, Boutron I, Hoffmann TC, Mulrow CD, Shamseer L, Tetzlaff JM, Akl EA, Brennan SE, Chou R, Glanville J, Grimshaw JM, Hróbjartsson A, Lalu MM, Li T, Loder EW, Mayo-Wilson E, McDonald S, McGuinness LA, Stewart LA, Thomas J, Tricco AC, Welch VA, Whiting P, Moher D (2021) The PRISMA 2020 statement: an updated guideline for reporting systematic reviews. BMJ 372:n71 https://dx.doi.org/10.1136/bmj.n71

[57] Bramer WM, Giustini D, de Jonge GB, Holland L, Bekhuis T (2016) De-duplication of database search results for systematic reviews in EndNote. J Med Libr Assoc 104:240-243 https://dx.doi.org/10.3163/1536-5050.104.3.014

[58] Ouzzani M, Hammady H, Fedorowicz Z, Elmagarmid A (2016) Rayyan-a web and mobile app for systematic reviews. Syst Rev 5:210 https://dx.doi.org/10.1186/s13643-016-0384-4

References

[59] Han C, Dilxat D, Zhang X, Li H, Chen J, Liu L (2018) Does Intraoperative Navigation Improve the Anatomical Reduction of Intracapsular Condylar Fractures? J Oral Maxillofac Surg 76:2583-2591 https://dx.doi.org/10.1016/j.joms.2018.07.030

[60] He Y, Huang T, Zhang Y, An J, He L (2017) Application of a computer-assisted surgical navigation system in temporomandibular joint ankylosis surgery: a retrospective study. Int J Oral Maxillofac Surg 46:189-197 https://dx.doi.org/10.1016/j.ijom.2016.10.006

[61] Jones R (2013) The use of virtual planning and navigation in the treatment of temporomandibular joint ankylosis. Aust Dent J 58:358-367 https://dx.doi.org/10.1111/adj.12086

[62] Kong XZ, Duan XG, Wang YG (2016) An integrated system for planning, navigation and robotic assistance for mandible reconstruction surgery. Intelligent Serv Rob 9:113-121 https://dx.doi.org/10.1007/s11370-015-0189-7

[63] Malis DD, Xia JJ, Gateno J, Donovan DT, Teichgraeber JF (2007) New protocol for 1-stage treatment of temporomandibular joint ankylosis using surgical navigation. J Oral Maxillofac Surg 65:1843-1848 https://dx.doi.org/10.1016/j.joms.2005.11.080

[64] Mazzoni S, Badiali G, Lancellotti L, Babbi L, Bianchi A, Marchetti C (2010) Simulation-guided navigation: a new approach to improve intraoperative three-dimensional reproducibility during orthognathic surgery. J Craniofac Surg 21:1698-1705 https://dx.doi.org/10.1097/SCS.0b013e3181f3c6a8

[65] Schmelzeisen R, Gellrich NC, Schramm A, Schon R, Otten JE (2002) Navigation-guided resection of temporomandibular joint ankylosis promotes safety in skull base surgery. J Oral Maxillofac Surg 60:1275-1283 https://dx.doi.org/10.1053/joms.2002.35724

[66] Shim BK, Shin HS, Nam SM, Kim YB (2013) Real-time navigation-assisted orthognathic surgery. J Craniofac Surg 24:221-225 https://dx.doi.org/10.1097/SCS.0b013e318267bb76

[67] Sun G, Wang Z, Yang X, Hu Q, Tang E (2015) The application of surgical navigation in the treatment of temporomandibular joint ankylosis. Int J Oral Maxillofac Surg 44:e293 https://dx.doi.org/10.1016/j.ijom.2015.08.336

[68] Wagner A, Undt G, Watzinger F, Wanschitz F, Schicho K, Yerit K, Kermer C, Birkfellner W, Ewers R (2001) Principles of computer-assisted arthroscopy of the temporomandibular joint with optoelectronic tracking technology. Oral Surg Oral Med Oral Pathol Oral Radiol 92:30-37 https://dx.doi.org/10.1067/moe.2001.114384

[69] Wang Y, Duan X (2015) Spatial Registration for a Three-Arm Robot Assisted Mandible Reconstruction Surgery. Math Probl Eng 2015: https://dx.doi.org/10.1155/2015/689278

[70] Wu J, Hui W, Chen S, Niu J, Lin Y, Luan N, Zhang S, Shen SGF (2020) Error Analysis of Robot-Assisted Orthognathic Surgery. J Craniofac Surg 31:2324-2328 https://dx.doi.org/10.1097/SCS.0000000000006767

[71] Yu HB, Shen GF, Zhang SL, Wang XD, Wang CT, Lin YP (2009) Navigation-guided gap arthroplasty in the treatment of temporomandibular joint ankylosis. Int J Oral Maxillofac Surg 38:1030-1035 https://dx.doi.org/10.1016/j.ijom.2009.05.008

[72] Zhu JH, Deng J, Liu XJ, Wang J, Guo YX, Guo CB (2016) Prospects of Robot-Assisted Mandibular Reconstruction with Fibula Flap: Comparison with a Computer-Assisted Navigation System and Freehand Technique. J Reconstr Microsurg 32:661-669 https://dx.doi.org/10.1055/s-0036-1584805

[73] Suenaga H, Tran HH, Liao H, Masamune K, Dohi T, Hoshi K, Takato T (2015) Vision-based markerless registration using stereo vision and an augmented reality surgical navigation system: a pilot study. BMC Med Imaging 15:51 https://dx.doi.org/10.1186/s12880-015-0089-5

[74] Bayrak M, Alsadoon A, Prasad PWC, Venkata HS, Ali RS, Haddad S (2020) A novel rotation invariant and Manhattan metric-based pose refinement: Augmented reality-based oral and maxillofacial surgery. Int J Med Robotics Comput Assist Surg 16:e2077 https://dx.doi.org/10.1002/rcs.2077

[75] Murugesan YP, Alsadoon A, Manoranjan P, Prasad PWC (2018) A novel rotational matrix and translation vector algorithm: geometric accuracy for augmented reality in oral and maxillofacial surgeries. Int J Med Robotics Comput Assist Surg 14:e1889 https://dx.doi.org/10.1002/rcs.1889

[76] Gerbino G, Zavattero E, Berrone M, Berrone S (2013) Management of needle breakage using intraoperative navigation following inferior alveolar nerve block. J Oral Maxillofac Surg 71:1819-1824 https://dx.doi.org/10.1016/j.joms.2013.07.023

[77] Holmes PJ, Miller JR, Gutta R, Louis PJ (2005) Intraoperative imaging techniques: a guide to retrieval of foreign bodies. Oral Surg Oral Med Oral Pathol Oral Radiol 100:614-618 https://dx.doi.org/10.1016/j.tripleo.2005.02.072

[78] Lee SJ, Woo SY, Huh KH, Lee SS, Heo MS, Choi SC, Han JJ, Yang HJ, Hwang SJ, Yi WJ (2016) Virtual skeletal complex model- and landmark-guided orthognathic surgery system. J Craniomaxillofac Surg 44:557-568 https://dx.doi.org/10.1016/j.jcms.2016.02.009

[79] Lee SJ, Yang HJ, Choi MH, Woo SY, Huh KH, Lee SS, Heo MS, Choi SC, Hwang SJ, Yi WJ (2019) Real-time augmented model guidance for mandibular proximal segment repositioning in orthognathic surgery, using electromagnetic tracking. J Craniomaxillofac Surg 47:127-137 https://dx.doi.org/10.1016/j.jcms.2018.10.016

[80] Lübbers HT, Jacobsen C, Matthews F, Grätz KW, Kruse A, Obwegeser JA (2011) Surgical navigation in craniomaxillofacial surgery: Expensive toy or useful tool? A classification of different indications. J Oral Maxillofac Surg 69:300-308 https://dx.doi.org/10.1016/j.joms.2010.07.016

[81] Maeda K, Yamamoto S, Nashi M, Mukainaka Y, Taniike N, Takenobu T (2020) Navigation surgery with an all-in-one splint for impacted tooth root removal. J. Oral Maxillofacial Surg. Med. Pathol. 32:296-299 https://dx.doi.org/10.1016/j.ajoms.2020.04.002

[82] Marmulla R, Mühling J, Eggers G (2007) Image-to-patient registration by natural anatomical surfaces of the head. Cent Eur J Med 2:89-102 https://dx.doi.org/10.2478/s11536-006-0042-7

[83] Ohba S, Yoshimura H, Ishimaru K, Awara K, Sano K (2015) Application of a real-time three-dimensional navigation system to various oral and maxillofacial surgical procedures. Odontology/The Society of the Nippon Dental University 103:360-366 https://dx.doi.org/10.1007/s10266-014-0156-3

[84] Schultes G, Zimmermann V, Feichtinger M, Gaggl A, Karcher H (2003) Removal of osteosynthesis material by minimally invasive surgery based on 3-dimensional computed tomography-guided navigation. J Oral Maxillofac Surg 61:401-405 https://dx.doi.org/10.1053/joms.2003.50067

[85] Shen SY, Yu Y, Zhang WB, Liu XJ, Peng X (2017) Angle-to-Angle Mandibular Defect Reconstruction With Fibula Flap by Using a Mandibular Fixation Device and Surgical Navigation. J Craniofac Surg 28:1486-1491 https://dx.doi.org/10.1097/SCS.0000000000003891

[86] Stein KM (2015) Use of intraoperative navigation for minimally invasive retrieval of a broken dental needle. J Oral Maxillofac Surg 73:1911-1916 https://dx.doi.org/10.1016/j.joms.2015.04.033

[87] Sukegawa S, Kanno T, Shibata A, Matsumoto K, Sukegawa-Takahashi Y, Sakaida K, Furuki Y (2017) Intraoperative navigation-assisted accurate bone lid surgery to remove a mandibular

lesion: A case report. Oral Maxillofac Surg Cases 3:15-19
https://dx.doi.org/10.1016/j.omsc.2017.01.008

[88] Sun H, Li B, Shen S, Yang T, Zhang L, Shen SG, Wang X (2013) Image-guided endoscopic navigation for the precise resection of a mandibular condylar osteochondroma. J Craniofac Surg 24:e573-579 https://dx.doi.org/10.1097/SCS.0b013e31829ad374

[89] Takeda A, Iwai T, Sugiyama S, Ohashi N, Kitajima H, Yajima Y, Hirota M, Mitsudo K (2020) Image-guided removal of deeply impacted mandibular third molar using a navigation system. J. Oral Maxillofacial Surg. Med. Pathol. 32:529-533
https://dx.doi.org/10.1016/j.ajoms.2020.07.012

[90] Yamamoto S, Taniike N, Takenobu T (2020) Application of an open position splint integrated with a reference frame and registration markers for mandibular navigation surgery. Int J Oral Maxillofac Surg 49:686-690 https://dx.doi.org/10.1016/j.ijom.2019.09.015

[91] Yu Y, Zhang WB, Liu XJ, Guo CB, Yu GY, Peng X (2016) A New Procedure Assisted by Digital Techniques for Secondary Mandibular Reconstruction With Free Fibula Flap. J Craniofac Surg 27:2009-2014 https://dx.doi.org/10.1097/SCS.0000000000003096

[92] Yu Y, Zhang WB, Wang Y, Liu XJ, Guo CB, Peng X (2016) A Revised Approach for Mandibular Reconstruction With the Vascularized Iliac Crest Flap Using Virtual Surgical Planning and Surgical Navigation. J Oral Maxillofac Surg 74:1285.e1281-1285.e1211
https://dx.doi.org/10.1016/j.joms.2016.02.021

[93] Zhang W, Li B, Gui H, Zhang L, Wang X, Shen G (2013) Reconstruction of complex mandibular defect with computer-aided navigation and orthognathic surgery. J Craniofac Surg 24:e229-233 https://dx.doi.org/10.1097/SCS.0b013e3182869b00

[94] Badiali G, Cutolo F, Roncari A, Marchetti C, Bianchi A (2017) Simulation-guided navigation for vector control in pediatric mandibular distraction osteogenesis. J Craniomaxillofac Surg 45:969-980 https://dx.doi.org/10.1016/j.jcms.2017.02.006

[95] Berger M, Nova I, Kallus S, Ristow O, Eisenmann U, Dickhaus H, Engel M, Freudlsperger C, Hoffmann J, Seeberger R (2018) Electromagnetic navigated condylar positioning after high oblique sagittal split osteotomy of the mandible: a guided method to attain pristine temporomandibular joint conditions. Oral Surg Oral Med Oral Pathol Oral Radiol 125:407-414.e401 https://dx.doi.org/10.1016/j.oooo.2017.12.007

[96] Bianchi A, Badiali G, Piersanti L, Marchetti C (2015) Computer-assisted piezoelectric surgery: a navigated approach toward performance of craniomaxillofacial osteotomies. J Craniofac Surg 26:867-872 https://dx.doi.org/10.1097/SCS.0000000000001360

[97] Cao J, Shen S, Liu Z, Dai J, Wang X (2020) Evaluation of Mandibular Symmetry in Patients With Condylar Osteochondroma Who Underwent Intro-Oral Condylar Resection and Simultaneous Bimaxillary Orthognathic Surgery. J Craniofac Surg 31:1390-1394
https://dx.doi.org/10.1097/SCS.0000000000006432

[98] Catanzaro S, Copelli C, Manfuso A, Tewfik K, Pederneschi N, Cassano L, Cocchi R (2017) Intraoperative navigation in complex head and neck resections: indications and limits. Int J CARS 12:881-887 https://dx.doi.org/10.1007/s11548-016-1486-0

[99] Hoffmann J, Troitzsch D, Westendorff C, Weinhold O, Reinert S (2004) Temporary intermaxillary fixation using individualized acrylic splints permits image-data-based surgery of the lower jaw and oropharynx. Laryngoscope 114:1506-1509
https://dx.doi.org/10.1097/00005537-200408000-00035

[100] Kang SH, Kim MK, Choi YS, Park W, Lee SH (2011) Navigation-assisted intraoral vertical ramus osteotomy. J Oral Maxillofac Surg 69:931-934
https://dx.doi.org/10.1016/j.joms.2010.05.021

[101] Lubbers HT, Obwegeser JA, Matthews F, Eyrich G, Gratz KW, Kruse A (2011) A simple and flexible concept for computer-navigated surgery of the mandible. J Oral Maxillofac Surg 69:924-930 https://dx.doi.org/10.1016/j.joms.2010.01.009

[102] Marmulla R, Muhling J (2007) Computer-assisted condyle positioning in orthognathic surgery. J Oral Maxillofac Surg 65:1963-1968 https://dx.doi.org/10.1016/j.joms.2006.11.024

[103] Neuhaus MT, Zeller AN, Jehn P, Lethaus B, Gellrich NC, Zimmerer RM (2021) Intraoperative real-time navigation and intraoperative three-dimensional imaging for patient-specific total temporomandibular joint replacement. Int J Oral Maxillofac Surg https://dx.doi.org/10.1016/j.ijom.2021.02.020

[104] Ni Y, Zhang X, Meng Z, Li Z, Li S, Xu ZF, Sun C, Liu F, Duan W (2020) Digital navigation and 3D model technology in mandibular reconstruction with fibular free flap: A comparative study. J Stomatol Oral Maxillofac Surg 24:24 https://dx.doi.org/10.1016/j.jormas.2020.11.002

[105] Qu M, Hou Y, Xu Y, Shen C, Zhu M, Xie L, Wang H, Zhang Y, Chai G (2015) Precise positioning of an intraoral distractor using augmented reality in patients with hemifacial microsomia. J Craniomaxillofac Surg 43:106-112 https://dx.doi.org/10.1016/j.jcms.2014.10.019

[106] Shan XF, Chen HM, Liang J, Huang JW, Zhang L, Cai ZG, Guo C (2016) Surgical navigation-assisted mandibular reconstruction with fibula flaps. Int J Oral Maxillofac Surg 45:448-453 https://dx.doi.org/10.1016/j.ijom.2015.08.1006

[107] Wu J, Sun J, Shen SG, Xu B, Li J, Zhang S (2016) Computer-assisted navigation: its role in intraoperatively accurate mandibular reconstruction. Oral Surg Oral Med Oral Pathol Oral Radiol 122:134-142 https://dx.doi.org/10.1016/j.oooo.2016.02.001

[108] Yanping L, Xiaojun C, Ming Y, Xudong W, Guofang S, Chengtao W (2010) A pilot application of image-guided navigation system in mandibular angle reduction surgery. J Plast Reconstr Aesthet Surg 63:e593-596 https://dx.doi.org/10.1016/j.bjps.2009.11.043

[109] Yu HB, Li B, Zhang L, Shen SG, Wang XD (2015) Computer-assisted surgical planning and intraoperative navigation in the treatment of condylar osteochondroma. Int J Oral Maxillofac Surg 44:113-118 https://dx.doi.org/10.1016/j.ijom.2014.08.009

[110] Yu Y, Zhang WB, Liu XJ, Guo CB, Yu GY, Peng X (2016) Three-Dimensional Accuracy of Virtual Planning and Surgical Navigation for Mandibular Reconstruction With Free Fibula Flap. J Oral Maxillofac Surg 74:1503.e1501-1503.e1510 https://dx.doi.org/10.1016/j.joms.2016.02.020

[111] Yu Y, Zhang WB, Liu XJ, Guo CB, Yu GY, Peng X (2020) Selection of Guiding Plate Combined With Surgical Navigation for Microsurgical Mandibular Reconstruction. J Craniofac Surg 31:960-965 https://dx.doi.org/10.1097/SCS.0000000000006295

[112] Zhang W, Wang X, Zhang J, Shen G (2016) Application of preoperative registration and automatic tracking technique for image-guided maxillofacial surgery. Computer Assisted Surgery 21:137-142 https://dx.doi.org/10.1080/24699322.2016.1187767

[113] Zhu M, Chai G, Zhang Y, Ma X, Gan J (2011) Registration strategy using occlusal splint based on augmented reality for mandibular angle oblique split osteotomy. J Craniofac Surg 22:1806-1809 https://dx.doi.org/10.1097/SCS.0b013e31822e8064

[114] Zhu M, Liu F, Chai G, Pan JJ, Jiang T, Lin L, Xin Y, Zhang Y, Li Q (2017) A novel augmented reality system for displaying inferior alveolar nerve bundles in maxillofacial surgery. Sci Rep 7:42365 https://dx.doi.org/10.1038/srep42365

[115] Zhu M, Liu F, Zhou C, Lin L, Zhang Y, Chai G, Xie L, Qi F, Li Q (2018) Does intraoperative navigation improve the accuracy of mandibular angle osteotomy: Comparison between augmented reality navigation, individualised templates and free-hand techniques. J Plast Reconstr Aesthet Surg 71:1188-1195 https://dx.doi.org/10.1016/j.bjps.2018.03.018

References

[116] Boeckx P, Essig H, Kokemuller H, Tavassol F, Gellrich NC, Swennen GR (2015) Presentation and Evaluation of a Modified Wax-Bite Dental Splint for Surgical Navigation in Craniomaxillofacial Surgery. J Oral Maxillofac Surg 73:2189-2195 https://dx.doi.org/10.1016/j.joms.2015.03.057

[117] Feichtinger M, Schultes G, Karcher H (2008) The use of a 3D navigation system in the treatment of mandibular angle fractures by minimally invasive insertion of Herbert screws for osteosynthesis. Computer Aided Surgery 13:47-54 https://dx.doi.org/10.3109/10929080701882572

[118] Gao Y, Lin L, Chai G, Xie L (2019) A feasibility study of a new method to enhance the augmented reality navigation effect in mandibular angle split osteotomy. J Craniomaxillofac Surg 47:1242-1248 https://dx.doi.org/10.1016/j.jcms.2019.04.005

[119] Kang SH, Kim MK, Kim JH, Park HK, Lee SH, Park W (2013) The validity of marker registration for an optimal integration method in mandibular navigation surgery. J Oral Maxillofac Surg 71:366-375 https://dx.doi.org/10.1016/j.joms.2012.03.037

[120] Lin L, Shi Y, Tan A, Bogari M, Zhu M, Xin Y, Xu H, Zhang Y, Xie L, Chai G (2016) Mandibular angle split osteotomy based on a novel augmented reality navigation using specialized robot-assisted arms--A feasibility study. J Craniomaxillofac Surg 44:215-223 https://dx.doi.org/10.1016/j.jcms.2015.10.024

[121] Lubbers HT, Kruse A, Messmer P, Gratz KW, Obwegeser JA, Matthews F (2011) Precise screw positioning at the mandibular angle: computer assisted versus template coded. J Craniofac Surg 22:620-624 https://dx.doi.org/10.1097/SCS.0b013e3182085519

[122] Lubbers HT, Messmer P, Gratz KW, Ellis RE, Matthews F (2010) Misjudgments at the mandibular angle: freehand versus computer-assisted screw positioning. J Craniofac Surg 21:1012-1017 https://dx.doi.org/10.1097/SCS.0b013e3181e20a37

[123] Ma Q, Kobayashi E, Suenaga H, Hara K, Wang J, Nakagawa K, Sakuma I, Masamune K (2020) Autonomous Surgical Robot with Camera-Based Markerless Navigation for Oral and Maxillofacial Surgery. IEEE ASME Trans Mechatron 25:1084-1094 https://dx.doi.org/10.1109/TMECH.2020.2971618

[124] Ma Q, Kobayashi E, Wang J, Hara K, Suenaga H, Sakuma I, Masamune K (2019) Development and preliminary evaluation of an autonomous surgical system for oral and maxillofacial surgery. Int J Med Robotics Comput Assist Surg 15:e1997 https://dx.doi.org/10.1002/rcs.1997

[125] Pietruski P, Majak M, Swiatek-Najwer E, Popek M, Szram D, Zuk M, Jaworowski J (2016) Accuracy of experimental mandibular osteotomy using the image-guided sagittal saw. Int J Oral Maxillofac Surg 45:793-800 https://dx.doi.org/10.1016/j.ijom.2015.12.018

[126] Pietruski P, Majak M, Swiatek-Najwer E, Zuk M, Popek M, Mazurek M, Swiecka M, Jaworowski J (2019) Supporting mandibular resection with intraoperative navigation utilizing augmented reality technology - A proof of concept study. J Craniomaxillofac Surg 47:854-859 https://dx.doi.org/10.1016/j.jcms.2019.03.004

[127] Tsuji M, Noguchi N, Shigematsu M, Yamashita Y, Ihara K, Shikimori M, Goto M (2006) A new navigation system based on cephalograms and dental casts for oral and maxillofacial surgery. Int J Oral Maxillofac Surg 35:828-836 https://dx.doi.org/10.1016/j.ijom.2006.02.024

[128] Wang J, Suenaga H, Liao H, Hoshi K, Yang L, Kobayashi E, Sakuma I (2015) Real-time computer-generated integral imaging and 3D image calibration for augmented reality surgical navigation. Comput Med Imaging Graph 40:147-159 https://dx.doi.org/10.1016/j.compmedimag.2014.11.003

[129] Woo SY, Lee SJ, Yoo JY, Han JJ, Hwang SJ, Huh KH, Lee SS, Heo MS, Choi SC, Yi WJ (2017) Autonomous bone reposition around anatomical landmark for robot-assisted

orthognathic surgery. J Craniomaxillofac Surg 45:1980-1988
https://dx.doi.org/10.1016/j.jcms.2017.09.001

[130] Augello M, Baetscher C, Segesser M, Zeilhofer HF, Cattin P, Juergens P (2018) Performing partial mandibular resection, fibula free flap reconstruction and midfacial osteotomies with a cold ablation and robot-guided Er:YAG laser osteotome (CARLO^R) - A study on applicability and effectiveness in human cadavers. J Craniomaxillofac Surg 46:1850-1855 https://dx.doi.org/10.1016/j.jcms.2018.08.001

[131] Bouchard C, Magill JC, Nikonovskiy V, Byl M, Murphy BA, Kaban LB, Troulis MJ (2012) Osteomark: a surgical navigation system for oral and maxillofacial surgery. Int J Oral Maxillofac Surg 41:265-270 https://dx.doi.org/10.1016/j.ijom.2011.10.017

[132] d'Hauthuille C, Taha F, Devauchelle B, Testelin S (2005) Comparison of two computer-assisted surgery techniques to guide a mandibular distraction osteogenesis procedure. Technical note. Int J Oral Maxillofac Surg 34:197-201 https://dx.doi.org/10.1016/j.ijom.2004.04.001

[133] Cai M, Chen Y, Lu X, Xu L, Wang X, Shen G (2017) Application of a newly designed mandibular distraction device for navigation surgery in goats. J Craniomaxillofac Surg 45:1704-1709 https://dx.doi.org/10.1016/j.jcms.2017.08.003

[134] Cai M, Shen G, Cheng AH, Lin Y, Yu D, Ye M (2014) Navigation-assisted mandibular body distraction osteogenesis: a preliminary study in goats. J Oral Maxillofac Surg 72:168.e161-167 https://dx.doi.org/10.1016/j.joms.2013.09.016

[135] Jiang T, Zhu M, Chai G, Li Q (2019) Precision of a Novel Craniofacial Surgical Navigation System Based on Augmented Reality Using an Occlusal Splint as a Registration Strategy. Sci Rep 9:501 https://dx.doi.org/10.1038/s41598-018-36457-2

[136] Hasan W, Daly MJ, Chan HHL, Qiu J, Irish JC (2020) Intraoperative cone-beam CT-guided osteotomy navigation in mandible and maxilla surgery. Laryngoscope 130:1166-1172 https://dx.doi.org/10.1002/lary.28082

[137] Naujokat H, Rohnen M, Lichtenstein J, Birkenfeld F, Gerle M, Florke C, Wiltfang J (2017) Computer-assisted orthognathic surgery: evaluation of mandible registration accuracy and report of the first clinical cases of navigated sagittal split ramus osteotomy. Int J Oral Maxillofac Surg 46:1291-1297 https://dx.doi.org/10.1016/j.ijom.2017.05.003

[138] Peacock ZS, Magill JC, Tricomi BJ, Murphy BA, Nikonovskiy V, Hata N, Chauvin L, Troulis MJ (2015) Assessment of the OsteoMark-Navigation System for Oral and Maxillofacial Surgery. J Oral Maxillofac Surg 73:2005-2016 https://dx.doi.org/10.1016/j.joms.2015.03.017

[139] Wang J, Shen Y, Yang S (2019) A practical marker-less image registration method for augmented reality oral and maxillofacial surgery. Int J CARS 14:763-773 https://dx.doi.org/10.1007/s11548-019-01921-5

[140] Wang J, Suenaga H, Yang L, Kobayashi E, Sakuma I (2017) Video see-through augmented reality for oral and maxillofacial surgery. Int J Med Robotics Comput Assist Surg 13: https://dx.doi.org/10.1002/rcs.1754

[141] Fitzpatrick JM, West JB (2001) The distribution of target registration error in rigid-body point-based registration. IEEE Trans Med Imaging 20:917-927 https://dx.doi.org/10.1109/42.952729

[142] Maurer CR, Jr., Fitzpatrick JM, Wang MY, Galloway RL, Jr., Maciunas RJ, Allen GS (1997) Registration of head volume images using implantable fiducial markers. IEEE Trans Med Imaging 16:447-462 https://dx.doi.org/10.1109/42.611354

[143] Ulrich M, Wiedemann C, Steger C (2012) Combining scale-space and similarity-based aspect graphs for fast 3D object recognition. IEEE Trans Pattern Anal Mach Intell 34:1902-1914 https://dx.doi.org/10.1109/tpami.2011.266

References

[144] van Baar GJC, Liberton N, Winters HAH, Leeuwrik L, Forouzanfar T, Leusink FKJ (2020) A Postoperative Evaluation Guideline for Computer-Assisted Reconstruction of the Mandible. J Vis Exp 155:28 https://dx.doi.org/10.3791/60363

[145] van Baar GJC, Forouzanfar T, Liberton N, Winters HAH, Leusink FKJ (2018) Accuracy of computer-assisted surgery in mandibular reconstruction: A systematic review. Oral Oncol 84:52-60 https://dx.doi.org/10.1016/j.oraloncology.2018.07.004

[146] "Aurora Tools." Northern Digital Inc. https://www.ndigital.com/products/aurora/aurora-tools/ (accessed November 19, 2021).

[147] Fedorov A, Beichel R, Kalpathy-Cramer J, Finet J, Fillion-Robin J-C, Pujol S, Bauer C, Jennings D, Fennessy F, Sonka M, Buatti J, Aylward S, Miller JV, Pieper S, Kikinis R (2012) 3D Slicer as an image computing platform for the Quantitative Imaging Network. Magnetic Resonance Imaging 30:1323-1341 https://dx.doi.org/10.1016/j.mri.2012.05.001

[148] Ungi T, Lasso A, Fichtinger G (2016) Open-source platforms for navigated image-guided interventions. Med Image Anal 33:181-186 https://dx.doi.org/10.1016/j.media.2016.06.011

[149] Lasso A, Heffter T, Rankin A, Pinter C, Ungi T, Fichtinger G (2014) PLUS: open-source toolkit for ultrasound-guided intervention systems. IEEE Trans Biomed Eng 61:2527-2537 https://dx.doi.org/10.1109/tbme.2014.2322864

[150] Tokuda J, Fischer GS, Papademetris X, Yaniv Z, Ibanez L, Cheng P, Liu H, Blevins J, Arata J, Golby AJ, Kapur T, Pieper S, Burdette EC, Fichtinger G, Tempany CM, Hata N (2009) OpenIGTLink: an open network protocol for image-guided therapy environment. Int J Med Robot 5:423-434 https://dx.doi.org/10.1002/rcs.274

[151] "Using BioMed Clear Resin." Formlabs. https://support.formlabs.com/s/article/Using-BioMed-Clear-Resin?language=en_US#resources (accessed November 9, 2021).

[152] Jacobs P, Kowatsch R (1993) Sterrad Sterilization System: a new technology for instrument sterilization. Endosc Surg Allied Technol 1:57-58

[153] Brouwer de Koning SG, Riksen JJM, Ter Braak TP, van Alphen MJA, van der Heijden F, Schreuder WH, Karssemakers LHE, Karakullukcu MB, van Veen RLP (2020) Utilization of a 3D printed dental splint for registration during electromagnetically navigated mandibular surgery. Int J CARS 15:1997-2003 https://dx.doi.org/10.1007/s11548-020-02271-3

[154] Mascott CR, Sol JC, Bousquet P, Lagarrigue J, Lazorthes Y, Lauwers-Cances V (2006) Quantification of true in vivo (application) accuracy in cranial image-guided surgery: influence of mode of patient registration. Neurosurgery 59:146-156 https://dx.doi.org/10.1227/01.Neu.0000220089.39533.4e

[155] Chang CM, Fang KM, Huang TW, Wang CT, Cheng PW (2013) Three-dimensional analysis of the surface registration accuracy of electromagnetic navigation systems in live endoscopic sinus surgery. Rhinology 51:343-348 https://dx.doi.org/10.4193/Rhino12.165

[156] Schicho K, Figl M, Seemann R, Donat M, Pretterklieber ML, Birkfellner W, Reichwein A, Wanschitz F, Kainberger F, Bergmann H, Wagner A, Ewers R (2007) Comparison of laser surface scanning and fiducial marker-based registration in frameless stereotaxy. Technical note. J Neurosurg 106:704-709 https://dx.doi.org/10.3171/jns.2007.106.4.704

[157] Block MS, Emery RW, Cullum DR, Sheikh A (2017) Implant Placement Is More Accurate Using Dynamic Navigation. J Oral Maxillofac Surg 75:1377-1386 https://dx.doi.org/10.1016/j.joms.2017.02.026

[158] Edelmann C, Wetzel M, Knipper A, Luthardt RG, Schnutenhaus S (2021) Accuracy of Computer-Assisted Dynamic Navigation in Implant Placement with a Fully Digital Approach: A Prospective Clinical Trial. J Clin Med 10: https://dx.doi.org/10.3390/jcm10091808

[159] Scheyer ET, Mandelaris GA, McGuire MK, AlTakriti MA, Stefanelli LV (2020) Implant Placement Under Dynamic Navigation Using Trace Registration: Case Presentations. Int J Periodontics Restorative Dent 40:e241-e248 https://dx.doi.org/10.11607/prd.4479

[160] Berger M, Nova I, Kallus S, Ristow O, Freudlsperger C, Eisenmann U, Dickhaus H, Engel M, Hoffmann J, Seeberger R (2017) Can electromagnetic-navigated maxillary positioning replace occlusional splints in orthognathic surgery? A clinical pilot study. J Craniomaxillofac Surg 45:1593-1599 https://dx.doi.org/10.1016/j.jcms.2017.08.005

[161] Lutz JC, Nicolau S, Agnus V, Bodin F, Wilk A, Bruant-Rodier C, Rémond Y, Soler L (2015) A novel navigation system for maxillary positioning in orthognathic surgery: Preclinical evaluation. J Craniomaxillofac Surg 43:1723-1730 https://dx.doi.org/10.1016/j.jcms.2015.08.001

[162] West JB, Fitzpatrick JM, Toms SA, Maurer CR, Jr., Maciunas RJ (2001) Fiducial point placement and the accuracy of point-based, rigid body registration. Neurosurgery 48:810-816; discussion 816-817 https://dx.doi.org/10.1097/00006123-200104000-00023

[163] Eggers G, Muhling J, Marmulla R (2006) Image-to-patient registration techniques in head surgery. Int J Oral Maxillofac Surg 35:1081-1095 https://dx.doi.org/10.1016/j.ijom.2006.09.015

[164] Yang J, Li H, Jia Y, "Go-ICP: Solving 3D Registration Efficiently and Globally Optimally," in *2013 IEEE International Conference on Computer Vision*, 1-8 Dec. 2013 2013, pp. 1457-1464, doi: https://dx.doi.org/10.1109/ICCV.2013.184.

[165] Mémoli F, Sapiro G, "Comparing Point Clouds," in *Eurographics/ACM SIGGRAPH symposium on Geometry processing*, 2004, vol. 71, pp. 33-42, doi: https://dx.doi.org/10.1145/1057432.1057436.

[166] Javaheri A, Brites C, Pereira F, Ascenso J, "A generalized Hausdorff distance based quality metric for point cloud geometry," in *Twelfth International Conference on Quality of Multimedia Experience (QoMEX)*, 2020, pp. 1-6, doi: https://dx.doi.org/10.1109/QoMEX48832.2020.9123087.

[167] Caiti G, Dobbe JGG, Strackee SD, Strijkers GJ, Streekstra GJ (2020) Computer-Assisted Techniques in Corrective Distal Radius Osteotomy Procedures. IEEE Rev Biomed Eng 13:233-247 https://dx.doi.org/10.1109/RBME.2019.2928424

[168] Wong KC, Kumta SM (2013) Computer-assisted tumor surgery in malignant bone tumors. Clin Orthop Relat Res 471:750-761 https://dx.doi.org/10.1007/s11999-012-2557-3

[169] Van Vlaenderen ARW, "Renewed Mandibular Reconstruction Process: the development of a universal fibula cutting guide and evaluation of a semi-automatic mandible reconstruction planning software," Master of Science, Universiteit Twente, 2020.

References

80

Appendices

Appendix I Search queries used in the systematic review

Embase.com, searched on March 25, 2021
("mandible resection"/exp or "mandible reconstruction"/exp or "orthognathic surgery"/exp or "maxillofacial surgery"/exp or (("mandible"/exp or "temporomandibular joint"/exp) and "Surgery"/exp) or (("sagittal split ram* osteotomy" or SSRO or "intraoral vertical ram* osteotomy" or IVRO or genioplasty or mandibulectom*) or ((Jaw or mandible or mandibula* or maxillofacial or "temporomandibular joint" or TMJ or orthognathic) NEAR/3 (reconstruct* or osteotom* or resect* or surger*))):ti,ab,kw)
AND
(((("computer assisted surgery"/exp OR (CAS OR AR OR "augmented reality" OR "mixed reality" OR "cutting guide*" OR ((computer OR image OR robot*) NEAR/1 (guided OR aided OR assisted) NEAR/1 (reconstruct* OR osteotom* OR resect* OR surger*)) OR (virtual NEAR/1 (reconstruct* OR osteotom* OR resect* OR surger*))):ti,ab,kw) AND (((guid* NEAR/2 (surger* or surgical or intraoperative or robot*)):ti,ab,kw) OR ("orthopedic fixation device"/exp OR (regist* OR splint OR screw* OR frame OR landmark* OR marker* OR tracker* OR "mark* point*"):ti,ab,kw))   ) OR (((guid* NEAR/2 (surger* or surgical or intraoperative or robot*)):ti,ab,kw) AND ("orthopedic fixation device"/exp OR (regist* OR splint OR screw* OR frame OR landmark* OR marker* OR tracker* OR "mark* point*"):ti,ab,kw)) OR ("surgical navigation system"/de OR (navigat* OR ((optic* OR electromagnet* OR EM) NEAR/1 track*)):ti,ab,kw))

Scopus, searched on March 25, 2021
((TITLE-ABS-KEY(("sagittal split ram* osteotomy" OR ssro OR "intraoral vertical ram* osteotomy" OR ivro OR genioplasty OR mandibulectom*) OR ((jaw OR mandible OR mandibula* OR maxillofacial OR "temporomandibular joint" OR tmj OR orthognathic) W/3 (reconstruct* OR osteotom* OR resect* OR surger*)))))
AND
((((TITLE-ABS-KEY("CAS" OR "AR" OR "augmented reality" OR "mixed reality" OR "cutting guide*" OR ((((computer OR image OR robot*) W/1 (guided OR aided OR assisted)) OR virtual) W/1 (reconstruct* OR osteotom* OR resect* OR surger*))))) AND (((TITLE-ABS-KEY(guid* W/2 (surger* OR surgical OR intraoperative OR robot*)))) OR ((TITLE-ABS-KEY(regist* OR splint OR screw* OR frame OR landmark* OR marker* OR tracker* OR "mark* point*"))))) OR (((TITLE-ABS-KEY(guid* W/2 (surger* OR surgical OR intraoperative OR robot*)))) AND ((TITLE-ABS-KEY(regist* OR splint OR screw* OR frame OR landmark* OR marker* OR tracker* OR "mark* point*")))) OR ((TITLE-ABS-KEY(navigat* OR ((optic* OR electromagnet* OR em) W/1 track*))))))

Medline Ovid, searched on March 25, 2021
(exp "orthognathic surgical procedures"/ or exp "Osteotomy, Sagittal Split Ramus"/ or exp "maxillofacial surgery"/ or ((exp "mandible"/ or exp "temporomandibular joint"/) and exp "Surgical Procedures, Operative"/) or (("sagittal split ram* osteotomy" or SSRO or "intraoral vertical ram* osteotomy" or IVRO or genioplasty or mandibulectom*) or ((Jaw or mandible or mandibula* or maxillofacial or "temporomandibular joint" or TMJ or orthognathic) adj3 (reconstruct* or osteotom* or resect* or surger*))).ti,ab,kf.)
AND (((exp "Surgery, Computer-Assisted"/ or (CAS or AR or "augmented reality" or "mixed reality" or "cutting guide*" or (((((computer or image or robot*) adj1 (guided or aided or assisted)) or virtual) adj1 (reconstruct* or osteotom* or resect* or surger*)))).ti,ab,kf.) and ((guid* adj2 (surger* or surgical or intraoperative or robot*)).ti,ab,kf. or (exp "orthopedic fixation device"/ or exp "Jaw Fixation Techniques"/ or (regist* or splint or screw* or frame or landmark* or marker* or tracker* or "mark*

point*").ti,ab,kf.))) OR ((guid* adj2 (surger* or surgical or intraoperative or robot*)).ti,ab,kf. and (exp "orthopedic fixation device"/ or exp "Jaw Fixation Techniques"/ or (regist* or splint or screw* or frame or landmark* or marker* or tracker* or "mark* point*").ti,ab,kf.)) OR (exp "Surgical Navigation Systems"/ or (navigat* or ((optic* or electromagnet* or EM) adj1 track*)).ti,ab,kf.))

Line-by-line search Medline Ovid

The line-by-line search is identical to the cope + paste search and is added to improve the readability of the search strategy

Ovid MEDLINE(R) ALL <1946 to March 25, 2021>

1	exp "orthognathic surgical procedures"/	5934
2	exp "Osteotomy, Sagittal Split Ramus"/	853
3	exp "maxillofacial surgery"/	8574
4	(exp "mandible"/ or exp "temporomandibular joint"/) and exp "Surgical Procedures, Operative"/	22725
5	("sagittal split ram* osteotomy" or SSRO or "intraoral vertical ram* osteotomy" or IVRO or genioplasty or mandibulectom*).ti,ab,kf.	2640
6	((Jaw or mandible or mandibula* or maxillofacial or "temporomandibular joint" or TMJ or orthognathic) adj3 (reconstruct* or osteotom* or resect* or surger*)).ti,ab,kf.	20561
7	1 or 2 or 3 or 4 or 5 or 6	46740
8	exp "Surgery, Computer-Assisted"/	29198
9	(CAS or AR or "augmented reality" or "mixed reality" or "cutting guide*").ti,ab,kf.	80998
10	((((computer or image or robot*) adj1 (guided or aided or assisted)) or virtual) adj1 (reconstruct* or osteotom* or resect* or surger*)).ti,ab,kf.	6626
11	8 or 9 or 10	112523
12	(guid* adj2 (surger* or surgical or intraoperative or robot*)).ti,ab,kf.	13083
13	exp "orthopedic fixation device"/	79716
14	exp "Jaw Fixation Techniques"/	1020
15	(regist* or splint or screw* or frame or landmark* or marker* or tracker* or "mark* point*").ti,ab,kf.	1405849
16	13 or 14 or 15	1457891
17	exp "Surgical Navigation Systems"/	12
18	navigat*.ti,ab,kf.	44557
19	((optic* or electromagnet* or EM) adj1 track*).ti,ab,kf.	1960
20	17 or 18 or 19	46076
21	7 and ((11 and (12 or 16)) or (12 and 16) or 20)	895

Appendix II Application form for sensor applicator

DOSSIER ACCEPTATIE MEDISCH HULPMIDDEL

NKI-AvL		DOSSIERNUMMER:
		AUTORISATIE
Verwervingsproces		
De transactie vindt plaats d.m.v. N.v.t.		
aankoop	Nee	
Consignatie	Nee	Zo ja zijn er afspraken gemaakt over beschadigde en/of vermiste artikelen Ja/nee
Bruikleen/zicht	Nee	Zo ja de zichtperiode aangeven: ...-…..-…. t/m ..-….-….
Anders:	Bedoeld voor klinisch onderzoek	
Indien van bekend geef hier de geldende garantietermijn aan	N.v.t.	
PRODUCTGEGEVENS		
Generieke naam		Sensorapplicator mandibula navigatie
Model (indien van toepassing)		N.v.t.
	Leverancier:	N.v.t.
	Telefoon	
	Fax	
	e-mail	
	Contactpersoon	
	Fabrikant:	NKI
	Telefoon	6142
	Fax	
	e-mail	r.v.veen@nki.nl
	Contactpersoon	Robert van Veen
Gebruiksdoel (intended purpose) ; functie		Applicator waar een electromagnetische sensor (NDI Aurora Cable Tool) mee kan worden bevestigd op de mandibula (bot) om beweging van de mandibula te tracken tijdens operaties. Bevestiging vindt plaats met CE gemarkeerde steriele schroeven van KLS Martin.

| Specialisme	HOD
Artikelnummer(s) leverancier	N.v.t.
Registratie nummer (identificerend kenmerk per artikel) aangebracht op het medisch hulpmiddel:	N.v.t

CE markering

Draagt het product CE markering	Nee
Zo ja:n.v.t.	

Onder welke directieven

a.	MDD 93/42 EEC of 90/385/EEC welke in de Nederlandse wetgeving is geharmoniseerd met het "Besluit medische hulpmiddelen" (aandachtspunt is de Nederlandse taaleis art 6 lid 2)	N.v.t.

Is het product

a.	Een "naar maat gemaakt medisch hulpmiddel" (art 1 a besluit medische hulpmiddelen/ MDD 93/42 art 2 d)	Nee
Zo ja patiëntennummer opgeven		
b.	Een product bedoeld voor klinisch onderzoek	Ja
Zo ja toestemmingsnummer Medisch Ethische Commissie opgeven (MEC)		N17TOT

DECONTAMINATIE/HERGEBRUIK

a.	Is het product bedoeld voor hergebruik	Ja	
b.	Zo ja is de gebruiksstatus		
c.	Is er een voorgeschreven beperking in het aantal malen hergebruik	Nee	
d.	Zijn er her-verwerkingsinstructies beschikbaar	Ja	Standaard machinale reiniging en sterilisatie in Sterrad
e.	Zijn er speciale gereedschappen/applicaties nodig voor Herverwerking	Nee	

f. Zijn er smeermiddelen of andere onderhoudsmiddelen voorgeschreven in het verwerkingstraject	Nee	
a. Is alleen handmatige reiniging voorgeschreven	Nee	
b. Is machinale reiniging mogelijk	Ja	
c. Wat is de maximale temperatuur voor thermische desinfectie	70 graden	
d. Zijn er beperkingen met betrekking tot de te gebruiken reiniging en desinfectie middelen:	Nee	
a. Is het product geschikt voor stoomsterilisatie:	Nee	
b. Is het product geschikt voor Sterrad sterilisatie (H2O2)	Ja	
Is er training nodig,beschikbaar voor de sterilisatieafdeling	Nee	
Indien ja zijn hier kosten aan verbonden	Nee	

GEBRUIKERSHANDLEIDING

Is er een handleiding beschikbaar	n.v.t.	
Zo Ja voldoet deze aan het gestelde in het Besluit medische hulpmiddelen *(b.v. taaleis Nederlandse handleiding)*		

Verpakking / aandachtspunten

Zijn er specifieke verpakkingsvoorschriften van toepassing:	Ja
Zo ja welke	**Dubbele laminaatverpakking**

Autorisatie:			
	NAAM & FUNCTIE	**DATUM: (dd-mnd-jr)**	**HANDTEKENING:**
Samengesteld door:			
Autorisatie DSMH:			
Autorisatie bedrijfsleider Clinium			
Clinium			
De CSA functionaris vult het dossier aan met de volgende documenten als bijlage		Aanwezig Ja/nee	**PARAAF:**
1. Handleiding fabrikant			
2. Steri setomschrijving			
3. Foto			
Indien van toepassing			
a. Kwaliteitscertificaten artikelen zonder CE zie blok 4			
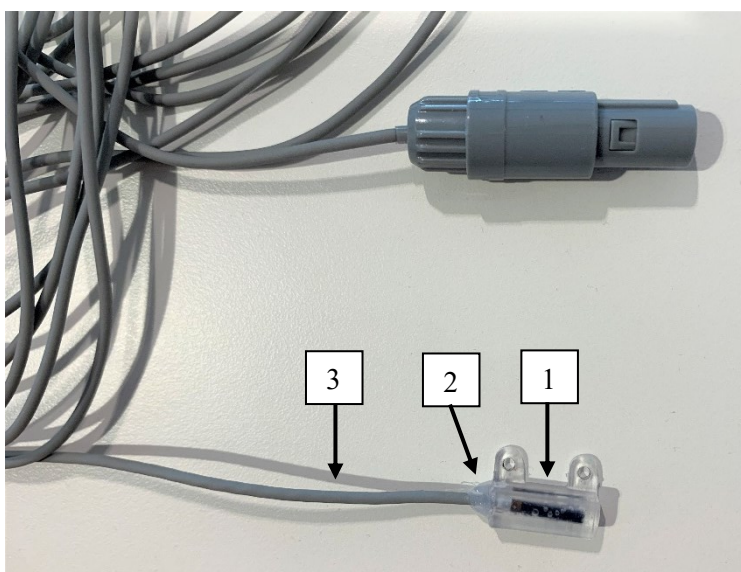
Item number	Part description	Material	Supplier
1	Applicator	BioMed Clear Resin	Formlabs
2	Elastocil V41 glue	Silicone	De Hazelaar
3	Aurora cable tool	Silicone	Northern Digital Inc.

Appendix III Additional table to Chapter 6

Table A3 *Results of the phantom experiment. The TRE and 95% Hausdorff distance are shown for the original registration, and after applying a transformation of -2, -1, 2, and 2 mm (A) or degrees (B) in three directions. All values are in mm.*

A	Original registration	Translation in LR direction (mm)				Translation in PA direction (mm)				Translation in IS direction (mm)			
		-2	-1	1	2	-2	-1	1	2	-2	-1	1	2
TRE	1.13	2.38	1.57	1.44	2.21	2.81	1.90	0.98	1.63	1.90	1.20	1.77	2.64
95% HD	0.57	2.01	1.23	1.30	2.27	2.12	1.27	0.82	1.47	1.83	1.08	0.86	1.39

B	Original registration	Rotation around LR axis (degrees)				Rotation around PA axis (degrees)				Rotation around IS axis (degrees)			
		-2	-1	1	2	-2	-1	1	2	-2	-1	1	2
TRE	1.13	15.64	8.00	7.50	15.13	5.22	2.92	2.34	4.60	15.03	7.67	7.29	14.64
95% HD	0.57	9.05	5.20	5.94	12.54	3.83	2.19	2.51	5.05	14.25	6.22	8.27	16.47

TRE = target registration error. HD = Hausdorff distance. LR = left right. PA = posterior anterior. IS = inferior superior.